UNIVERSITY OF SOUTHAMPTON

FURTHER DEVELOPMENT IN THE CAUCHY–CHARACTERISTIC MATCHING
APPROACH TO NUMERICAL RELATIVITY

Elizabeth Ann Sarkies

Master of Philosophy

FACULTY OF MATHEMATICAL STUDIES

DEPARTMENT OF MATHEMATICS

September 1998

UNIVERSITY OF SOUTHAMPTON

ABSTRACT

FACULTY OF MATHEMATICAL STUDIES

DEPARTMENT OF MATHEMATICS

Master of Philosophy

FURTHER DEVELOPMENT IN THE CAUCHY–CHARACTERISTIC MATCHING
APPROACH TO NUMERICAL RELATIVITY

by Elizabeth Ann Sarkies

Numerical relativity is a relatively small but growing area of research in General Relativity. The background and motivation for this type of work is first described. The major project of the Southampton Relativity group, CCM (Cauchy–characteristic matching) is next outlined and the initial work on cylindrical symmetry is subjected to a complete and detailed analysis to ascertain its validity. The next stage of the project was to extend the CCM scheme in cylindrical symmetry to two degrees of freedom using a solution due to Piran, Safier and Katz which possesses both gravitational degrees of freedom. This family of solutions is derived, and the modifications required to be made to the existing code are described. The problems that were encountered, and the means by which they were overcome are considered, and error and convergence results are presented. Finally, a new approach to CCM is considered in which the principal null directions of the system are calculated, rather than the metric functions which are inherently coordinate dependent. However the practical application of this method turns out to be less successful than had originally been hoped for, and the major problems which arise are discussed. Some final comments are made as to the successes and drawbacks of the various methods, and suggestions are made to possible future areas of development.

Contents

List of Figures

Acknowledgements

Introduction

0.1 Numerical Relativity

In this introduction the origins of the subject of Numerical Relativity are outlined. We shall describe how the natural human desire to know and understand more about the world around us has driven people through the ages to learn more about the universe. From early speculation, which was based mainly upon ideology, to observations made with the telescopes and satellite probes of today, the main pioneers and procedures are described. We then conclude by outlining the growing status of numerical relativity, and the increasing contribution that this field is making to our understanding of the universe in which we live.

In the early ages of man there was little if any knowledge of any countries and civilisations beyond their own. Most ideas about what lay beyond immediate experience was founded on myths and legends, and the world was believed to be flat. Greek philosophers began to question this belief, and early mathematics also seemed not to support this theory. An experiment was designed to test the notion. By placing two identical sticks many miles apart and observing that the shadows that these cast at the same time of day had different lengths, it was demonstrated that the Earth's surface was in fact curved. Thus began a slow development which reconciled scientific theory with observation. The Greeks believed that the planets should be perfect spheres which described perfectly circular orbits about the Earth. However observed orbits were not quite like this. Ptolemy succeeded in adding slight circular corrections to circular orbits to achieve a theory which matched observation of the time, and this theory survived for over 1500 years. By the 16th century more accurate observations of planetary orbits were available, and Ptolemy's model no longer fitted completely with these. Copernicus

determined that circular orbits would very nearly fit with the new observations with the provision that the centre of the system be the Sun rather than the Earth. Later in around 1600 Johannes Kepler devised a theory which also had the Sun at the centre, but where the planets described eliptical orbits. The Church refuted these ideas, believing rather that God created the Earth as the centre of his universe, but when in 1609 Galileo observed with a telescope that Jupiter had satellites, the Earth–centred model was finally laid to rest.

From the middle of the seventeenth century Isaac Newton began to study the laws and factors that governed motion. He produced his three laws of motion, and also gave some thought to forces that exist between objects. Whether an apple really fell and gave him a flash of inspiration or whether this story is just a myth is not certain. But regardless of the method, he devised a theory of gravitation which for the first time gave a means of understanding everyday gravitational phenomena. Newton's theory of gravity was based on the theory that every piece of matter pulls every other piece of matter towards it. In the case of a body falling under the force of the Earth's local gravity, the Earth does move towards the body but the motion is too small relatively to be detected. He stated that quantitively a gravitational force exists between two objects of masses m_1 and m_2 say, the force F of attraction between them being given by

$$F = \frac{Gm_1m_2}{r^2} \tag{0.1}$$

where r is the distance between the two centres of gravity and G is Newton's Gravitiational constant.

In our lifetime the idea of gravity is second nature, and few would dispute the maxim 'what goes up must come down'. In Newton's time though this theory represented a great breakthrough, and when he applied his laws of gravitation and motion to the solar system he found that his predictions were the first which actually matched the observed universe. This model produced a universe that was infinite and forever unchanging. However, as the resolution of telescopes improved, more and more detail of the stars and planets was able to be observed and strange whirlpool configurations were discovered. These were found to be galaxies in their own right. Furthermore spectroscopic analysis of light coming from these galaxies showed that they exhibited a red–shift, that is the

universe was in fact expanding. Theoreticians were uneasy with this idea however, and still favoured a static model.

In 1915 Albert Einstein proposed his celebrated General Theory of Relativity which unified space and time into one theory. One consequence of the theory was that a static universe was not possible. Instead the universe must either be expanding or contracting. Einstein thought that this was a flaw in his theory, and added in a term known as the cosmological constant in order to allow the universe to remain a constant size. He later described this move as 'the biggest blunder of his life', after George Le Maître had worked through Einstein's theory and showed that expansion of the universe was indeed what was observed, and that the cosmological constant was not needed. Several famous experiments have supported Einstein's theory, including the observed advance of the perihelion of Mercury, and the bending of light as it passes massive objects such as planets. There is still not conclusive proof that General Relativity is in fact the correct theory, but it remains the most likely candidate at present, and that which best fits with observation. Since Einstein first proposed his theory, many people have worked on his ideas and sought further proof to support it.

Einstein's equations are extremely complex, but the emergence of computer technology suggested that computers might be a useful tool in further exploring implications of the theory. Moreover, despite a large amount of analytical work it became clear that there were practical limitations in using a purely analytical approach, in that there are only a limited number of physically realistic exact solutions. At the same time exact solutions of Einstein's equations do not exist for many physically significant scenarios, including the two body problem, radiative sources and the interior of a rotating body undergoing gravitational collapse. A greater understanding of problems such as these would help to combine the mathematical theory with the observations of astrophysicists and cosmologists. Numerical simulations could also produce more evidence to support the General Relativistic theory. For example gravitational waves are generally believed to be one consequence of the theory, and have not as yet been detected directly. This is due to the tiny size of signal that could be detected in relation to the accuracy of the detection instruments at this stage. The next generation of detectors (LIGO, VIRGO etc) may finally have the resolution needed to pick up these faint signals when they come on line in a few years time. If these do detect gravitational waves, this will provide firm

evidence in support of the General Theory of Relativity. A procedure for experimentally testing the strong–field predictions of General Relativity using data from these detectors is considered in [1].

0.1.1 A new approach to solving Einstein's equations

Classical mechanics, which governs the macroscopic motion of objects, is now well understood. In this case, experiments could be performed to analyse how various factors (mass of objects, initial velocities etc.) affected the resultant motion. Understanding the behaviour of our universe is a very involved problem which classical Newtonian theory cannot fully handle. The General Theory of Relativity best fits with what has been observed, but the universe is not like a laboratory where factors can be varied at will to examine patterns of behaviour. The elegance of the General Theory is only matched by the complexity of the equations, which are second order partial differential equations and highly non–linear. Consequently purely theoretical work has been mainly restricted to special cases, usually of high symmetry, where the equations simplify and become soluable. The great challenge is to harness the power of the new generation of supercomputers to solve the complex equations for *any* given spacetime.

In the 1960s a small number of people began to attempt to solve Einstein's equations via computer simulation – thus numerical relativity was born. The first numerical general relativistic calculations were performed by May and White [2], and Hahn and Lindquist [3]. The former investigated spherical matter collapse and the formation of neutron stars, and the latter looked into black hole collision. Although both studies made some progress, the work was hampered by the underdevelopment of the necessary theoretical techniques and the available computer power of the time. A number of new numerical techniques needed to be developed in order to cope with the complexities of a four–dimensional system. One such technique was based on the so–called ADM '3+1' formalism [4] which, in essence, involves splitting spacetime into a series of 3–dimensional spacelike hypersurfaces which are connected by 1–dimensional timelike lines. This method is addressed in, for example, [5]. Essentially the four–dimensional problem can be addressed by considering the 3–geometry on the series of spacelike hypersufaces. The geometries of successive slices can be related through the evolution equations, which

come directly from the Einstein field equations. The fundamental components to the formalism are the choice of an initial three–surface Σ, and the construction of a family of slices $\{\Sigma\}$, along with a congruence of curves along which the data is propagated from one slice to the next. In order to uniquely describe the four–metric in this new way it is neccessary to know the three–metric g_{ij} on each slice, and also the shift vector N^i and lapse function α. The lapse function specifies the normal separation of the slices while the shift vector defines where the normal intersects the upper slice in relation to the lower.
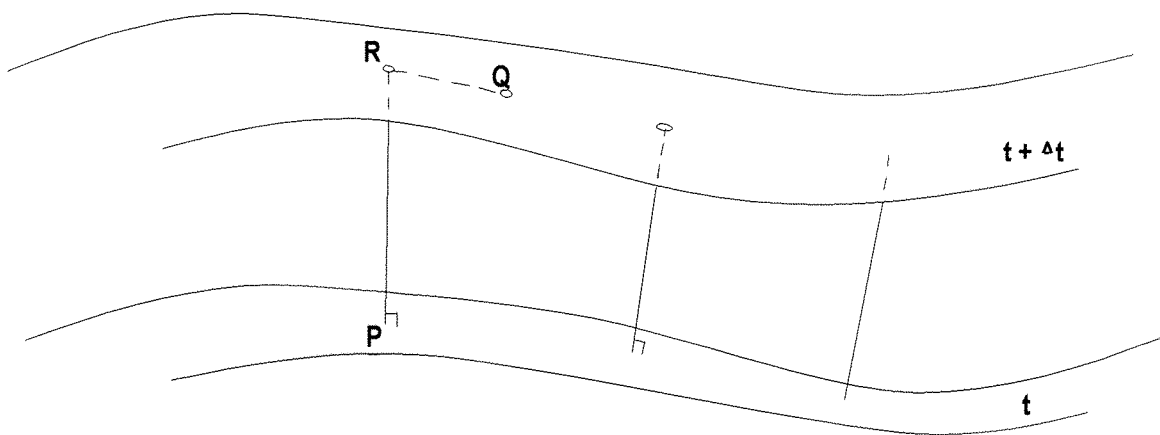
Figure 0.1: An illustration of the '3+1' set up

As an illustration, consider Figure 0.1 which shows two adjacent three–surfaces. The time–like normal vector at the point P, (t, x^i) on the surface $t = constant$, intersects the next surface, $t + \Delta t = constant$ at the point R. When the normal vector intersects the upper slice it has been displaced due to the shift vector $\vec{RQ}$ which has components N^i in the upper slice , and so R has coordinates $(t + \delta t, x^i - N^i \delta t)$. The proper time that elapses is $\alpha \delta t$ where α is the lapse function. Note that $\alpha = 1/\sqrt{g^{00}}$.

We now present a derivation of the '3+1' decomposition of the metric. We choose a family of spacelike hypersurfaces, Σ which form a foliation of spacetime. These hyper-

surfaces are given by

$$\phi(x^a) = constant. \tag{0.2}$$

$w_a = \phi_{,a}$ is the covariant normal to the family and $w^a = g^{ab}w_b$ is the contravariant normal from it. If n^a is the unit normal to the foliation, which must naturally be proportional to w^a, then it satisfies

$$n^a n_a = -1 \tag{0.3}$$

with the standard signature (-1,+1,+1,+1). We then define the projection operator by

$$B_a{}^b = \delta_a^b + n_a n^b \tag{0.4}$$

This is used to project tensors into the foliation. From equations (0.3 – 0.4), $B_a{}^b n^a = 0$, and we can obtain the induced 3–metric by projecting the 4–dimensional metric into Σ, viz

$$^3g_{ab} = B_a^c B_a^c g_{cd} \tag{0.5}$$

From (0.3– 0.4),

$$^3g_{ab} = g_{ab} + n_a n_b \tag{0.6}$$

or,

$$^3g^{ab} = g^{ab} + n^a n^b \tag{0.7}$$

The next step is to choose a rigging vector field t^a that lies nowhere in the foliation. It can therefore be decomposed into components parallel to and orthogonal to n^a, i.e.

$$t^a = \alpha n^a + N^a \tag{0.8}$$

where again α is the lapse function and N^a the shift vector, satisfying

$$N^a n_a = 0 \tag{0.9}$$

We find from (0.7 – 0.8) that

$$g^{ab} = -\frac{1}{\alpha^2}(t^a - N^a)(t^b - N^b) + {}^3g^{ab} \tag{0.10}$$

Coordinates $(x^a) = (x^0, x^\mu) = (t, x^1, x^2, x^3)$ are chosen where the hypersurfaces are the slices

$$t = constant$$

6

The rigging vector field is $\frac{\delta}{\delta t}$. With this choice of coordinates the induced 3–metric and the shift vector are entirely spacial. We have

$$^3 g^{ab} = \delta^a_\mu \delta^b_\nu \gamma^{\mu\nu} \tag{0.11}$$

and

$$N^a = \delta^a_\mu N^\mu \tag{0.12}$$

Combining (0.10) and (0.11– 0.12) we find that

$$g^{ab} = \frac{1}{\alpha^2} \begin{pmatrix} -1 & N^\mu \\ N^\mu & \alpha^2 \gamma^{\mu\nu} - N^\mu N^\nu \end{pmatrix} \tag{0.13}$$

Now define the induced covariant metric $\gamma_{\mu\nu}$ by

$$\gamma_{\mu\nu} \gamma^{\nu\sigma} = \delta^\sigma_\mu \tag{0.14}$$

so that Greek indices can be raised and lowered with $\gamma^{\mu\nu}$ and $\gamma_{\mu\nu}$. Thus

$$N_\mu = \gamma_{\mu\sigma} N^\sigma \tag{0.15}$$

Since the covariant and contravariant metrics must satify the relation

$$g_{ac} g^{cb} = \delta^b_a \tag{0.16}$$

we deduce from (0.13) that

$$g_{ab} = \begin{pmatrix} -\alpha^2 + N^\sigma N_\sigma & N_\mu \\ N_\mu & \gamma_{\mu\nu} \end{pmatrix} \tag{0.17}$$

Therefore the line element in canonical form is

$$ds^2 = - \left(\alpha^2 - N^\sigma N_\sigma \right) dt^2 + 2 N_\mu dx^\mu dt + \gamma_{\mu\nu} dx^\mu dx^\nu. \tag{0.18}$$

Thus knowing the three–geometry, the lapse function and the shift vector, the four–metric can be uniquely reconstructed. For a more detailed discussion of the '3 + 1' formalism see, for example [5] or [6]. Basic methods and issues related to numerical relativity are addressed in [7].

The ability to express a four–geometry in terms of 3–geometries and these other functions makes it possible to study general relativity via computer modelling. Einstein's equations

are second order partial differential equations, and standard finite differencing techniques such as those used in the study of fluid mechanics can be applied. The principles of the finite difference method as used in the Southampton work are outlined in section 1.2, or for a more general description see [8]. Once the evolution equations for the system being considered have been put into finite difference form, and any necessary boundary conditions have been enforced, the initial conditions are applied. The simulation can then run, and the output is compared with analytical or semi–analytical results to assess the reliability of the code. Self–consistency checks, such as convergence tests, are also a way by which the model's validity can be evaluated. Early simulations were limited by the memory and speed of the computers that were available to researchers. Modern codes are increasingly complex, and cover a wide range of research interests. The Grand Challenge project in the United States involves a large scale collaboration to investigate gravitational radiation resulting from the coalescence of a binary black hole system (some examples of recent work in this project are described in [9] [10] [11] [12]). While this may be regarded as, in a sense, the holy grail of numerical relativity, many other projects contribute to the greater understanding of the big picture. For example, comparing the results from numerical gravitational wave simulations with physical evidence when (or if) gravitational waves are detected will provide evidence to support or contradict General Relativity. Many examples of recent work and ideas can be found in proceedings from workshops and conferences related to numerical relativity, such as that held in Southampton a few years ago [13].

As with any numerical approach, there is an amount of scepticism as to whether the results obtained are realistic, for by its nature a computer simulation will always generate a numerical solution of some form. A similar situation existed when computer algebra systems were first developed. In General Relativity, SHEEP (d'Inverno, Frick) was able to compute metric tensors and associated 'objects' which previously would have taken days or even months to calculate by hand. Confidence in the answers generated was eventually obtained by performing the same calculation using other algebra systems. The answers obtained were consistent between the systems and were also consistent with hand calculations, when they were available. Thus the validity of these systems was confirmed, and subsequently the computer tools were accepted into general use.

Similarly, computer simulations must be benchmarked, and a level of consistency

is required to confirm their validity. Benchmarking is achieved by requiring that the results obtained are in keeping with analytic predictions or other similar simulations. Consistency is achieved by performing convergence tests on any particular simulation. Thus most models begin by examining special cases, or spacetimes with certain symmetries so that the behaviour is already understood. Hence if the results produced by the simulation differ vastly from the expected solution, the code needs further refinement. However if the results are consistent the model can be developed further with some confidence that the basic hypotheses of the model are correct.

The ultimate aim of numerical relativists is to develop a reliable computer code which, when given the initial configuration of *any* spacetime or universe could then calculate the subsequent behaviour. This is obviously a lot to ask, but the benefits would be great. It would bring relativity into the position where, just as a mechanical system can be carefully scrutinised, each parameter could be adjusted to examine how this affected the large picture. As a result, a far greater understanding of complex problems could be achieved. However, to arrive at this final stage one must begin with what is already known and hope to learn from this at each stage, as progression to this final goal occurs. There would then be a great opportunity for numericists and theoreticians to work more closely together to produce a better and more complete understanding of the universe.

0.2   The Southampton project

Southampton is one of the main centres for Numerical Relativity in the UK. The main project consists of attempting to combine interior Cauchy codes with exterior characteristic codes connected across an interface, in order to model scenarios of astrophysical interest. This area has now become known as CCM – Cauchy–characteristic matching. Moreover, the exterior vacuum region is compactified so as to include future null infinity into the regime where gravitational radiation can be unambiguously defined. This overcomes one of the main drawbacks of existing codes on finite grids, namely their reliance on ad–hoc definitions of gravitational radiation at the boundary.

The project has four main stages in its development, namely showing that the method works in (i) flat space (ii) cylindrical symmetry (iii) axial symmetry (iv) full generality. The work on stage (ii) of this scheme is described in [14] and [15]. The group is

currently focussing on (iii). The major difficulties lie in coping with the transfer of information at the interface between the regions, and in obtaining regular compactified equations in the exterior region. The ultimate aim of the project is to produce a fully general code which can take any appropriate initial conditions and produce from them a series of evolution slices. However, it is hoped that through examining the procedures neccessary in the steps labelled (i)–(iii) above, a greater understanding of the problems associated with the process, especially the matching of the two regimes at the interface, will be achieved.

0.3   Motivation for this work

The computer code that had been developed by the Southampton group at stage (ii) mentioned above, that is in the case of cylindrical symmetry, had only fully considered the case with one gravitational degree of freedom, and where there was no rotational degree of freedom. It was thought that it would be of interest in this case to also consider a vacuum solution with two gravitational degrees of freedom. The results obtained via the computer evolution could then be compared with the exact prescription of the solution in question. The solution chosen for this purpose was given in [16], and appeared at first sight to be fairly simple. However, in the implementation of this comparison the existing code was subjected to a much harsher test that had been expected, and also required some modifications in order that the evolution grid could include future null infinity. The convergence results and errors obtained, as stated in [15], showed the code to give very successful reproduction of the expected data.

Further to testing how well the numerical scheme dealt with the presence of the rotational element in this solution, the existing code was a useful tool with which new numerical methods and ideas could be examined. Due to the results obtained previously, the code was reliable enough to try out a method suggested in [17]. This involved calculating the principal null directions which contain coordinate–invariant information about the spacetime. This approach, if successful, could be an important new numerical approach because it is often the metric functions which are evolved in numerical simulations of this nature, but these are heavily dependant upon the coordinate system being used. Thus this new idea was applied to the computer code, in order to investi-

gate the practicality of this approach, and to aim to test the accuracy of the computer simulations further.

The work described in this thesis deals with the development of the coding in these two areas, giving details of what was done and comments on the success and merits of these methods. Attention is also drawn to areas which generate problems, or where practicalities of implementation restrict the efficiency and desirability of the methods.

Chapter 1

Validation of the computer code

1.1 Verifying the equations

A first step in the process of verifying the work was to go through the derivation of all equations that were used. We began with [14], the first paper in which vacuum cylindrical symmetry is considered by the Southampton group. The starting point for this work is the standard general cylindrically symmetric line element due to Jordan, Ehlers, Kundt and Kompaneets [18], [19]. Using the coordinates $(x^\alpha) = (x^0, x^1, x^2, x^3) = (t, r, \phi, z)$ in the Cauchy region the line element, or metric, is given by (1) :

$$ds^2 = e^{2(\gamma-\psi)}(-dt^2 + dr^2) + r^2 e^{-2\psi}d\phi^2 + e^{2\psi}(\omega d\phi + dz)^2 \tag{1.1}$$

where the metric functions ψ, ω and γ are functions only of t and r, ie

$$\psi = \psi(t,r), \qquad \omega = \omega(t,r), \qquad \gamma = \gamma(t,r) \tag{1.2}$$

We compute the Ricci tensor, R_{ab}, for this metric and then use the fact that for vacuum solutions we have the identity

$$R_{ab} = 0 \tag{1.3}$$

This gives us six non–trivial equations, from the non–identically zero components, viz. $R_{00}, R_{01}, R_{11}, R_{22}, R_{23}$ and R_{33}. After some simple manipulation, involving merely taking linear combinations of these quantities, we obtain the equations labelled (6)–(9) in [14].

ie

$$e^{2\gamma - 4\psi} R_{33} = \Box\psi + \frac{1}{2}r^{-2}e^{4\psi}(\omega_{,r}^2 - \omega_{,t}^2) = 0 \qquad (1.4)$$

$$2e^{2\gamma - 4\psi}(R_{23} - \omega R_{33}) - = \Box\omega + 2r^{-1}\omega_{,r} + 4(\omega_{,t}\psi_{,t} - \omega_{,r}\psi_{,r}) = 0 \qquad (1.5)$$

$$rR_{01} = \gamma_{,t} - 2r\psi_{,t}\phi_{,r} - \frac{1}{2}r^{-1}e^{4\psi}\omega_{,t}\omega_{,r} = 0 \qquad (1.6)$$

$$\frac{1}{2}r(R_{00} + R_{11}) = \gamma_{,r} - r(\psi_{,r}^2 + \psi_{,t}^2) - \frac{1}{4}r^{-1}e^{4\psi}(\omega_{,t}^2 + \omega_{,r}^2) = 0 \qquad (1.7)$$

$$(1.8)$$

where

$$\Box \equiv \frac{\partial^2}{\partial t^2} - \frac{1}{r}\frac{\partial}{\partial r} - \frac{\partial^2}{\partial r^2} \qquad (1.9)$$

These are the field equations for this problem in the Cauchy region of our spacetime. The contracted Bianchi identities can be expressed

$$\left(-2R_m^l + R_k^k\delta_m^l\right)_{;n} = 0 \qquad (1.10)$$

These show that $R_{22,t}$ and the combination $\left(2R_{11} - r^{-1}e^{2\gamma}R_{22,r}\right)$ are functions of equation (1.7). Due to the cylindrical symmetry, we also have the identity

$$R_{22} + (r^2 e^{-4\phi} - \omega^2)R_{33} + 2\omega\left(\omega R_{33} - R_{23}\right) \equiv 0 \qquad (1.11)$$

These put together imply that R_{11} and R_{22} are determined in terms of the main evolution equations. Hence if ψ, $\psi_{,t}$, ω and $\omega_{,t}$ are prescribed on an initial $t = constant$ slice then the coupled wave equations (1.4 – 1.5) can be used to evolve ψ and ω into the future. γ, which represents the energy of the system, can be obtained by quadrature once the other two metric functions are known.

In the characteristic region we introduce a null coordinate, u. Then the evolution slices in this region are given by a series of hypersurfaces where u takes a constant value. We set

$$u = t - r \qquad (1.12)$$

and thus our line element in terms of our new coordinates (u, r, ϕ, z) becomes

$$ds^2 = -e^{(\gamma - \psi)}(du^2 + 2dudr) + r^2 e^{-2\psi}d\phi^2 + e^{2\phi}(\omega\phi + dz)^2 \qquad (1.13)$$

13

This is equation (16) in [14]. We compute the Ricci tensor components for this metric, and then by taking similar linear combinations of the non–identically zero components as in the Cauchy region, we produce the field equations (18)–(20) :

$$2\psi_{,ur} - \psi_{,rr} + r^{-1}(\psi_{,u} - \psi_{,r}) + \frac{1}{2}r^{-2}e^{4\phi}(\omega_{,r}^2 - 2\omega_{,u}\omega_{,r}) = 0 \tag{1.14}$$

$$2\omega_{,ur} - \omega_{,rr} - r^{-1}(\omega_{,u} - \omega_{,r}) + 4(\psi_{,u}\omega_{,r} + \psi_{,r}\omega_{,u} - \psi_{,r}\omega_{,r}) = 0 \tag{1.15}$$

$$\gamma_{,u} + 2r(\psi_{,u}^2 - \psi_{,u}\psi_{,r}) + \frac{1}{2}r^{-1}e^{4\psi}(\omega_{,u}^2 - \omega_{,u}\omega_{,r}) = 0 \tag{1.16}$$

The corresponding fourth equation in this set should be

$$\gamma_{,r} - r\psi_{,r}^2 - \frac{1}{4}e^{4\psi}r^{-1}\omega_{,r}^2 = 0 \tag{1.17}$$

This equation is incorrectly stated in [14], for taking coordinates (u, r, ϕ, z) we have

$$R_{00} = -2\psi_{,r}^2 + 2r^{-1}\gamma_{,r} - \frac{1}{2}r^{-2}e^{4\psi}\omega_{,r}^2 = 0 \tag{1.18}$$

which, on multiplication by $\frac{1}{2}r$ yields equation (1.17). However, this mistake is not passed through to the computer code itself.

These characteristic field equations cannot be regularised as they stand, and so we need to consider a mechanism that will put them into a regularised form. We shall apply the method of Geroch decomposition. The formalism developed by Geroch, [20] enables us to 'factor out' one direction by means of an appropriate Killing vector, and from thence forwards concentrate fully on the remaining 3–space. This, it turns out, enables us to regularise our field equations. In the case of vacuum cylindrical symmetry, since all the functions are independent of z, it seems desirable to remove this direction and turn our full attention to what remains. Applying the method and general equations of the Appendix of [20], we obtain new (though equivalent) forms for the field equations. The wave equations can then be simultaneously regularised, to remove the singularities at infinity.

Two metrics are conformally related when we can write

$$\bar{g}_{ab} = \Omega^2 g_{ab} \tag{1.19}$$

for some Ω. If we rescale ϕ so that

$$\bar{\phi} = \Omega^s \phi \tag{1.20}$$

14

then for some appropriate value of s we may be able to regularise the field equations. We follow the method of Appendix D in [21] (particularly using (D.14)), and discover that if $s = -1/2$ then the 3-dimensional wave equation is then conformally invariant. This suggests that we can regularise the equations in the characteristic regime by means of a rescaling. Thus the characteristic region can be regularised by introducing a new radial coordinate,

$$x = \frac{1}{r} \tag{1.21}$$

we then set $y = x^{-\frac{1}{2}}$, and following Geroch set $e^{2\psi} = \lambda = 1 + mx^{\frac{1}{2}}$ to obtain new parameters,

$$m = \frac{\lambda - 1}{y} \tag{1.22}$$

and

$$w = yo \tag{1.23}$$

We rescale our former parameters by $x^{-\frac{1}{2}}$ so that

$$\bar{\psi} = x^{-\frac{1}{2}}\psi = y\psi, \tag{1.24}$$

$$\bar{o} = x^{-\frac{1}{2}}o = yo, \tag{1.25}$$

Proceeding in this way we finally obtain compactified, regular forms for the field equations in the characteristic region ((59) – (62))

$$\begin{aligned} M_{,y} &= -\lambda^{-1}(yw)_{,y}W + \frac{1}{4}\lambda^{-1}[-y(m + y^2 m_{,yy} + 3y m_{,y}) \\ &\quad + y^2\lambda^{-1}(m^2 + 2ymm_{,y} - w^2 - 2yww_{,y} + y^2 m_{,y}^2 - y^2 w_{,y}^2)] \end{aligned} \tag{1.26}$$

$$\begin{aligned} W_{,y} &= \lambda^{-1}(yw)_{,y}M + \frac{1}{4}\lambda^{-1}[-y(w + y^2 w_{,yy} + 3y w_{,y}) \\ &\quad + 2y^2\lambda^{-1}(mw + ymw_{,y} + ywm_{,y} + y^2 m_{,y}w_{,y})] \end{aligned} \tag{1.27}$$

$$\gamma_{,y} = -\frac{1}{8}y\lambda^{-2}[m^2 + w^2 + 2y(mm_{,y} + ww_{,y}) + y^2(m_{,y}^2 + w_{,y}^2)] \tag{1.28}$$

$$\gamma_{,u} = -\frac{1}{2}\{M^2 + W^2 + \frac{1}{2}y^2\lambda^{-1}[(m + ym_{,y})M + (w + yw_{,y})W]\} \tag{1.29}$$

where

$$M = \lambda^{-1} m_{,u} \qquad (1.30)$$

$$W = \lambda^{-1} w_{,u} \qquad (1.31)$$

These equations are used directly in the computer coding used in the numerical model.

In the second paper in the on–going series by the Southampton relativity group, [15], the framework of the numerical scheme is developed, and the details of the interface matching method are presented. The line element in the Cauchy region is, as before, given by

$$ds^2 = e^{2(\gamma - \psi)}(-dt^2 + dr^2) + r^2 e^{-2\psi} d\phi^2 + e^{2\psi}(\omega d\phi + dz)^2 \qquad (1.32)$$

We follow the ADM $3+1$ formalism [4] and impose the slicing condition

$$K^\phi_\phi + K^z_z = 0 \qquad (1.33)$$

where K^i_j are the mixed components of the extrinsic curvature, defined shortly. If we set $\chi = \gamma - \psi$ then the lapse function N is defined as

$$N \equiv e^\chi \qquad (1.34)$$

The extrinsic curvature components can be computed from the formulae

$$K_{ij} = -\frac{1}{2N}\frac{\partial h_{ij}}{\partial t} + D_i N_j + D_j N_i \qquad (1.35)$$

Here h_{ij} is the three–metric of the $t = constant$ hypersurfaces, N^i are the components of the shift vector, and D_i is the covariant derivative compatible with the three–metric. The shift–vector has all components set to zero, so that $N^i = 0$. h_{ij} is used to raise and lower spacial indices in the usual way. With coordinates $(x^\alpha) = (r, \phi, z)$, the covariant components of the three–metric are

$$h_{ij} = \begin{pmatrix} e^{2(\psi - \gamma)} & 0 & 0 \\ 0 & r^2 e^{-2\psi} + \omega^2 e^{2\psi} & \omega e^{2\psi} \\ 0 & \omega e^{2\psi} & e^{2\psi} \end{pmatrix} \qquad (1.36)$$

while the contravariant components are given by

$$h^{ij} = \begin{pmatrix} e^{2(\gamma-\psi)} & 0 & 0 \\ 0 & r^{-2}e^{2\psi} & -\omega r^{-2}e^{2\psi} \\ 0 & -\omega r^{-2}e^{2\psi} & e^{-2\psi} + \omega^2 r^{-2}e^{2\psi} \end{pmatrix} \tag{1.37}$$

Since the shift vector components are identically zero in this case, the expression for the extrinsic curvature components simplifies to

$$K_{ij} = -\frac{1}{2N}\frac{\partial h_{ij}}{\partial t} \tag{1.38}$$

Thus the covariant components are given by the following. Note that in the simplified form of (1.38), this tensor is symmetric.

$$K_{rr} = -\frac{1}{2e^{\chi}}\frac{\partial}{\partial t}\left(e^{2\chi}\right) = -\chi_{,t}e^{\chi} \tag{1.39}$$

$$K_{r\phi} = 0 \tag{1.40}$$

$$K_{rz} = 0 \tag{1.41}$$

$$K_{\phi\phi} = -\frac{1}{2e^{\chi}}\frac{\partial}{\partial t}\left(-2r^2\psi_{,t}e^{-2\psi} + 2\omega\omega_{,t}e^{2\psi} + 2\psi_{,t}\omega^2 e^{2\psi}\right)$$
$$= r^2\psi_{,t}e^{-\psi-\gamma} - \omega\omega_{,t}e^{3\psi-\gamma} - \omega^2\psi_{,t}e^{3\psi-\gamma} \tag{1.42}$$

$$K_{\phi z} = -\frac{1}{2e^{\chi}}\frac{\partial}{\partial t}\left(\omega_{,t}e^{2\psi} + 2\omega\psi_{,t}e^{2\psi}\right) = -e^{3\psi-\gamma}\left(\frac{1}{2}\omega_{,t} + \omega\psi_{,t}\right) \tag{1.43}$$

$$K_{zz} = -\frac{1}{2e^{\chi}}\frac{\partial}{\partial t}\left(2\psi_{,t}e^{2\psi}\right) = -\psi_{,t}e^{3\psi-\gamma} \tag{1.44}$$

$$\tag{1.45}$$

Thus the mixed forms are

$$K_r^r = h^{r\alpha}K_{\alpha r} = h^{rr}Krr = -\chi_{,t}e^{-\chi} \tag{1.46}$$

$$K_\phi^r = h^{r\alpha}K_{\alpha\phi} = h^{rr}K_{r\phi} = 0 \tag{1.47}$$

$$K_z^r = h^{r\alpha}K_{\alpha z} = h^{rr}K_{rz} = 0 \tag{1.48}$$

$$K_r^\phi = h^{\phi\alpha}K_{\alpha r} = h^{\phi\phi}K_{\phi r} + h^{\phi z}K_{zr} = 0 \tag{1.49}$$

$$K_\phi^\phi = h^{\phi\alpha}K_{\alpha\phi} = h^{\phi\phi}K_{\phi\phi} + h^{\phi z}K_{z\phi}$$
$$= r^{-2}e^{2\psi}\left(r^2\psi_{,t}e^{-\psi-\gamma} - \omega\omega_{,t}e^{3\psi-\gamma} - \omega^2\psi_{,t}e^{3\psi-\gamma}\right)$$

17

$$+\omega r^{-2}e^{2\psi}\left(\frac{1}{2}\omega_{,t}+\omega\psi_{,t}\right)e^{3\psi-\gamma}$$

$$\Rightarrow K_\phi^\phi = \psi_{,t}e^{\psi-\gamma} - \frac{1}{2}\omega\omega_{,t}e^{5\psi-\gamma} \tag{1.50}$$

$$K_z^\phi = h^{\phi\alpha}K_{\alpha z} = h^{\phi\phi}K_{\phi z} + h^{\phi z}K_{zz}$$

$$= r^{-2}e^{5\psi-\gamma}\left(\omega\psi_{,t} - \frac{1}{2}\omega_{,t} - \omega\psi_{,t}\right) \tag{1.51}$$

$$\Rightarrow K_z^\phi = -\frac{1}{2}r^{-2}\omega_{,t}e^{5\psi-\gamma} \tag{1.52}$$

These are sufficient to determine evolution expressions for the three metric functions ψ, γ (via $\chi = \gamma - \psi$), and ω. Equation (1.46) yields equation (6) of [15], (1.52) can be rearranged into (8) of [15], and (1.52) with (1.50) gives equation (7) of the same.

If L_r^r, L_z^ϕ and $\tilde{L}$ are defined as given in (12) and (13) of [15] then we readily obtain (14)–(17). An error occurs in the statement of the next equation, for from (3)

$$e^{-2\psi}\left[\frac{1}{4}(\omega_{,r})^2e^{4\psi} - r\left(\chi_{,r} + \psi_{,r}\right) + r^2(\psi_{,r})^2\right]$$
$$+ r^2(K_\phi^\phi - \omega K_z^\phi)^2 + r^4e^{-4\psi}(K_z^\phi)^2 = 0 \tag{1.53}$$

then

$$\chi_{,r} = r^{-1}e^{2\psi}\left(\frac{1}{4}e^{2\psi}(\omega_{,r})^2 - re^{-2\psi}\psi_{,r} + r^2e^{-2\psi}(\psi_{,r})^2\right.$$
$$\left.+ r^2\left(\frac{\tilde{L}}{re^\chi}\right)^2 + r^4e^{-4\psi}\left(\frac{L_z^\phi}{r^2e^\chi}\right)^2\right)$$
$$\chi_{,r} = \frac{1}{4r}e^{4\psi}(\omega_{,r})^2 - \psi_{,r} - r(\psi_{,r})^2 + \frac{1}{r}\left[\tilde{L}^2e^{2\psi-2\chi} + (L_z^\phi)^2e^{-2\psi-2\chi}\right] \tag{1.54}$$

The remaining equations of section A follow simply from the earlier ones. Section B restates the main equations of [14].

The interface equations of part III section B were verified with the exception that errors were discovered in (56) & (70). From (55), we have

$$\omega_{,r} = \frac{W}{y\lambda} \tag{1.55}$$

But from the chain rule as in (50),

$$\frac{\partial}{\partial r}f(u,y) = -\frac{\partial f}{\partial u} - \frac{y^3}{2}\frac{\partial f}{\partial y} \tag{1.56}$$

18

Thus, making use of relation (54) of [14],

$$\lambda = 1 + my \tag{1.57}$$

$$\lambda_{,u} = (my)_{,u} = ym_{,u} \tag{1.58}$$

$$\lambda_{,y} = (my)_{,y} \tag{1.59}$$

and from (57) of [14],

$$M = \frac{m_{,u}}{\lambda} \tag{1.60}$$

we obtain

$$
\begin{aligned}
\omega_{,rr} &= -\frac{\partial}{\partial u}\left(\frac{W}{y\lambda}\right) - \frac{y^3}{2}\frac{\partial}{\partial y}\left(\frac{W}{y\lambda}\right) \\
&= -\left(\frac{W_{,u}}{y\lambda} - \frac{W}{y^2\lambda^2}(y\lambda_{,u} + y_{,u}\lambda)\right) - \frac{y^3}{2}\left(\frac{W_{,y}}{y\lambda} - \frac{W}{y^2\lambda^2}(y\lambda_{,y} + y_{,y}\lambda)\right) \\
&= -\frac{W_{,u}}{y\lambda} + \frac{Wm_{,u}}{\lambda^2} - \frac{y^3}{2}\left(\frac{W_{,y}}{y\lambda} - \frac{W}{y^2\lambda} - \frac{W}{y\lambda^2}(my)_{,y}\right) \\
&= -\frac{W_{,u}}{y\lambda} + \frac{W}{\lambda}\left(\frac{m_{,u}}{\lambda}\right) - \frac{y^2}{2\lambda}W_{,y} + \frac{yW}{2\lambda} + \frac{y^2W}{2\lambda^2}(my)_{,y} \tag{1.61}
\end{aligned}
$$

Therefore,

$$\omega_{,rr} = -\frac{W_{,u}}{y\lambda} + \frac{MW}{\lambda} + \frac{1}{2}\frac{yW}{\lambda} + \frac{1}{2}\frac{y^2W}{\lambda^2}(my)_{,y} - \frac{1}{2}\frac{y^2W_{,y}}{\lambda} \tag{1.62}$$

Note that the last term in the published equation (56) is therefore incorrect. Also in 70 there is a surplus factor of 2 on the last term in the first round bracket. The equation should read

$$
\begin{aligned}
w_{,yy} &= 2r^{5/2}e^{4\psi}(8\psi_{,t}\omega_{,r} + 2\omega_{,tr} + 3r^{-1}\omega_{,r} + 8\psi_{,r}\omega_{,r} + 2\omega_{,rr} + r^{-1}\omega_{,t}) \\
&\quad - 8r^{5/2}(L^\phi_{z,t} + L^\phi_{z,r} + r^{-1}L^\phi_z) + 2\int r^{1/2}e^{4\psi}\omega_{,r}\,dt \tag{1.63}
\end{aligned}
$$

For from (69) of [15] we have

$$w_{,y} = 4rL^\phi_z - 2r\lambda^2\omega_{,r} - r^{1/2}w \tag{1.64}$$

$$
\begin{aligned}
w_{,yy} &= \frac{\partial}{\partial y}\left(4rL_z^\phi - 2r\lambda^2\omega_{,r} - r^{1/2}w\right)\\[2mm]
&= -2r^{3/2}\left(\frac{\partial}{\partial r} + \frac{\partial}{\partial t}\right)\left(4rL_z^\phi - 2r\lambda^2\omega_{,r} - r^{1/2}w\right)\\[2mm]
&= -2r^{3/2}\Big(4L_z^\phi + 4rL_{z,r}^\phi - 2e^{4\psi}\omega_r - 8r\psi_{,r}e^{4\psi}\omega_{,r} - 2re^{4\psi}\omega_{,rr}\\
&\quad -\frac{1}{2}r^{-1/2}w - r^{1/2}w_{,r} + 4rL_{z,t}^\phi - 8r\psi_{,t}e^{4\psi}\omega_{,r} - 2re^{4\psi}\omega_{,rt} - r^{1/2}w_{,t}\Big)\\[2mm]
&= -2r^{3/2}\Big(4L_z^\phi + 4rL_{z,r}^\phi + 4rL_{z,t}^\phi - 2e^{4\psi}\omega_r - 8r\psi_{,r}e^{4\psi}\omega_{,r} - 8r\psi_{,t}e^{4\psi}\omega_{,r}\\
&\quad -2re^{4\psi}\omega_{,rr} - 2re^{4\psi}\omega_{,rt} - \frac{1}{2}o - r^{1/2}\left(or^{1/2}\right)_{,r} - r^{1/2}\left(or^{1/2}\right)_{,t}\Big)\\[2mm]
&= -2r^{3/2}\Big(-2re^{4\psi}\omega_{,rr} - 2re^{4\psi}\omega_{,rt} - 8r\psi_{,r}e^{4\psi}\omega_{,r} - 8r\psi_{,t}e^{4\psi}\omega_{,r} - 2e^{4\psi}\omega_r\\
&\quad +4L_z^\phi + 4rL_{z,r}^\phi + 4rL_{z,t}^\phi - \frac{1}{2}o - r^{1/2}\left(r^{1/2}o_{,r} + \frac{1}{2}or^{-1/2}\right) - ro_{,t}\Big) \qquad (1.65)
\end{aligned}
$$

Recall that from (60) we can extract expressions for the derivatives of o with respect to t and r:

$$
o = r^{-1/2}w = \int r^{-1}e^{4\psi}\omega_{,r}\,dt + \int r^{-1}e^{4\psi}\omega_{,t}\,dr \qquad (1.66)
$$

$$
\Rightarrow o_{,r} = r^{-1}e^{4\psi}\omega_{,t} \qquad (1.67)
$$

$$
\Rightarrow o_{,t} = r^{-1}e^{4\psi}\omega_{,r} \qquad (1.68)
$$

If we now use substitute these expressions into (1.65) then we obtain

$$
\begin{aligned}
w_{,yy} &= 2r^{5/2}e^{4\psi}\left(2\omega_{,rr} + 2\omega_{,rt} + 8\psi_{,t}\omega_{,r} + 8\psi_{,r}\omega_{,r} + 2r^{-1}\omega_{,r}\right)\\
&\quad -8r^{5/2}\left(L_{z,r}^\phi + L_{z,t}^\phi + r^{-1}L_z^\phi\right) + 2r^{3/2}o + 2r^{5/2}\left(r^{-1}e^{4\psi}\omega_{,t}\right) + 2r^{5/2}\left(r^{-1}e^{4\psi}\omega_{,t}\right)\\
w_{,yy} &= 2r^{5/2}e^{4\psi}\left(8\psi_{,t}\omega_{,r} + 2\omega_{,rt} + 3r^{-1}\omega_{,t} + 8\psi_{,r}\omega_{,r} + 2\omega_{,rr} + r^{-1}\omega_{,t}\right)\\
&\quad -8r^{5/2}\left(L_{z,t}^\phi + L_{z,r}^\phi + r^{-1}L_z^\phi\right) + 2\int r^{1/2}e^{4\psi}\omega_{,r}dt \qquad (1.69)
\end{aligned}
$$

In the characteristic region, by finite differencing equations (59) & (60) of [14] in the case where $\omega = W = 0$, we obtained (72) of [15] with the exception that the last term in the first square bracket needed to be corrected to

$$
3\mu y_{i+1}\frac{\Delta m_{i+1}}{\Delta y_{i+1}} \qquad (1.70)
$$

Thus the equations derived and developed in both [14] and [15] are verified, with the exception of a few slight discrepancies. We shall find however that these errors are not

critical errors, and that they have not contaminated the numerical scheme developed from them.

1.2   Finite Difference methods

The validity of the equations which form the basis for our scheme has now been established. The next step is to put them into a form compatible with a numerical evolution. We shall illustrate the principles involved in the Cauchy region, although the same methods are applied in the characteristic region.

Firstly we need to set up our grid in the Cauchy region. Since we are concerned with cylindrically symmetric systems, we only need to consider points at various radial distances from the origin. We define a radial axis, starting from the origin where clearly $r = 0$. Here r is the distance of the points from the origin in the xy plane. The distance of the interface from the origin is purely arbitrary, but for numerical convenience we let the interface lie on the infinite cylinder $r = 1$. Thus the Cauchy region can be described by equally spaced points along the radial axis between the values of 0 and 1. In the characteristic region, we have a similar scheme, but the radial coordinate used is y, which runs from 1 at the interface to 0 at future null infinity. Thus on each iteration we calculate the values of each evolution variable at each relevant point along the radial axis. Therefore $\psi, \chi, \tilde{L}, L_z^\phi$ are calculated for $0 \leq r \leq 1$, and m, w, M, W are evaluated for $1 \leq y \leq 0$. The values of these functions can then be determined at any point in the slice by symmetry.

The numbers of grid–points in each of the two regions are specified at the start of each run of the program. If we suppose that the number of grid–points in the Cauchy region is given by n and the corresponding number in the characteristic region is given by n_C then the spacing between adjacent points in each region is respectively

$$dr = \frac{1}{n-1} \tag{1.71}$$

$$dy = \frac{1}{n_C - 1} \tag{1.72}$$

so that

$$r(i) = (i-1)dr \tag{1.73}$$

$$y(j) = 1 - (j-1)dy \tag{1.74}$$

for $1 \leq i \leq n$ and $1 \leq j \leq n_C$.

These points are retained throughout the evolution. However, the value of t in the Cauchy region, and u in the characteristic region, is repeatedly increased by a constant increment in order to produce a series of evolution slices. It is shown in section III, part A of [15] how in order to keep the Cauchy and characteristic slices 'in step', we need to fix the value of Δu to be equal to the time spacing, Δt.

We next introduce the Courant stability condition which is effectively a condition on the ratio of the grid spacing with respect to the time direction against that for the space direction. In order to maintain stability of the evolution, we find that the following condition must be observed:

$$\frac{\Delta t}{\Delta r} \leq 1 \tag{1.75}$$

Thus in the Cauchy region, the distance between time slices must not exceed that between adjacent points in the same time slice. Similarly in the characteristic region

$$\frac{\Delta u}{\Delta y} \leq 1 \tag{1.76}$$

We see therefore that the time that elapses between one time level and the next is very much limited by the grid spacing within each slice. However, by having the grid points closer together on each time–step, there is greater accuracy than on a coarser mesh. A balance must thus be found between the accuracy required and the time for which we wish to evolve our problem.

Having established the grid to be used, we can now address the methods for calculating and evolving the variables. The set–up is described in detail in section C of [15]. We require initial values for the functions ψ and $\tilde{L}$ in the Cauchy region, and m in the characteristic region. We also need the value of M on the interface, i.e. $M(y(1))$. These are computed depending on the option invoked at the commencement of the program. For example, in the case of the comparison with the Weber–Wheeler wave, [22], we have

explicit expressions for the metric functions ψ and γ, whilst ω is zero everywhere. The values of the $\psi(i)$ are thus readily obtained, the values of $\tilde{L}$ are calculated via equation (14) of [15], and m in the characteristic region is found from (37) of [15]. The value of M on the interface follows from (54) of that paper.

Hence the initial values for the evolution variables are set. The next step is to use the evolution equations to produce a succession of evolution slices. We use a centred second–order finite difference scheme known as the leapfrog evolution scheme. This scheme uses information from three successive evolution slices, and therefore three levels of information are stored . The evolution equations are the mechanism by which this information is passed between the adjacent slices. In the Cauchy region these are the equations which describe the time derivatives of the evolution variables, equations (14) – (17) of [15], while in the characteristic region they are the equations giving the u derivatives of the evolution variables, (38) – (39). We also make use of (40) and (41) to calculate the values of M and W out along the slices as y runs from 1 to 0.

The main principles of the finite difference method are now illustrated. If we begin with (14) of [15], viz.

$$\psi_{,t} = \frac{1}{r}\tilde{L} \tag{1.77}$$

then this needs to be transformed into an expression where each function is represented by the function at certain grid–points. The notation which is used is that the value of function f at the ith grid–point on the nth time–slice is written as f_i^n. If we centre our difference scheme at the point r_i^n and apply the scheme to the above equation, we obtain the following. Functions are replaced by their respective values at the central point, and derivatives take standard forms. In the case of a first derivative, the second–order expression is closely related to the definition of a derivative from first principles. We have

$$\psi_{,t}(i) = \frac{\psi_i^{n+1} - \psi_i^{n-1}}{r_i^{n+1} - r_i^{n-1}} \tag{1.78}$$

Note that the distance between the time slices u^{n+1} and u^{n-1} is $\Delta t + \Delta t = 2\Delta t$. Thus (1.77) becomes

$$\frac{\psi_i^{n+1} - \psi_i^{n-1}}{2\Delta t} = \frac{1}{r_i^n}\tilde{L}_i^n \tag{1.79}$$

This is then rearranged to explicitly express the value of ψ on the time–slice u^{n+1} in terms of data from previous time–slices thus:

$$\psi_i^{n+1} = \psi_i^{n-1} + 2\Delta t \frac{\tilde{L}_i^n}{r_i^n} \tag{1.80}$$

Other standard derivatives, centred at r_i^n are given by the following:

$$\psi_{,r}(i) \quad = \quad \frac{\psi_{i+1}^n - \psi_{i-1}^n}{r_{i+1}^n - r_{i-1}^n} \tag{1.81}$$

$$\psi_{,tt}(i) \quad = \quad \frac{\psi_i^{n+1} - 2\psi_i^n + \psi_i^{n-1}}{(r_i^{n+1} - r_i^n)(r_i^n - r_i^{n-1})} \tag{1.82}$$

$$\psi_{,rr}(i) \quad = \quad \frac{\psi_{i+1}^n - 2\psi_i^n + \psi_{i-1}^n}{(r_{i+1}^n - r_i^n)(r_i^n - r_{i-1}^n)} \tag{1.83}$$

and so on. The form that the expressions for the various derivatives take are obviously similar when ψ is replaced by another function, except that wherever a ψ appears above it is to be replaced by the new function as appropriate. Thus for example if we require a finite–differnce expression for $\omega_{,r}$ then by analogy with (1.81) we obtain

$$\omega_{,r}(i) = \frac{\omega_{i+1}^n - \omega_{i-1}^n}{r_{i+1}^n - r_{i-1}^n} \tag{1.84}$$

These principles are applied to all the evolution equations. These then allow the evolution of the information through the grid. The same procedure is followed in the characteristic region for m and w, and a complicated subroutine enables the calculation of the values for M and W, via (40) and (41). Due to the strong coupling of these two equations, they need to be solved in combination, by quadrature.

This thus gives an apparatus for the evolution of the two schemes, one in the Cauchy regime and the other in the characteristic region. However a key aim of this work is to be able to pass information across the interface by which the two regions are joined. This calls for very careful matching of the variables in the two regions, especially with regards to the radial derivatives across the interface. Second–order accuracy can be maintained via the use of ghost points in the characteristic region, and the extension of the Cauchy slices beyond the interface for the initial start–up procedures. This issue is discussed in [15]. However, the principles of the finite difference method as applied to these interface–matching procedures remain as previously described.

24

1.3 Checking the numerical scheme

The final stage in double–checking the work that had been done was to establish that the equations had been correctly encoded. This involved both ensuring that the equations had been accurately put into the finite differenced form, and also that the variables and constants were passed between main program and subroutines in a consistent manner.

The main program takes the following shape:

1) Initial values are set for ψ, ω, $\tilde{L}$ and L_z^ϕ on the Cauchy grid, M on the interface and for m in the characteristic grid.

2) A thick sandwich method is employed as described in III C of [15], to evolve this initial data backwards. Thus there are three slices of initial data as required for a scheme of second–order accuracy.

3) The evolution equations are applied, in conjuction with equations to match the two sets of variables at the interface, to produce a series of evolution slices.

4) The inherent error, in the form of an $l2$ norm is calculated and a graphics output is obtained for each metric function.

In order to check through the computer code, each of these four stages must be examined carefully. For the first point, it is important to ensure that each of the required variables is initialised correctly. A failure to initialise any of the variables required at the set–up stage will lead to the value of that variable at each point being set to zero. The way in which ψ, ω, $\tilde{L}$ and L_z^ϕ are calculated for the initial slice depends upon whether general initial conditions are being used, as described in section IV B of [15], or whether an exact solution is being used, in which case the metric functions are known explicitly and thus these quantities are readily obtained. The initialising routines were thoroughly checked, and found to be correct.

The next stage was to work through the thick sandwich scheme, which applies only in the Cauchy region. The initial data is evolved via an explicit first–order Euler method onto a slice at time $t - \frac{1}{2}\Delta t$, and then this slice in conjunction with the first can generate a slice at time $t - \Delta t$ using the usual leapfrog method. Finally the first slice and that at $t - \Delta t$ produce the last set-up slice at $t - 2\Delta t$. The code was again found to be correct.

The main part of the code which required to be carefully worked through was the

third part listed above. The subroutine calls from main program to subroutines and vice versa showed no discrepancies. The subroutines themselves were rigourously checked, and finally found to match the equations already verified exactly. The interface matching routines were long and complicated, but these were also found to be without error.

Finally the $l2$ norm is defined by

$$l_2 = \frac{1}{N} \sum_{i=1}^{N} \xi_i^2 \tag{1.85}$$

This is calculated on each slice for the non–zero metric functions ψ and γ. Graphics display is via Matt Choptuick's visualisation tool. All this section of the code was found to be satisfactory.

Thus the computer code described in [14] and [15] by the Southampton group was fully checked and verified. The scheme can simulate the general vacuum cylindrically symmetric case, however only the case where $\omega = 0$ had been examined in detail. In the next chapter a solution due to Piran et al. [16] is introduced, which was studied and used to explore the behaviour and performance of the code when the rotational degree of freedom was present.

Chapter 2

Extension to two gravitational degrees of freedom

2.1 The family of exact solutions due to Piran, Safier and Katz

We have described how the computer code developed by Dubal, d'Inverno and Clarke [15] had been subjected to a number of consistency checks, in order to establish its validity as a code to model the evolution of cylindrically symmetric vacuum spacetimes. It had been used to compare the output obtained by numerically evolving a given set of initial conditions with the output from the exact solution due to Weber and Wheeler [22] at the same times. This comparison yielded very encouraging results, with an error of less than 0.1% between the evolved data and the computed values for the specified exact solution, at a resolution of 300 grid–points in each of the Cauchy and characteristic grids.

However, one limitation of this Weber-Wheeler wave was that it constrained one of the three metric functions, ω, to be zero. It was felt that a further step in the investigative process would be to see how the code coped with solutions which included a rotational element, i.e. where ω was non–zero, since this involves passing derivative information across the interface. Fortunately, an exact solution for non–zero ω has been found by Piran, Safier and Katz [16]. In the remainder of this chapter, we shall employ the convention that numerically generated functions are written in lower case, ψ, γ, ω,

while the analytic forms of [16] are written in upper case Ψ, Γ, Ω.

This two-parameter family of solutions is given by the general cylindrically symmetric vacuum line element due to Jordan, Ehlers, Kundt and Kompaneets, namely

$$ds^2 = e^{2(\Gamma - \Psi)}(dT^2 - dR^2) - e^{2\Psi}(dZ + \Omega d\Phi)^2 - e^{-2\Psi}R^2 d\Phi^2 \qquad (2.1)$$

where the three metric functions, Ψ, Γ and Ω are functions of $U = T - R$ and $V = T + R$ and are given as follows:

$$e^{2\Psi} = \frac{\alpha^2(1 - \lambda_u\lambda_v)^2 + (\lambda_v + \lambda_u)^2}{\alpha^2\Xi^2 + (\lambda_v - \lambda_u)^2} \qquad (2.2)$$

$$e^{2\Gamma} = 1 + \frac{(\alpha^2 - 1)(1 - \lambda_u\lambda_v)^2}{(1 + \lambda_u^2)(1 + \lambda_v^2)} \qquad (2.3)$$

$$\Omega = \tilde{a}(\alpha^2 - 1)^{\frac{1}{2}}\left(2[1 + (1 - \alpha^{-2})^{-\frac{1}{2}}] - \frac{\Xi(\lambda_v + \lambda_u)^2}{\lambda_u\lambda_v^{\frac{1}{2}}[\alpha^2(1 - \lambda_u\lambda_v)^2 + (\lambda_v + \lambda_u)^2]}\right) \qquad (2.4)$$

where

$$\lambda_u = \tilde{a}^{-1}[(\tilde{a}^2 + U^2)^{\frac{1}{2}} - U] \qquad (2.5)$$

$$\lambda_v = \tilde{a}^{-1}[(\tilde{a}^2 + V^2)^{\frac{1}{2}} + V] \qquad (2.6)$$

$$\Xi = 1 + \lambda_u\lambda_v + 2[(1 - \alpha^{-2})\lambda_u\lambda_v]^{\frac{1}{2}} \qquad (2.7)$$

The two parameters that govern the solutions are α, which determines the total energy of the waves, and $\tilde{a}$ which acts as a length scale, where $1 \leq \alpha \leq \infty$ and $0 \leq \tilde{a} \leq \infty$. The special case $\alpha = 1$ corresponds to flat space.

We first wanted to check that this was indeed a solution of the vacuum field equations directly, by computing the Ricci tensor and showing it to be identically zero. However the nature of the forms of the metric functions, in particular the existance of nested square roots, meant that a calculation by hand would be very protracted and messy. Rather disappointingly, both the computer algebra packages SHEEP and GRTENSOR were unable to complete the calculation. We were however able to confirm that the solutions were vacuum for particular choices of the parameters α and $\tilde{a}$.

2.1.1 Derivation of the family of exact solutions

Here we shall lay out the method that was used to show indirectly that the exact solution of Piran, Safier and Katz is indeed a solution of Einstein's Vacuum Field Equations.

We begin with the Kerr solution in Boyer–Lindquist coordinates, $(x^a) = (x^0, r, \theta, \phi)$

$$ds^2 = \frac{\Delta}{\rho^2}(dx^0 - a\sin^2\theta d\phi)^2 - \frac{\sin^2\theta}{\rho^2}\left[(r^2 + a^2)d\phi - adx^0\right]^2 - \frac{\rho^2}{\Delta}dr^2 - \rho^2 d\theta^2 \qquad (2.8)$$

where

$$\rho^2 = r^2 + a^2\cos^2\theta \qquad (2.9)$$

$$\Delta = (r - m)^2 + a^2 - m^2 \qquad (2.10)$$

The method consists of considering a sequence of coordinate transformations:

New coordinates 1: $(x^a) = (x^0, \tilde{R}, \theta, \phi)$

where $$r = m + \tilde{R} + \frac{\mu^2}{4\tilde{R}} \qquad \text{and} \qquad \mu^2 = \mathrm{m}^2 - \mathrm{a}^2. \qquad (2.11)$$

Then $$dr = \left(1 - \frac{\mu^2}{4\tilde{R}^2}\right)d\tilde{R} \qquad (2.12)$$

and so

$$ds^2 = \frac{\Delta}{\rho^2}(dx^0 - a\sin^2\theta d\phi)^2 - \frac{\rho^2}{\Delta}\left(1 - \frac{\mu^2}{4\tilde{R}^2}\right)^2 d\tilde{R}^2 - \rho^2 d\theta^2$$
$$- \frac{\sin^2\theta}{\rho^2}\left[\left(\left(m + \tilde{R} + \frac{\mu^2}{4\tilde{R}}\right)^2 + a^2\right)d\phi - adx^0\right]^2 \qquad (2.13)$$

where

$$\rho^2 = \left(m + \tilde{R} + \frac{\mu^2}{4\tilde{R}}\right)^2 + a^2\cos^2\theta, \qquad (2.14)$$

$$\Delta = \left(\tilde{R} + \frac{\mu^2}{4\tilde{R}}\right)^2 + a^2 - m^2. \qquad (2.15)$$

New Coordinates 2: $(x^a) = (x^0, \tilde{\rho}, \tilde{z}, \phi)$

where $$\tilde{\rho} = \tilde{R}\sin\theta, \qquad\qquad \tilde{z} = \tilde{R}\cos\theta, \qquad (2.16)$$

$$\tilde{R} = (\tilde{\rho}^2 + \tilde{z}^2)^{\frac{1}{2}}, \qquad\qquad \theta = arctan(\tilde{\rho}/\tilde{z}). \qquad (2.17)$$

29

Then
$$sin\theta = \frac{\tilde{\rho}}{\tilde{R}} = \frac{\tilde{\rho}}{(\tilde{\rho}^2 + \tilde{z}^2)^{\frac{1}{2}}} \tag{2.18}$$

$$cos\theta = \frac{\tilde{z}}{\tilde{R}} = \frac{\tilde{z}}{(\tilde{\rho}^2 + \tilde{z}^2)^{\frac{1}{2}}} \tag{2.19}$$

$$d\tilde{R} = (\tilde{\rho}d\tilde{\rho} + \tilde{z}d\tilde{z})(\tilde{\rho}^2 + \tilde{z}^2)^{-\frac{1}{2}} \tag{2.20}$$

$$d\theta = \left(\frac{d\tilde{\rho}}{\tilde{z}} - \frac{\tilde{\rho}d\tilde{z}}{\tilde{z}^2}\right)(1 + (\tilde{\rho}/\tilde{z})^2)^{-1} = \frac{\tilde{z}d\tilde{\rho} - \tilde{\rho}d\tilde{z}}{\tilde{\rho}^2 + \tilde{z}^2} \tag{2.21}$$

and so

$$
\begin{aligned}
ds^2 &= \frac{\Delta}{\rho^2}\left(dx^0 - \frac{a\tilde{\rho}^2}{(\tilde{\rho}^2 + \tilde{z}^2)}d\phi\right)^2 - \frac{\rho^2}{\Delta}\left(1 - \frac{\mu^2}{4(\tilde{\rho}^2 + \tilde{z}^2)}\right)^2 \frac{(\tilde{\rho}d\tilde{\rho} + \tilde{z}d\tilde{z})^2}{(\tilde{\rho}^2 + \tilde{z}^2)} \\
&\quad - \frac{\tilde{\rho}^2}{\rho^2(\tilde{\rho}^2 + \tilde{z}^2)}\left[\left(\left(m + (\tilde{\rho}^2 + \tilde{z}^2)^{\frac{1}{2}} + \frac{\mu^2}{4(\tilde{\rho}^2 + \tilde{z}^2)^{\frac{1}{2}}}\right)^2 + a^2\right)d\phi - adx^0\right]^2 \\
&\quad - \frac{\rho^2(\tilde{z}d\tilde{\rho} - \tilde{\rho}d\tilde{z})^2}{(\tilde{\rho}^2 + \tilde{z}^2)^2}
\end{aligned}
\tag{2.22}
$$

where

$$\rho^2 = \left(m + (\tilde{\rho}^2 + \tilde{z}^2)^{\frac{1}{2}} + \frac{\mu^2}{4(\tilde{\rho}^2 + \tilde{z}^2)^{\frac{1}{2}}}\right)^2 + \frac{a^2\tilde{z}^2}{\tilde{\rho}^2 + \tilde{z}^2} \tag{2.23}$$

$$\Delta = \left((\tilde{\rho}^2 + \tilde{z}^2)^{\frac{1}{2}} + \frac{\mu^2}{4(\tilde{\rho}^2 + \tilde{z}^2)^{\frac{1}{2}}}\right)^2 + a^2 - m^2 \tag{2.24}$$

We next apply a trick involving the complex coordinate transformation:

$$x^0 \to iz, \qquad \tilde{z} \to i\tilde{t}, \qquad a \to i\tilde{a}, \qquad \tilde{\rho} \to \tilde{\rho}, \qquad \phi \to \phi, \qquad \mu^2 \to M^2$$

Then

$$
\begin{aligned}
ds^2 &= -\frac{\Delta}{\rho^2}\left(dz - \frac{\tilde{a}\tilde{\rho}^2 d\phi}{(\tilde{\rho}^2 - \tilde{t}^2)}\right)^2 - \frac{\rho^2}{\Delta}\left(1 - \frac{M^2}{4(\tilde{\rho}^2 - \tilde{t}^2)}\right)^2 \frac{(\tilde{\rho}d\tilde{\rho} - \tilde{t}d\tilde{t})^2}{(\tilde{\rho}^2 - \tilde{t}^2)} \\
&\quad - \frac{\tilde{\rho}^2}{\rho^2(\tilde{\rho}^2 - \tilde{t}^2)}\left[\left(\left(m + (\tilde{\rho}^2 - \tilde{t}^2)^{\frac{1}{2}} + \frac{M^2}{4(\tilde{\rho}^2 - \tilde{t}^2)^{\frac{1}{2}}}\right)^2 - \tilde{a}^2\right)d\phi + \tilde{a}dz\right]^2 \\
&\quad + \frac{\rho^2(\tilde{t}d\tilde{\rho} - \tilde{\rho}d\tilde{t})^2}{(\tilde{\rho}^2 - \tilde{t}^2)^2}
\end{aligned}
\tag{2.25}
$$

where
$$\rho^2 = \left(m + (\tilde{\rho}^2 - \tilde{t}^2)^{\frac{1}{2}} + \frac{M^2}{4(\tilde{\rho}^2 - \tilde{t}^2)^{\frac{1}{2}}}\right)^2 + \frac{\tilde{a}^2\tilde{t}^2}{(\tilde{\rho}^2 - \tilde{t}^2)} \tag{2.26}$$

30

$$\Delta = \left((\tilde{\rho}^2 - \tilde{t}^2)^{\frac{1}{2}} + \frac{M^2}{4(\tilde{\rho}^2 - \tilde{t}^2)^{\frac{1}{2}}} \right)^2 - \tilde{a}^2 - m^2$$

$$= \left[(\tilde{\rho}^2 - \tilde{t}^2)^{\frac{1}{2}} + \frac{M^2}{4(\tilde{\rho}^2 - \tilde{t}^2)^{\frac{1}{2}}} \right]^2 - M^2$$

$$= (\tilde{\rho}^2 - \tilde{t}^2) + \frac{M^2}{2} + \frac{M^4}{16(\tilde{\rho}^2 - \tilde{t}^2)} - M^2$$

$$= \left[(\tilde{\rho}^2 - \tilde{t}^2)^{\frac{1}{2}} - \frac{M^2}{4(\tilde{\rho}^2 - \tilde{t}^2)^{\frac{1}{2}}} \right]^2$$

Thus
$$\Delta = \left(\tilde{R} - \frac{M^2}{4\tilde{R}} \right)^2 = \frac{1}{16\tilde{R}^2}[4\tilde{R}^2 - M^2]^2 \tag{2.27}$$

since $\tilde{R}^2 = \tilde{\rho}^2 + \tilde{z}^2 = \tilde{\rho}^2 - \tilde{t}^2$, and so we obtain

$$ds^2 = -\frac{\Delta}{\rho^2} \left(dz - \frac{\tilde{a}\tilde{\rho}^2}{\tilde{R}^2}d\phi \right)^2 - \frac{\tilde{\rho}^2}{\rho^2 \tilde{R}^2} \left[\left(\left(m + \tilde{R} + \frac{M^2}{4\tilde{R}} \right)^2 - \tilde{a}^2 \right) d\phi + \tilde{a}dz \right]^2$$
$$- \frac{\rho^2}{\Delta} \left(1 - \frac{M^2}{4\tilde{R}^2} \right)^2 \frac{1}{\tilde{R}^2}(\tilde{t}d\tilde{t} - \tilde{\rho}d\tilde{\rho})^2 + \frac{\rho^2}{\tilde{R}^4}(\tilde{\rho}d\tilde{t} - \tilde{t}d\tilde{\rho})^2$$

i.e.
$$ds^2 = \left[\frac{\rho^2 \tilde{\rho}^2}{\tilde{R}^4} - \frac{\rho^2 \tilde{t}^2}{\Delta \tilde{R}^2} \left(1 - \frac{M^2}{4\tilde{R}^2} \right)^2 \right] d\tilde{t}^2 + \left[\frac{\rho^2 \tilde{t}^2}{\tilde{R}^4} - \frac{\rho^2 \tilde{\rho}^2}{\Delta \tilde{R}^2} \left(1 - \frac{M^2}{4\tilde{R}^2} \right)^2 \right] d\tilde{\rho}^2$$
$$+ 2 \left[-\frac{\rho^2 \tilde{\rho}\tilde{t}}{\tilde{R}^4} + \frac{\rho^2 \tilde{\rho}\tilde{t}}{\Delta \tilde{R}^2} \left(1 - \frac{M^2}{4\tilde{R}^2} \right)^2 \right] d\tilde{t}d\tilde{\rho} - \left[\frac{\tilde{a}^2 \tilde{\rho}^2}{\rho^2 \tilde{R}^2} + \frac{\Delta}{\rho^2} \right] dz^2$$
$$+ 2 \left[\frac{\Delta \tilde{a}\tilde{\rho}^2}{\rho^2 \tilde{R}^2} - \frac{\tilde{\rho}^2 \tilde{a}}{\rho^2 \tilde{R}^2} \left[\left(m + \tilde{R} + \frac{M^2}{4\tilde{R}} \right)^2 - \tilde{a}^2 \right] \right] dzd\phi$$
$$- \left[\frac{\Delta \tilde{a}^2 \tilde{\rho}^4}{\rho^2 \tilde{R}^4} + \frac{\tilde{\rho}^2}{\rho^2 \tilde{R}^2} \left(\left(m + \tilde{R} + \frac{M^2}{4\tilde{R}} \right)^2 - \tilde{a}^2 \right)^2 \right] d\phi^2 \tag{2.28}$$

Moreover, we find

$$\Delta = \left(\tilde{R} - \frac{M^2}{4\tilde{R}} \right)^2 \tag{2.29}$$

$$\tilde{r} = m + \tilde{R} + \frac{M^2}{4\tilde{R}} \tag{2.30}$$

$$\rho^2 = \left(m + \tilde{R} + \frac{M^2}{4\tilde{R}} \right) + \frac{\tilde{a}^2 \tilde{t}^2}{\tilde{R}^2} \tag{2.31}$$

and so

$$ds^2 = \tilde{g}_{00}d\tilde{t}^2 + 2\tilde{g}_{01}d\tilde{t}d\tilde{\rho} + \tilde{g}_{11}d\tilde{\rho}^2 + \tilde{g}_{22}dz^2 + 2\tilde{g}_{23}dzd\phi + \tilde{g}_{33}d\phi^2 \tag{2.32}$$

where

$$\tilde{g}_{00} = \frac{\rho^2}{16\Delta \tilde{R}^6}\left[16\tilde{\rho}^2\tilde{R}^2\Delta - \tilde{t}^2(4\tilde{R}^2 - M^2)^2\right] \tag{2.33}$$

$$\tilde{g}_{01} = \frac{\rho^2}{16\Delta \tilde{R}^6}\left[-16\tilde{\rho}\tilde{t}\tilde{R}^2\Delta + \tilde{\rho}\tilde{t}(4\tilde{R}^2 - M^2)^2\right] \tag{2.34}$$

$$\tilde{g}_{11} = \frac{\rho^2}{16\Delta \tilde{R}^6}\left[16\tilde{t}^2\tilde{R}^2\Delta - \tilde{\rho}^2(4\tilde{R}^2 - M^2)^2\right] \tag{2.35}$$

$$\tilde{g}_{22} = -\frac{1}{\rho^2\tilde{R}^2}\left[\tilde{a}^2\tilde{\rho}^2 + \tilde{R}^2\Delta\right] \tag{2.36}$$

$$\tilde{g}_{23} = \frac{\tilde{a}\tilde{\rho}^2}{\rho^2\tilde{R}^2}\left[\Delta - \left(\left(m + \tilde{R} + \frac{M^2}{4\tilde{R}}\right)^2 - \tilde{a}^2\right)\right] \tag{2.37}$$

$$\tilde{g}_{33} = -\frac{\tilde{\rho}^2}{\rho^2\tilde{R}^4}\left[\Delta\tilde{a}^2\tilde{\rho}^2 + \tilde{R}^2\left(\left(m + \tilde{R} + \frac{M^2}{4\tilde{R}}\right)^2 - \tilde{a}^2\right)^2\right] \tag{2.38}$$

New Coordinates 3: $(x^a) = (T, R, Z, \Phi)$

where

$$T = \frac{\tilde{a}\tilde{t}}{M}\left(1 + \frac{M^2}{4\tilde{R}^2}\right) = \frac{\tilde{a}\tilde{t}}{M}\left(1 + \frac{M^2}{4(\tilde{\rho}^2 - \tilde{t}^2)}\right) \tag{2.39}$$

$$R = \frac{\tilde{a}\tilde{\rho}}{M}\left(1 - \frac{M^2}{4\tilde{R}^2}\right) = \frac{\tilde{a}\tilde{\rho}}{M}\left(1 - \frac{M^2}{4(\tilde{\rho}^2 - \tilde{t}^2)}\right) \tag{2.40}$$

$$Z = z - 2\frac{m}{\tilde{a}}(m + M)\phi \tag{2.41}$$

$$\Phi = \frac{M}{\tilde{a}}\phi \tag{2.42}$$

New Coordinates 4: $(x^a) = (U, V, Z, \Phi)$

where

$$U = T - R = \frac{\tilde{a}\tilde{t}}{M} + \frac{\tilde{a}\tilde{t}M}{4(\tilde{\rho} - \tilde{t})(\tilde{\rho} + \tilde{t})} - \frac{\tilde{a}\tilde{\rho}}{M} + \frac{\tilde{a}\tilde{\rho}M}{4(\tilde{\rho} - \tilde{t})(\tilde{\rho} + \tilde{t})}$$

$$= \frac{\tilde{a}}{M}(\tilde{t} - \tilde{\rho}) + \frac{\tilde{a}M(\tilde{\rho} + \tilde{t})}{4(\tilde{\rho} - \tilde{t})(\tilde{\rho} + \tilde{t})}$$

$$U = \frac{\tilde{a}}{M}(\tilde{t} - \tilde{\rho}) + \frac{\tilde{a}M}{4(\tilde{\rho} - \tilde{t})} \tag{2.43}$$

$$V = T + R = \frac{\tilde{a}}{M}(\tilde{t} + \tilde{\rho}) - \frac{\tilde{a}M}{4(\tilde{\rho} + \tilde{t})}$$

$$V = \frac{\tilde{a}}{M}(\tilde{\rho} + \tilde{t}) - \frac{\tilde{a}M}{4(\tilde{\rho} + \tilde{t})} \tag{2.44}$$

$$Z = z - 2\frac{m}{\tilde{a}}(m + M)\phi \tag{2.45}$$

$$\Phi = \frac{M}{\tilde{a}}\phi \tag{2.46}$$

Letting $\tilde{v} = \tilde{\rho} + \tilde{t}, \quad \tilde{u} = \tilde{\rho} - \tilde{t}$ then

$$U = -\frac{\tilde{a}\tilde{u}}{M} + \frac{\tilde{a}M}{4\tilde{u}} \tag{2.47}$$

$$V = \frac{\tilde{a}\tilde{v}}{M} - \frac{\tilde{a}M}{4\tilde{v}} \tag{2.48}$$

Multiplying (2.47) by $-\dfrac{\tilde{u}M}{\tilde{a}}$ we obtain

$$\tilde{u}^2 + \left(\frac{MU}{\tilde{a}}\right)\tilde{u} - \frac{M^2}{4} = 0 \tag{2.49}$$

$$\Rightarrow \qquad\qquad \tilde{u} = \frac{1}{2}\left[-\frac{MU}{\tilde{a}} \pm \sqrt{\frac{M^2U^2}{\tilde{a}^2} + M^2}\right]$$

i.e.

$$\tilde{u} = \frac{M}{2\tilde{a}}\left[-U \pm \sqrt{U^2 + \tilde{a}^2}\right] \tag{2.50}$$

Similarly,

$$\tilde{v} = \frac{M}{2\tilde{a}}\left[V \pm \sqrt{V^2 + \tilde{a}^2}\right] \tag{2.51}$$

Taking positive square roots, so that $\tilde{u} > 0$ and $\tilde{v} > 0$, we obtain

$$\tilde{u} = \tilde{\rho} - \tilde{t} = \frac{M}{2\tilde{a}}\left[\sqrt{\tilde{a}^2 + U^2} - U\right] \tag{2.52}$$

$$\tilde{v} = \tilde{\rho} + \tilde{t} = \frac{M}{2\tilde{a}}\left[\sqrt{\tilde{a}^2 + V^2} + V\right] \tag{2.53}$$

In these coordinates, the metric tensor takes the form,

$$ds^2 = -e^{2\Gamma - 2\Psi}dUdV + e^{2\Psi}dZ^2 + 2e^{2\Psi}\Omega dZd\Phi + (e^{2\Phi}\Omega^2 + e^{2\Psi}R^2)d\Phi^2 \qquad (2.54)$$

i.e.

$$ds^2 = 2g_{01}dx^0 dx^1 + g_{22}(dx^2)^2 + 2g_{23}dx^2 dx^3 + g_{33}(dx^3)^2 \qquad (2.55)$$

where

$$g_{01} = -\frac{1}{2}e^{2\Gamma - 2\Psi} \qquad (2.56)$$

$$g_{22} = e^{2\Psi} \qquad (2.57)$$

$$g_{23} = \Omega e^{2\Psi} \qquad (2.58)$$

$$g_{33} = \Omega^2 e^{2\Psi} + \frac{1}{4}e^{-2\Psi}(V - U)^2 \qquad (2.59)$$

Change of Coordinates : $(\tilde{x}^a) = (\tilde{x}^0, \tilde{x}^1, \tilde{x}^2, \tilde{x}^3) = (\tilde{t}, \tilde{\rho}, z, \phi)$

$$U = \frac{\tilde{a}}{M}(\tilde{t} - \tilde{\rho}) - \frac{\tilde{a}M}{4(\tilde{t} - \tilde{\rho})} \qquad (2.60)$$

$$V = \frac{\tilde{a}}{M}(\tilde{t} + \tilde{\rho}) - \frac{\tilde{a}M}{4(\tilde{t} + \tilde{\rho})} \qquad (2.61)$$

$$Z = z - \frac{2m}{\tilde{a}}(m + M)\phi \qquad (2.62)$$

$$\Phi = \frac{M}{\tilde{a}}\phi \qquad (2.63)$$

where

$$M = (m^2 + \tilde{a}^2)^{\frac{1}{2}} \qquad (2.64)$$

34

Jacobean Matrix, $\left(\dfrac{\partial x^a}{\partial \tilde{x}^b}\right)$

This has seven non–zero components, namely

$$\frac{\partial U}{\partial \tilde{t}} = \frac{\tilde{a}}{M} + \frac{\tilde{a}M}{4(\tilde{t} - \tilde{\rho})^2} \tag{2.65}$$

$$\frac{\partial U}{\partial \tilde{\rho}} = -\left(\frac{\tilde{a}}{M} + \frac{\tilde{a}M}{4(\tilde{t} - \tilde{\rho})^2}\right) \tag{2.66}$$

$$\frac{\partial V}{\partial \tilde{t}} = \frac{\tilde{a}}{M} + \frac{\tilde{a}M}{4(\tilde{t} + \tilde{\rho})^2} \tag{2.67}$$

$$\frac{\partial V}{\partial \tilde{\rho}} = \frac{\tilde{a}}{M} + \frac{\tilde{a}M}{4(\tilde{t} + \tilde{\rho})^2} \tag{2.68}$$

$$\frac{\partial Z}{\partial z} = 1 \tag{2.69}$$

$$\frac{\partial Z}{\partial \phi} = -\frac{2m}{\tilde{a}}(m + M) \tag{2.70}$$

$$\frac{\partial \Phi}{\partial \phi} = \frac{M}{\tilde{a}} \tag{2.71}$$

We now perform a transformation of the metric, using the transformation relationship

$$\tilde{g}_{ab} = \frac{\partial x^c}{\partial \tilde{x}^a} \frac{\partial x^d}{\partial \tilde{x}^b} g_{cd} \tag{2.72}$$

The non–zero components of the original metric here are g_{01}, g_{22}, g_{23} and g_{33}, and the new metric components we obtain via this transformation are

$$\begin{aligned}
\tilde{g}_{00} &= \frac{\partial x^c}{\partial \tilde{t}} \frac{\partial x^d}{\partial \tilde{t}} g_{cd} \\
&= \left(\frac{\partial U}{\partial \tilde{t}}\right)^2 g_{00} + 2\left(\frac{\partial U}{\partial \tilde{t}} \frac{\partial V}{\partial \tilde{t}}\right) g_{01} + \left(\frac{\partial V}{\partial \tilde{t}}\right)^2 g_{11} \\
&= 0 + \frac{2}{2}\left(\frac{\tilde{a}}{M} + \frac{\tilde{a}M}{4(\tilde{t} - \tilde{\rho})^2}\right)\left(\frac{\tilde{a}}{M} + \frac{\tilde{a}M}{4(\tilde{t} + \tilde{\rho})^2}\right)e^{2\Gamma - 2\Psi} + 0
\end{aligned}$$

i.e. $$\tilde{g}_{00} = \left(\frac{\tilde{a}}{M} + \frac{\tilde{a}M}{4(\tilde{t} - \tilde{\rho})^2}\right)\left(\frac{\tilde{a}}{M} + \frac{\tilde{a}M}{4(\tilde{t} + \tilde{\rho})^2}\right)e^{2\Gamma - 2\Psi} \tag{2.73}$$

$$\tilde{g}_{01} = \frac{\partial x^c}{\partial \tilde{t}} \frac{\partial x^d}{\partial \tilde{\rho}} g_{cd}$$

$$= \left(\frac{\partial U}{\partial \tilde{t}}\frac{\partial U}{\partial \tilde{\rho}}\right)g_{00} + \left(\frac{\partial U}{\partial \tilde{t}}\frac{\partial V}{\partial \tilde{\rho}}\right)g_{01} + \left(\frac{\partial U}{\partial \tilde{\rho}}\frac{\partial V}{\partial \tilde{t}}\right)g_{10} + \left(\frac{\partial V}{\partial \tilde{t}}\frac{\partial V}{\partial \tilde{\rho}}\right)g_{11}$$

i.e. $\quad \tilde{g}_{01} = 0 + \left(\dfrac{\partial U}{\partial \tilde{t}}\dfrac{\partial V}{\partial \tilde{\rho}}\right)g_{01} + \left(\dfrac{\partial U}{\partial \tilde{\rho}}\dfrac{\partial V}{\partial \tilde{t}}\right)g_{10} + 0$ $\qquad$ (2.74)

But from (2.65 – 2.68), $V_{,\tilde{t}} = V_{,\tilde{\rho}}$ and $U_{,\tilde{\rho}} = -U_{,\tilde{t}}$, while the metric tensor is symmetric, so that $g_{01} = g_{10}$.

Thus

$$\tilde{g}_{01} = \left[\frac{\partial U}{\partial \tilde{t}}\frac{\partial V}{\partial \tilde{\rho}} + -\frac{\partial U}{\partial \tilde{t}}\frac{\partial V}{\partial \tilde{\rho}}\right]g_{01} = 0 \qquad (2.75)$$

$$\tilde{g}_{11} = 2\left(\frac{\partial U}{\partial \tilde{\rho}}\frac{\partial V}{\partial \tilde{\rho}}\right)g_{01} = \left(\frac{\tilde{a}}{M} + \frac{\tilde{a}M}{4(\tilde{t}-\tilde{\rho})^2}\right)\left(\frac{\tilde{a}}{M} + \frac{\tilde{a}M}{4(\tilde{t}+\tilde{\rho})^2}\right)e^{2\Gamma - 2\Psi} \qquad (2.76)$$

$$\tilde{g}_{22} = g_{22} = e^{2\Psi} \qquad (2.77)$$

$$\tilde{g}_{23} = \frac{\partial Z}{\partial \phi}g_{22} + \frac{\partial \Phi}{\partial \phi}g_{23} = -\frac{2m}{\tilde{a}}(m+M)e^{2\Psi} + \frac{M}{\tilde{a}}\Omega e^{2\Psi} \qquad (2.78)$$

$$\tilde{g}_{33} = \left(\frac{\partial Z}{\partial \phi}\right)^2 g_{22} + 2\left(\frac{\partial z}{\partial \phi}\frac{\partial \Phi}{\partial \phi}\right)g_{23} + \left(\frac{\partial \Phi}{\partial \phi}\right)^2 g_{33}$$

$$= \frac{4m^2}{\tilde{a}^2}(m+M)^2 e^{2\Psi} - \frac{4mM(m+M)}{\tilde{a}^2}\Omega e^{2\Psi} + \frac{M^2}{\tilde{a}^2}\Omega^2 e^{2\Psi} + \frac{M^2}{4\tilde{a}^2}e^{-2\Psi}(V-U)^2$$

$$\tilde{g}_{33} = \frac{4me^{2\Psi}}{\tilde{a}^2}(m+M)\left(m^2 + mM - M\Omega\right) + \frac{M^2}{\tilde{a}^2}\Omega^2 e^{2\Psi} + \frac{M^2}{4\tilde{a}^2}e^{-2\Psi}(V-U) \qquad (2.79)$$

Defining $\alpha = \dfrac{M}{\tilde{a}}$ then

$$\alpha^2 - 1 = \frac{M^2}{\tilde{a}^2} - 1 = \frac{M^2 - \tilde{a}^2}{\tilde{a}^2} = \frac{m^2 + \tilde{a}^2 - \tilde{a}^2}{\tilde{a}^2} = \frac{m^2}{\tilde{a}^2} \qquad (2.80)$$

$$1 - \alpha^{-2} = 1 - \frac{\tilde{a}^2}{M^2} = \frac{m^2 + \tilde{a}^2 - \tilde{a}^2}{M^2} = \frac{m^2}{M^2} \qquad (2.81)$$

We also require the following side relations:

$$\tilde{\rho} - \tilde{t} = \frac{M}{2\tilde{a}}[(\tilde{a}^2 + U^2)^{\frac{1}{2}} - U] = \frac{M}{2}\lambda_u \qquad (2.82)$$

$$\tilde{\rho} + \tilde{t} = \frac{M}{2\tilde{a}}[(\tilde{a}^2 + V^2)^{\frac{1}{2}} + V] = \frac{M}{2}\lambda_v \tag{2.83}$$

$$\tilde{\rho} = \frac{M}{4}(\lambda_v + \lambda_u) \tag{2.84}$$

$$\tilde{t} = \frac{M}{4}(\lambda_v - \lambda_u) \tag{2.85}$$

$$\tilde{R}^2 = \tilde{\rho}^2 - \tilde{t}^2 = \frac{1}{4}M^2\lambda_u\lambda_v \tag{2.86}$$

$$\tilde{R} = \frac{M}{2}\lambda_u^{1/2}\lambda_v^{1/2} \tag{2.87}$$

$$
\begin{aligned}
\tilde{r} &= \left(m + \tilde{R} + \frac{M^2}{4\tilde{R}}\right) \\
&= \frac{4m\tilde{R} + 4\tilde{R}^2 + M^2}{4\tilde{R}} \\
&= \frac{2mM\lambda_u^{1/2}\lambda_v^{1/2} + M^2\lambda_u\lambda_v + M^2}{2M\lambda_u^{1/2}\lambda_v^{1/2}} \\
&= \frac{M\left(1 + \lambda_u\lambda_v + 2\lambda_u^{1/2}\lambda_v^{1/2}m/M\right)}{2\lambda_u^{1/2}\lambda_v^{1/2}} \\
&= \frac{M\left(1 + \lambda_u\lambda_v + 2\lambda_u^{1/2}\lambda_v^{1/2}\sqrt{1-\alpha^{-2}}\right)}{2\lambda_u^{1/2}\lambda_v^{1/2}}
\end{aligned}
$$

i.e.
$$\tilde{r} = \frac{M\Xi}{2\lambda_u^{1/2}\lambda_v^{1/2}} \tag{2.88}$$

$$
\begin{aligned}
\Delta &= \left(\tilde{R} - \frac{M^2}{4\tilde{R}}\right)^2 = \tilde{R}^2 - \frac{M^2}{2} + \frac{M^4}{16\tilde{R}^2} \\
&= \frac{M^2}{4}\lambda_u\lambda_v - \frac{M^2}{2} + \frac{M^2}{4\lambda_u\lambda_v} \\
\Delta &= \frac{M^2}{4\lambda_u\lambda_v}(1 - \lambda_u\lambda_v)^2
\end{aligned}
\tag{2.89}
$$

$$\rho^2 = \left(m + \tilde{R} + \frac{M^2}{4\tilde{R}}\right)^2 + \frac{\tilde{a}^2\tilde{t}^2}{\tilde{R}^2}$$

$$= \frac{M^2 \Xi^2}{4\lambda_u \lambda_v} + \frac{\tilde{a}^2 M^2 (\lambda_v - \lambda_u)^2/16}{M^2 \lambda_u \lambda_v/4}$$

$$= \frac{M^2}{4\lambda_u \lambda_v} \Xi^2 + \frac{\tilde{a}^2 (\lambda_v - \lambda_u)^2}{4\lambda_u \lambda_v}$$

$$= \frac{\tilde{a}^2}{4\lambda_u \lambda_v} \left[\left(\frac{M}{\tilde{a}} \right)^2 \Xi^2 + (\lambda_v - \lambda_u)^2 \right]$$

i.e. $$\rho^2 = \frac{\tilde{a}^2}{4\lambda_u \lambda_v} \left[\alpha^2 \Xi^2 + (\lambda_v - \lambda_u)^2 \right] \qquad (2.90)$$

where

$$\Xi = 1 + \lambda_u \lambda_v + 2[(1 - \alpha^{-2})\lambda_u \lambda_v]^{1/2} \qquad (2.91)$$

Derivation of expressions for Ψ, Ω and Γ.

From equation(2.36),

$$e^{2\Psi} = -\tilde{g}_{22} = \frac{\tilde{a}^2 \tilde{\rho}^2 + \tilde{R}^2 \Delta}{\rho^2 \tilde{R}^2} \qquad (2.92)$$

Now,

$$\tilde{a}^2 \tilde{\rho}^2 + \tilde{R}^2 \Delta = \frac{\tilde{a}^2 M^2}{16} (\lambda_u + \lambda_v)^2 + \frac{M^4}{16} (1 - \lambda_u \lambda_v)^2 \qquad (2.93)$$

i.e.

$$\tilde{a}^2 \tilde{\rho}^2 + \tilde{R}^2 \Delta = \frac{\tilde{a}^2 M^2}{16} \left[(\lambda_u + \lambda_v)^2 + \alpha^2 (1 - \lambda_u \lambda_v)^2 \right]. \qquad (2.94)$$

Also,

$$\rho^2 \tilde{R}^2 = \frac{\tilde{a}^2 M^2}{16} [\alpha^2 \Xi^2 + (\lambda_v - \lambda_u)^2] \qquad (2.95)$$

so

$$e^{2\Psi} = \frac{\alpha^2 (1 - \lambda_u \lambda_v)^2 + (\lambda_u + \lambda_v)^2}{[\alpha^2 \Xi^2 + (\lambda_v - \lambda_u)^2]}. \qquad (2.96)$$

From (2.37),

$$\tilde{g}_{23} = \frac{\tilde{a} \tilde{\rho}^2}{\rho^2 \tilde{R}^2} \left[\Delta - \left(\left(m + \tilde{R} + \frac{M^2}{4\tilde{R}} \right)^2 - \tilde{a}^2 \right) \right]$$

$$= \frac{\tilde{a} \tilde{\rho}^2}{\rho^2 \tilde{R}^2} \left[\tilde{R}^2 - \frac{M^2}{2} + \frac{M^4}{16\tilde{R}^2} - \left(m^2 + \tilde{R}^2 + \frac{M^4}{16\tilde{R}^2} + 2m\tilde{R} + \frac{mM^2}{2\tilde{R}} + \frac{M^2}{2} \right) + \tilde{a}^2 \right]$$

$$= \frac{\tilde{a} \tilde{\rho}^2}{\rho^2 \tilde{R}^2} \left[\tilde{a}^2 - m^2 - M^2 - 2m\tilde{R} - \frac{mM^2}{2\tilde{R}} \right] = - \frac{2m\tilde{a} \tilde{\rho}^2}{\rho^2 \tilde{R}^2} \left[m + \tilde{R} + \frac{M^2}{4\tilde{R}} \right]$$

$$\tilde{g}_{23} = - \frac{2m\tilde{a} \tilde{\rho}^2 \tilde{r}}{\rho^2 \tilde{R}^2} \qquad (2.97)$$

Also from (2.78),

$$\tilde{g}_{23} = \frac{M}{\tilde{a}}\Omega e^{2\Psi} - \frac{2m}{\tilde{a}}(m + M)e^{2\Psi} \tag{2.98}$$

Hence,

$$\frac{M}{\tilde{a}}\Omega e^{2\Psi} - \frac{2m}{\tilde{a}}(m + M)e^{2\Psi} = -\frac{2m\tilde{a}\tilde{\rho}^2\tilde{r}}{\rho^2\tilde{R}^2} \tag{2.99}$$

thus

$$
\begin{aligned}
\Omega &= \frac{2m}{M}(m + M) - \frac{2m\tilde{a}^2\tilde{\rho}^2\tilde{r}}{M\,\tilde{R}^2\,\rho^2}\frac{\tilde{R}^2\,\rho^2}{(\tilde{a}^2\rho^2 + \tilde{R}^2\Delta)} \\
&= 2\tilde{a}\left(\frac{m}{\tilde{a}}\right)\left(1 + \frac{m}{M}\right) - \frac{2m\tilde{a}^2\left(M^2(\lambda_u + \lambda_v)^2/16\right)\left(M\Xi\lambda_u^{-1/2}\lambda_v^{-1/2}/2\right)}{M\left(\tilde{a}^2 M^2[\alpha^2(1 - \lambda_u\lambda_v)^2 + (\lambda_u + \lambda_v)^2]/16\right)} \\
&= 2\tilde{a}\left(\frac{m}{\tilde{a}}\right)\left(1 + \frac{m}{M}\right) - \frac{\frac{1}{16}\,M^3\,\tilde{a}^2\,m\Xi(\lambda_u + \lambda_v)^2\lambda_u^{-1/2}\lambda_v^{-1/2}}{\frac{1}{16}\,M^3\,\tilde{a}^2[\alpha^2(1 - \lambda_u\lambda_v)^2 + (\lambda_v + \lambda_u)^2]} \\
&= 2\tilde{a}\left(\frac{m}{\tilde{a}}\right)\left(1 + \frac{m}{M}\right) - \tilde{a}\left(\frac{m}{\tilde{a}}\right)\frac{\Xi(\lambda_u + \lambda_v)^2(\lambda_u\lambda_v)^{-1/2}}{[\alpha^2(1 - \lambda_u\lambda_v)^2 + (\lambda_v + \lambda_u)^2]}
\end{aligned}
\tag{2.100}
$$

so

$$
\begin{aligned}
\Omega = \tilde{a}(\alpha^2 - 1)^{1/2}\Big\{ &2[1 + (1 - \alpha^{-2})^{1/2}] - \Xi(\lambda_u\lambda_v)^{-1/2}(\lambda_u + \lambda_v)^2 \\
&\times[\alpha^2(1 - \lambda_u\lambda_v)^2 + (\lambda_v + \lambda_u)^2]^{-1}\Big\}
\end{aligned}
\tag{2.101}
$$

$$
\begin{aligned}
e^{2\Gamma} &= e^{2\Psi}e^{2\Gamma - 2\Psi} \\[2mm]
&= (-g_{22})(2g_{01}) \\
&= (-g_{22})\left(\tilde{g}_{00}/\left(\frac{\partial U}{\partial\tilde{t}}\frac{\partial V}{\partial\tilde{t}}\right)\right) \\
&= \frac{\rho^2}{16\Delta\tilde{R}^6}\left(16\Delta\tilde{\rho}^2\tilde{R}^2 - \tilde{t}^2(4\tilde{R}^2 - M^2)^2\right)\left(\frac{[\tilde{a}^2\rho^2 + \tilde{R}^2\Delta]}{\tilde{R}^2\rho^2}\right) \\
&\quad \times\left[\frac{\tilde{a}}{M}\left(1 + \frac{M^2}{4(\tilde{t} - \tilde{\rho})^2}\right)\frac{\tilde{a}}{M}\left(1 + \frac{M^2}{4(\tilde{t} + \tilde{\rho})^2}\right)\right]^{-1} \\[3mm]
&= \frac{[16\Delta\tilde{\rho}^2\tilde{R}^2 - \tilde{t}^2(4\tilde{R}^2 - M^2)^2][\tilde{a}^2\rho^2 + \tilde{R}^2\Delta]}{16\Delta\tilde{R}^8\tilde{a}^2 M^{-2}\left(1 + 1/\lambda_u^2\right)\left(1 + 1/\lambda_v^2\right)}
\end{aligned}
$$

i.e.

$$e^{2\Gamma} = \frac{n}{d}, \qquad \text{say.} \tag{2.102}$$

39

Now,

$$
\begin{aligned}
16\Delta\tilde{\rho}^2\tilde{R}^2 - \tilde{t}^2(4\tilde{R}^2 - M^2)^2 &= \frac{16M^2}{4\lambda_u\lambda_v}(1 - \lambda_u\lambda_v)^2\frac{M^2}{16}(\lambda_u + \lambda_v)^2\frac{M^2}{4}\lambda_u\lambda_v \\
&\quad - \frac{M^2}{16}(\lambda_v - \lambda_u)^2(M^2\lambda_u\lambda_v - M^2)^2 \\
&= \frac{M^6}{16}(1 - \lambda_u\lambda_v)^2[(\lambda_v + \lambda_u)^2 - (\lambda_v - \lambda_u)^2] \\
&= \frac{M^6}{16}(1 - \lambda_u\lambda_v)^2 \cdot 4\lambda_u\lambda_v
\end{aligned}
$$

i.e.
$$
16\Delta\tilde{\rho}^2\tilde{R}^2 - \tilde{t}^2(4\tilde{R}^2 - M^2)^2 = \frac{M^6\lambda_u\lambda_v(1 - \lambda_u\lambda_v)^2}{4} \tag{2.103}
$$

Then, from (2.94) and (2.103),

$$
n = \frac{\tilde{a}^2 M^8}{64}\lambda_u\lambda_v(1 - \lambda_u\lambda_v)^2[\alpha^2((1 - \lambda_u\lambda_v)^2 + (\lambda_u + \lambda_v)^2] \tag{2.104}
$$

$$
\begin{aligned}
d &= 16\Delta\tilde{R}^8\tilde{a}^2 M^{-2}\left(1 + \frac{1}{\lambda_u^2}\right)\left(1 + \frac{1}{\lambda_v^2}\right) \\
&= 16\frac{M^2}{4\lambda_u\lambda_v}(1 - \lambda_u\lambda_v)^2\lambda_u^4\lambda_v^4\frac{M^8}{256}\frac{\tilde{a}^2}{M^2}\frac{(1 + \lambda_u^2)(1 + \lambda_v^2)}{\lambda_u^2\lambda_v^2} \\
d &= \frac{\tilde{a}^2 M^8}{64}\lambda_u\lambda_v(1 - \lambda_u\lambda_v)^2(1 + \lambda_u^2)(1 + \lambda_v^2) \tag{2.105}
\end{aligned}
$$

Thus

$$
\begin{aligned}
e^{2\Gamma} &= \frac{n}{d} \tag{2.106} \\
&= \frac{[\alpha^2((1 - \lambda_u\lambda_v)^2 + (\lambda_u + \lambda_v)^2]}{(1 + \lambda_u^2)(1 + \lambda_v^2)} \tag{2.107} \\
&= \frac{\lambda_u^2 + 2\lambda_u\lambda_v + \lambda_v^2 + \alpha^2(1 - 2\lambda_u\lambda_v + \lambda_u^2\lambda_v^2)}{(1 + \lambda_u^2)(1 + \lambda_v^2)} \tag{2.108} \\
&= \frac{1 + \lambda_u^2 + \lambda_v^2 + \lambda_u^2\lambda_v^2 - 1 - \lambda_u^2\lambda_v^2 + 2\lambda_u\lambda_v + \alpha^2(1 - 2\lambda_u\lambda_v + \lambda_u^2\lambda_v^2)}{(1 + \lambda_u^2)(1 + \lambda_v^2)} \tag{2.109}
\end{aligned}
$$

$$
e^{2\Gamma} = \frac{(1 + \lambda_u^2)(1 + \lambda_v^2) + (\alpha^2 - 1)(1 - 2\lambda_u\lambda_v + \lambda_u^2\lambda_v^2)}{(1 + \lambda_u^2)(1 + \lambda_v^2)} \tag{2.110}
$$

and so finally,

$$
e^{2\Gamma} = 1 + (\alpha^2 - 1)(1 - \lambda_u\lambda_v)^2/[(1 + \lambda_u^2)(1 + \lambda_v^2)] \tag{2.111}
$$

We have therefore verified the forms for the metric functions Ψ, Γ and Ω as given by Piran, Safier and Katz in [16].

40

2.2 Derivation of the evolution variables

In order to initiate and evolve a numerical scheme, the theoretical framework must be put into the correct form for this purpose. The evolution is divided into two regions, each having different evolution variables which are meshed together across the interface. The interior region where $|r| \leq 1$ is known as the Cauchy region, and here the traditional '3+1' approach is used. For $|r| \geq 1$ null hypersurfaces are used for a sequence of successive values of the null coordinate $u = t - r$. The derivations of the forms of the evolution variables in each of these regions, and the corresponding evolution equations needed to sustain the evolution are given in the following sections.

2.2.1 The metric functions in the Cauchy region

The computer code requires certain specific quantities to be calculated and then evolved. In the case of our code, in the Cauchy region we require ω, ψ, $\tilde{L}$ and L_z^ϕ. We have explicit expressions for ω and ψ, so computing their values at each grid-point on the initial Cauchy slice merely involves substituting in the value chosen for the initial time, and the value of our radial parameter, r, at each point. However, we will need to determine the values for $\tilde{L}$ and L_z^ϕ in terms of the Piran metric expressions.

We have, via the evolution equations of [14] expressions for these variables in terms of Φ, Γ and Ω, and their derivatives. Explicitly, for our initial values for $\tilde{L}$ and L_z^ϕ we shall need to use

$$\psi_{,t} = \frac{1}{r}\tilde{L} \tag{2.112}$$

and

$$\omega_{,t} = -2e^{-4\psi}L_z^\phi \tag{2.113}$$

We shall therefore require the time derivatives of the metric functions Ψ and Ω. In order to derive these, we shall also require the time derivatives of the 'building block' functions, λ_u, λ_v and Ξ.

$$\lambda_u = \tilde{a}^{-1}[(\tilde{a}^2 + U^2)^{1/2} - U] \tag{2.114}$$

$$\lambda_u = \tilde{a}^{-1}[(\tilde{a}^2 + (t-r)^2)^{1/2} - (t-r)] \tag{2.115}$$

$$\lambda_{u,t} = \tilde{a}^{-1}\left(\frac{1}{2}(\tilde{a}^2 + (t-r)^2)^{-1/2}(2(t-r)) - 1\right) \tag{2.116}$$

$$\lambda_{u,t} = \tilde{a}^{-1}\left(\frac{U}{(\tilde{a}^2 + U^2)^{1/2}} - 1\right) \tag{2.117}$$

$$\lambda_v = \tilde{a}^{-1}[(\tilde{a}^2 + V^2)^{1/2} + V] \tag{2.118}$$

$$\lambda_v = \tilde{a}^{-1}[(\tilde{a}^2 + (t+r)^2)^{1/2} + (t+r)] \tag{2.119}$$

$$\lambda_{v,t} = \tilde{a}^{-1}\left(\frac{1}{2}(\tilde{a}^2 + (t+r)^2)^{-1/2}(2(t+r)) + 1\right) \tag{2.120}$$

$$\lambda_{v,t} = \tilde{a}^{-1}\left(\frac{V}{(\tilde{a}^2 + V^2)^{1/2}} + 1\right) \tag{2.121}$$

$$\Xi = 1 + \lambda_v\lambda_u + 2[(1 - \alpha^{-2})\lambda_v\lambda_u]^{1/2} \tag{2.122}$$

$$\Xi_{,t} = \lambda_u\lambda_{v,t} + \lambda_{u,t}\lambda_v + 2\sqrt{1 - \alpha^{-2}}\left(\frac{1}{2}(\lambda_u\lambda_{v,t} + \lambda_{u,t}\lambda_v)(\lambda_u\lambda_v)^{-1/2}\right) \tag{2.123}$$

$$\Xi_{,t} = \lambda_u\lambda_{v,t} + \lambda_{u,t}\lambda_v + \sqrt{1 - \alpha^{-2}}\frac{\lambda_u\lambda_{v,t} + \lambda_{u,t}\lambda_v}{(\lambda_u\lambda_v)^{1/2}} \tag{2.124}$$

$$\Xi_{,t} = \left(1 + \sqrt{\frac{1 - \alpha^{-2}}{\lambda_u\lambda_v}}\right)(\lambda_u\lambda_{v,t} + \lambda_{u,t}\lambda_v) \tag{2.125}$$

Similarly, the radial derivatives are given by

$$\lambda_{u,r} = \tilde{a}^{-1}\left(\frac{-U}{(\tilde{a}^2 + U^2)^{1/2}} + 1\right) \tag{2.126}$$

$$\lambda_{v,r} = \tilde{a}^{-1}\left(\frac{V}{(\tilde{a}^2 + V^2)^{1/2}} + 1\right) \tag{2.127}$$

$$\Xi_{,r} = \left(1 + \sqrt{\frac{1 - \alpha^{-2}}{\lambda_u\lambda_v}}\right)(\lambda_u\lambda_{v,r} + \lambda_{u,r}\lambda_v) \tag{2.128}$$

For Ψ,

$$e^{2\Psi} = \frac{\alpha^2(1 - \lambda_u\lambda_v)^2 + (\lambda_u + \lambda_v)^2}{[\alpha^2\Xi^2 + (\lambda_v - \lambda_u)^2]} \tag{2.129}$$

Thus differentiating with respect to t,

$$2\Psi_{,t}e^{2\Psi} = \frac{2\alpha^2(1 - \lambda_u\lambda_v)(-\lambda_u\lambda_{v,t} - \lambda_{u,t}\lambda_v) + 2(\lambda_v + \lambda_u)(\lambda_{v,t} + \lambda_{u,t})}{\alpha^2\Xi^2 + (\lambda_v - \lambda_u)^2}$$
$$- \frac{[\alpha^2(1 - \lambda_u\lambda_v)^2 + (\lambda_v + \lambda_u)^2]}{[\alpha^2\Xi^2 + (\lambda_v - \lambda_u)^2]^2}\left[2\alpha^2\Xi\Xi_{,t} + 2(\lambda_v - \lambda_u)(\lambda_{v,t} - \lambda_{u,t})\right]$$

$$\Psi_{,t} = \frac{1}{2}\left(\frac{\alpha^2\Xi^2 + (\lambda_v - \lambda_u)^2}{\alpha^2(1 - \lambda_u\lambda_v)^2 + (\lambda_v + \lambda_u)^2}\right) \times$$
$$\left(\frac{2\alpha^2(1 - \lambda_u\lambda_v)(-\lambda_u\lambda_{v,t} - \lambda_{u,t}\lambda_v) + 2(\lambda_v + \lambda_u)(\lambda_{v,t} + \lambda_{u,t})}{\alpha^2\Xi^2 + (\lambda_v - \lambda_u)^2}\right.$$
$$\left. - \frac{[\alpha^2(1 - \lambda_u\lambda_v)^2 + (\lambda_v + \lambda_u)^2]}{[\alpha^2\Xi^2 + (\lambda_v - \lambda_u)^2]^2}\left[2\alpha^2\Xi\Xi_{,t} + 2(\lambda_v - \lambda_u)(\lambda_{v,t} - \lambda_{u,t})\right]\right)$$

$$\Psi_{,t} = \frac{1}{2}e^{-2\Psi}\left(\frac{2\alpha^2(1 - \lambda_u\lambda_v)(-\lambda_u\lambda_{v,t} - \lambda_{u,t}\lambda_v) + 2(\lambda_v + \lambda_u)(\lambda_{v,t} + \lambda_{u,t})}{\alpha^2\Xi^2 + (\lambda_v - \lambda_u)^2}\right.$$
$$\left. - \frac{[\alpha^2(1 - \lambda_u\lambda_v)^2 + (\lambda_v + \lambda_u)^2]}{[\alpha^2\Xi^2 + (\lambda_v - \lambda_u)^2]^2}\left[2\alpha^2\Xi\Xi_{,t} + 2(\lambda_v - \lambda_u)(\lambda_{v,t} - \lambda_{u,t})\right]\right)$$
$$= \frac{\alpha^2(1 - \lambda_u\lambda_v)(-\lambda_u\lambda_{v,t} - \lambda_{u,t}\lambda_v) + (\lambda_v + \lambda_u)(\lambda_{v,t} + \lambda_{u,t})}{\alpha^2(1 - \lambda_u\lambda_v)^2 + (\lambda_v + \lambda_u)^2}$$
$$- \frac{\alpha^2\Xi\Xi_{,t} + (\lambda_v - \lambda_u)(\lambda_{v,t} - \lambda_{u,t})}{\alpha^2\Xi^2 + (\lambda_v - \lambda_u)^2}$$

i.e.

$$\Psi_{,t} = \frac{1}{\alpha^2(1 - \lambda_u\lambda_v)^2 + (\lambda_v + \lambda_u)^2}\Big((\lambda_v + \lambda_u)(\lambda_{v,t} + \lambda_{u,t}) \tag{2.130}$$
$$- \alpha^2(1 - \lambda_u\lambda_v)(\lambda_u\lambda_{v,t} + \lambda_{u,t}\lambda_v)\Big) \tag{2.131}$$
$$- \frac{1}{\alpha^2\Xi^2 + (\lambda_v - \lambda_u)^2}\Big(\alpha^2\Xi\Xi_{,t} + (\lambda_v - \lambda_u)(\lambda_{v,t} - \lambda_{u,t})\Big) \tag{2.132}$$

Initial values for $\tilde{L}$ can therefore be found from the expression

$$\tilde{L} = r\Psi_{,t} \tag{2.133}$$

43

where we calculate the value of $\Psi_{,t}$ from (2.133) above. To set our initial values of L_z^ϕ, we shall need to compute $\Omega_{,t}$.

$$\Omega = \tilde{a}\sqrt{\alpha^2 - 1}\left[2 + 2\sqrt{1 - \alpha^{-2}} - \frac{\Xi(\lambda_v + \lambda_u)^2}{(\lambda_u\lambda_v)^{1/2}[\alpha^2(1 - \lambda_u\lambda_v)^2 + (\lambda_v + \lambda_u)^2]}\right] \quad (2.134)$$

$$
\begin{aligned}
\Omega_{,t} = &-\tilde{a}\sqrt{\alpha^2 - 1}\left[\frac{\Xi_{,t}(\lambda_v + \lambda_u)^2 + 2\Xi(\lambda_v + \lambda_u)(\lambda_{v,t} + \lambda_{u,t})}{(\lambda_u\lambda_v)^{1/2}[\alpha^2(1 - \lambda_u\lambda_v)^2 + (\lambda_v + \lambda_u)^2]}\right. \\
&- \frac{\Xi(\lambda_v + \lambda_u)^2}{\lambda_u\lambda_v[\alpha^2(1 - \lambda_u\lambda_v)^2 + (\lambda_v + \lambda_u)^2]^2} \times \\
&\left((\lambda_u\lambda_v)^{1/2}[2\alpha^2(1 - \lambda_u\lambda_v)(-\lambda_u\lambda_{v,t} - \lambda_{u,t}\lambda_v) + 2(\lambda_v + \lambda_u)(\lambda_{v,t} + \lambda_{u,t})\right. \\
&\left.\left.+ \frac{1}{2}(\lambda_u\lambda_v)^{1/2}(\lambda_u\lambda_{v,t} + \lambda_{u,t}\lambda_v)[\alpha^2(1 - \lambda_u\lambda_v)^2 + (\lambda_v + \lambda_u)^2]\right)\right]
\end{aligned}
$$

$$
\begin{aligned}
\Omega_{,t} = &-\frac{\tilde{a}\sqrt{\alpha^2 - 1}}{(\lambda_u\lambda_v)^{1/2}}\left[\frac{(\lambda_v + \lambda_u)[\Xi_{,t}(\lambda_v + \lambda_u) + 2\Xi(\lambda_{v,t} + \lambda_{u,t})}{[\alpha^2(1 - \lambda_u\lambda_v)^2 + (\lambda_v + \lambda_u)^2]}\right. \\
&- \frac{\Xi(\lambda_v + \lambda_u)^2}{\lambda_u\lambda_v[\alpha^2(1 - \lambda_u\lambda_v)^2 + (\lambda_v + \lambda_u)^2]^2} \times \\
&\left(2\lambda_u\lambda_v[(\lambda_v + \lambda_u)(\lambda_{v,t} + \lambda_{u,t}) - \alpha^2(1 - \lambda_u\lambda_v)(\lambda_u\lambda_{v,t} + \lambda_{u,t}\lambda_v)]\right. \\
&\left.\left.+ \frac{1}{2}(\lambda_u\lambda_{v,t} + \lambda_{u,t}\lambda_v)[\alpha^2(1 - \lambda_u\lambda_v)^2 + (\lambda_v + \lambda_u)^2]\right)\right]
\end{aligned}
\quad (2.135)
$$

Therefore we can evaluate the values for L_z^ϕ on our initial slice via

$$\Omega_{,t} = -2e^{-4\Psi}L_z^\phi \quad (2.136)$$

i.e.

$$L_z^\phi = -\frac{1}{2}e^{4\Psi}\Omega_{,t} \quad (2.137)$$

Similarly, we shall require initial values for χ on our starting slice, which we can calculate via the equation

$$\chi_{,t} = -\frac{1}{r}L_r^r \quad (2.138)$$

Here $\chi = \gamma - \psi$, and so from the preceding expressions we have

$$L_r^r = r(\Psi_{,t} - \Gamma_{,t}) \tag{2.139}$$

Thus we are equipped with all we need to initialise all our evolution variables in the Cauchy region. We now turn our attention to the exterior characteristic region and the evolution variables in this regime.

2.2.2 The metric functions in the characteristic region

In the characteristic region, we introduce the null coordinate $u = t - r$ and use our rescaled radial coordinate $y = \dfrac{1}{r^{1/2}}$, where $y = 1$ at the interface and $y \to 0$ as $r \to \infty$. We therefore redefine our functions in terms of our variables u and y, thus:

$$v = t + r = t - r + 2r = u + 2y^{-2} \tag{2.140}$$

$$u = t_{CAUCHY} - r_{INTERFACE} \tag{2.141}$$

recalling that on each characteristic slice the value of u is constant. The functions λ_u, λ_v, Ξ, Γ, Ψ and Ω are defined in terms of u and v as before, but this time using v as given in equation (2.140).

In terms of the evolution variables in the characteristic region, we work with m,w,M,W as defined in [14]. For m, we have

$$e^{2\psi} = 1 + my \tag{2.142}$$

thus

$$m = \frac{e^{2\psi} - 1}{y} \tag{2.143}$$

where ψ is expressed in terms of our characteristic variables u and y. Our variable w is derived from the Geroch potential o, and is defined in the characteristic region as the integral:

$$w = oy^{-1} \tag{2.144}$$

where o is given by

$$
\begin{aligned}
o = {} & -\int_F^P e^{4\Psi(u,y)} \left(\frac{1}{2} y^5 \Omega(u,y)_{,y} + y^2 \Omega(u,y)_{,u} \right) du \\
& + \int_F^P e^{4\Psi(u,y)} y^2 \Omega(u,y)_{,y} \, dy
\end{aligned}
\tag{2.145}
$$

Here F is a fixed point and P is the point where o is being calculated. For convenience we shall set F as the interface point on the initial slice, that is $F = r(n) = y(1)$ on the slice at the starting time. If we define Q as the interface point on the slice upon which we wish to compute o, then we may rewrite the expression for o as follows

$$
\begin{aligned}
o = & -\int_F^Q e^{4\Psi(u,y)}\left(\frac{1}{2}y^5\Omega(u,y)_{,y} + y^2\Omega(u,y)_{,u}\right)\,du \\
& + \int_Q^P e^{4\Psi(u,y)}y^2\Omega(u,y)_{,y}\,dy
\end{aligned}
\tag{2.146}
$$

Thus the path of integration is from the fixed point F up the interface to the appropriate slice and then along that slice as far as the point in question.

We shall find that we encounter serious problems with the metric function Ω, for as $y \to 0$, $\Omega \to \infty$. Hence our variable w as defined above becomes a bad candidate for an evolution variable, and we shall find that we need to introduce a new variable when we include a rotational element in our spacetime. We shall address this problem in the next section.

The other two variables, M and W are calculated via their y–derivatives:

$$
M_{,y} = -\frac{1}{\lambda}(yw)_{,y}W + \frac{1}{4\lambda}\Big(-y(m + y^2 m_{,yy} + 3y m_{,y}) \tag{2.147}
$$
$$
+\frac{1}{\lambda}y^2(m^2 + 2ymm_{,y} - w^2 - 2yww_{,y} \tag{2.148}
$$
$$
+y^2 m_{,y}^2 - y^2 w_{,y}^2)\Big) \tag{2.149}
$$

$$
W_{,y} = \frac{1}{\lambda}(yw)_{,y}M + \frac{1}{4\lambda}\Big(-y(w + y^2 w_{,yy} + 3y w_{,y}) \tag{2.150}
$$
$$
+\frac{2}{\lambda}y^2(mw + ymw_{,y} + ywm_{,y} + y^2 m_{,y}w_{,y})\Big) \tag{2.151}
$$

Since we cannot use our w in this case, we shall obviously need to reformulate these equations in terms of our new variables. We shall give the amended versions of all the relevant equations in a later section.

2.3 Regularisation of the characteristic variables

Whilst in the Cauchy region, all our variables are well–behaved, and the Piran metric functions are all bounded. However, in the characteristic region, we cannot proceed merely by substituting for $v = u + 2y^{-2}$ without generating problems as we move towards future null infinity, for then $y \to 0$ and hence $v \to \infty$. Thus, although λ_u remains constant and is therefore bounded for all values of y, for λ_v we have

$$\lambda_v = \tilde{a}^{-1}\left[\left(\tilde{a}^2 + \left[u + \frac{2}{y^2}\right]^2\right)^{\frac{1}{2}} + u + \frac{2}{y^2}\right] \tag{2.152}$$

which 'blows up' as we approach ∞. This then makes all subsequent functions $(\Xi, \Psi, \Gamma, \Omega)$ unbounded, so we need to rescale the basic function λ_v, and then adjust the metric functions accordingly, in an attempt to write our metric functions as regular functions. Let

$$\overline{\lambda_v} = y^2 \lambda_v \tag{2.153}$$

i.e.

$$\overline{\lambda_v} = \tilde{a}^{-1}\left[\left(y^4[\tilde{a}^2 + (u + 2y^{-2})^2]\right)^{\frac{1}{2}} + uy^2 + 2\right] \tag{2.154}$$

$$\overline{\lambda_v} = \tilde{a}^{-1}\left[\left(y^4\tilde{a}^2 + (uy^2 + 2)^2\right)^{\frac{1}{2}} + uy^2 + 2\right] \tag{2.155}$$

Then we redefine our metric functions, replacing λ_v by $y^{-2}\overline{\lambda_v}$.

$$\overline{\Xi} = y^2 \Xi \tag{2.156}$$

$$\Xi = y^2 + \lambda_u(y^2\lambda_v) + 2y[(1 - \alpha^{-2})\lambda_u(y^2\lambda_v)]^{\frac{1}{2}} \tag{2.157}$$

$$\overline{\Xi} = y^2 + \lambda_u\overline{\lambda_v} + 2y[(1 - \alpha^{-2})\lambda_u\overline{\lambda_v}]^{\frac{1}{2}} \tag{2.158}$$

$$e^{2\Gamma} = 1 + \frac{(\alpha^2 - 1)(1 - \lambda_u\lambda_v)^2}{(1 + \lambda_u^2)(1 + \lambda_v^2)} \tag{2.159}$$

$$e^{2\Gamma} = 1 + \frac{(\alpha^2 - 1)(y^2 - \lambda_u y^2\lambda_v)^2}{(1 + \lambda_u^2)(y^4 + (y^2\lambda_v)^2)} \tag{2.160}$$

47

$$e^{2\Gamma} = 1 + \frac{(\alpha^2 - 1)(y^2 - \lambda_u \overline{\lambda_v})^2}{(1 + \lambda_u^2)(y^4 + \overline{\lambda_v}^2)} \tag{2.161}$$

$$e^{2\Psi} = \frac{\alpha^2(1 - \lambda_u \lambda_v)^2 + (\lambda_v + \lambda_u)^2}{\alpha^2 \Xi^2 + (\lambda_v - \lambda_u)^2} \tag{2.162}$$

$$e^{2\Psi} = \frac{\alpha^2(y^2 - \lambda_u y^2 \lambda_v)^2 + (y^2 \lambda_v + y^2 \lambda_u)^2}{\alpha^2(y^2 \Xi)^2 + (y^2 \lambda_v - y^2 \lambda_u)^2} \tag{2.163}$$

$$e^{2\Psi} = \frac{\alpha^2(y^2 - \lambda_u \overline{\lambda_v})^2 + (\overline{\lambda_v} + y^2 \lambda_u)^2}{\alpha^2 \overline{\Xi}^2 + (\overline{\lambda_v} - y^2 \lambda_u)^2} \tag{2.164}$$

$$\Omega = \tilde{a}(\alpha^2 - 1)^{1/2}\left(2 + 2(1 - \alpha^{-2})^{1/2} - \frac{\Xi(\lambda_u + \lambda_v)^2}{(\lambda_u \lambda_v)^{1/2}[\alpha^2(1 - \lambda_v \lambda_u)^2 + (\lambda_v + \lambda_u)^2]}\right) \tag{2.165}$$

$$\Omega = \tilde{a}(\alpha^2 - 1)^{1/2}\left(2 + 2(1 - \alpha^{-2})^{1/2}\right.$$
$$\left. - \frac{y^2 \Xi(y^2 \lambda_u + y^2 \lambda_v)^2}{y(\lambda_u y^2 \lambda_v)^{1/2}[\alpha^2(y^2 - y^2 \lambda_v \lambda_u)^2 + (y^2 \lambda_v + y^2 \lambda_u)^2]}\right) \tag{2.166}$$

$$\Omega = \tilde{a}(\alpha^2 - 1)^{1/2}\left(2 + 2(1 - \alpha^{-2})^{1/2} - \frac{\overline{\Xi}(y^2 \lambda_u + \overline{\lambda_v})^2}{y(\lambda_u \overline{\lambda_v})^{1/2}[\alpha^2(y^2 - \overline{\lambda_v}\lambda_u)^2 + (\overline{\lambda_v} + y^2 \lambda_u)^2]}\right) \tag{2.167}$$

We can now take the limit of all these functions as we approach future null infinity, i.e as $y \to 0$. We first note that λ_u is a constant and bounded on each characteristic hypersurface.

$$\begin{aligned}
\lim_{y \to 0}(\overline{\lambda_v}) &= \lim_{y \to 0}\left(\tilde{a}^{-1}\left[\left(y^4 \tilde{a}^2 + (uy^2 + 2)^2\right)^{\frac{1}{2}} + uy^2 + 2\right]\right) \\
&= \tilde{a}^{-1}[2 + 2]
\end{aligned}$$
$$\text{i.e.} \qquad \lim_{y \to 0}(\overline{\lambda_v}) = \frac{4}{\tilde{a}} \tag{2.168}$$

$$\begin{aligned}
\lim_{y \to 0}(\overline{\Xi}) &= \lim_{y \to 0}(y^2 + \lambda_u \overline{\lambda_v} + 2y[(1 - \alpha^{-2})\lambda_u \overline{\lambda_v}]^{\frac{1}{2}}) \\
&= \lim_{y \to 0}(\lambda_u \overline{\lambda_v})
\end{aligned}$$
$$\text{i.e.} \qquad \lim_{y \to 0}(\overline{\Xi}) = \frac{4\lambda_u}{\tilde{a}} \tag{2.169}$$

48

$$\lim_{y\to0}(e^{2\Psi}) = \lim_{y\to0}\left(\frac{\alpha^2(y^2 - \lambda_u\overline{\lambda_v})^2 + (\overline{\lambda_v} + y^2\lambda_u)^2}{\alpha^2\overline{\Xi}^2 + (\overline{\lambda_v} - y^2\lambda_u)^2}\right)$$

$$= \lim_{y\to0}\left(\frac{\alpha^2(\lambda_u\overline{\lambda_v})^2 + \overline{\lambda_v}^2}{\alpha^2\overline{\Xi}^2 + \overline{\lambda_v}^2}\right)$$

$$= \frac{\alpha^2\lambda_u^2(4\tilde{a}^{-1})^2 + (4\tilde{a}^{-1})^2}{\alpha^2(4\tilde{a}^{-1}\lambda_u)^2 + (4\tilde{a}^{-1})^2}$$

$$= \frac{16\alpha^2\tilde{a}^{-2}\lambda_u^2 + 16\tilde{a}^{-2}}{16\alpha^2\tilde{a}^{-2}\lambda_u^2 + 16\tilde{a}^{-2}}$$

Hence

$$\lim_{y\to0}(e^{2\Psi}) = 1. \tag{2.170}$$

$$\lim_{y\to0}(e^{2\Gamma}) = \lim_{y\to0}\left(1 + \frac{(\alpha^2 - 1)(y^2 - \lambda_u\overline{\lambda_v})^2}{(1 + \lambda_u^2)(y^4 + \overline{\lambda_v}^2)}\right)$$

$$= 1 + (\alpha^2 - 1)\lim_{y\to0}\left(\frac{(\lambda_u\overline{\lambda_v})^2}{(1 + \lambda_u^2)(\overline{\lambda_v}^2)}\right)$$

$$\Rightarrow \lim_{y\to0}(e^{2\Gamma}) = 1 + (\alpha^2 - 1)\frac{\lambda_u^2}{1 + \lambda_u^2} \tag{2.171}$$

which is clearly bounded for all values of y.

Finally, for Ω we have

$$\lim_{y\to0}(\Omega) = \lim_{y\to0}\left(\tilde{a}(\alpha^2 - 1)^{1/2}\left(2 + 2(1 - \alpha^{-2})^{1/2}\right.\right.$$

$$\left.\left. - \frac{\overline{\Xi}(y^2\lambda_u + \overline{\lambda_v})^2}{y(\lambda_u\overline{\lambda_v})^{1/2}[\alpha^2(y^2 - \overline{\lambda_v}\lambda_u)^2 + (\overline{\lambda_v} + y^2\lambda_u)^2]}\right)\right)$$

$$= \tilde{a}(\alpha^2 - 1)^{1/2}\left[2 + 2\sqrt{1 - \alpha^{-2}} - \lim_{y\to0}\left(\frac{\overline{\Xi}\,\overline{\lambda_v}^2}{y\sqrt{\lambda_u\overline{\lambda_v}}[\alpha^2\lambda_u^2\overline{\lambda_v}^2 + \overline{\lambda_v}^2]}\right)\right]$$

i.e.

$$\lim_{y\to0}(\Omega) = \tilde{a}(\alpha^2 - 1)^{1/2}[2 + 2\sqrt{1 - \alpha^{-2}} \times \tag{2.172}$$

$$\frac{(4\tilde{a}^{-1}\lambda_u)(4\tilde{a}^{-1})^2}{\sqrt{4\tilde{a}^{-1}\lambda_u}[\alpha^2\lambda_u^2(4\tilde{a}^{-1})^2 + (4\tilde{a}^{-1})^2]}\lim_{y\to0}\left(\frac{1}{y}\right) \tag{2.173}$$

Hence

$$\lim_{y\to0}(\Omega) = \infty \tag{2.174}$$

49

Thus, although the 'building–block' functions, λ_u and $\overline{\lambda}_v$ are regular for all values of y, and the metric functions Ψ and Γ are also made regular by this rescaling, the other function, Ω, which governs the rotation of the system, is not. Ω has a factor of y multiplying the denominator which it appears cannot be removed. Thus as y gets smaller and approaches zero, Ω is not well behaved.

This fact has serious implications in terms of which quantities we shall be able to use as comparison functions. That is, how to compare the values obtained through the evolution with those from the analytic prescription. In the past, it has generally been the metric functions themselves which have been used for this purpose, and indeed there is no problem in implementing this approach with Ψ and Γ, for both analytic expressions can be expressed in such a way that they are bounded for all values of our radial coordinates, r and y. In addition, the evolving ψ can be expressed directly in terms of our evolving characteristic variables m and y, and although this is not the case with the evolving γ, we can obtain an expression for γ at each point by integration along the null hypersurface which is sufficiently accurate for our purposes. It is to be noted here that the values for γ that we calculate in the characteristic region have no bearing on the evolving characteristic variables, they are merely computed for comparison with the expected values deduced from the analytic expression.

However, the third metric function, Ω, is clearly unsuitable for use as a comparison function, since it is not bounded for all values of y under consideration. We therefore need to find an alternative comparison function, which contains information about the rotational behaviour of the spacetime. A possible alternative candidate is the characteristic function w, which is derived from the Geroch potential o, where, in terms of our characteristic variables, $(x^\alpha) = (u, y, \phi, z)$,

$$o_{,\alpha} = \frac{1}{r} e^{4\Psi} \left(-\frac{1}{2} y^3 \Omega_{,y} - \Omega_{,u}, \Omega_{,y}, 0, 0 \right) \tag{2.175}$$

$$w = \frac{o}{y} \tag{2.176}$$

However, it transpires that w is also unbounded as $y \to 0$. For Ω is of order $\dfrac{1}{y}$, as we saw previously, hence $\Omega_{,y}$ is of order $\dfrac{1}{y^2}$. Consequently

$$o \sim y + \text{ constant} \tag{2.177}$$

and so

$$w \sim \frac{1}{y} \tag{2.178}$$

If instead we consider o, the Geroch potential directly, which from the above is regular for all values of y in the range $0 \le y \le 1$, we should then have a well–behaved comparison function as required. However, by virtue of w being unbounded for small y, it too is unsuitable for use as an evolution variable, for errors will rapidly be generated in w which will then be propagated through the other evolution variables, since all the variables are strongly inter–related. Thus we shall also need to rewrite the basic computer code in the characteristic region, and on the interface, replacing w by oy, and $W = \frac{w_{,u}}{\lambda}$ by an appropriate alternative.

2.4   Reformulation of the code

As suggested in the previous section, we shall replace w by oy and now investigate the relationship between O and W. Then

$$o_{,u} = (wy)_{,u} \tag{2.179}$$

$$= w_{,u}y + wy_{,u} \tag{2.180}$$

$$= yw_{,u} \tag{2.181}$$

$$= y\lambda W \tag{2.182}$$

$$= \lambda O \tag{2.183}$$

Hence this transformation between w and o and W and O is entirely consistent with the corresponding relations involving w and W. We have

$$o = wy \tag{2.184}$$

$$O = Wy \tag{2.185}$$

We shall now present the analogue o–equations to the w–equations given in [15]. These are then finite–differenced and used to write the adapted subroutines for the characteristic regions.

2.4.1 Interface relations involving w and W

We first state the existing equations involving w or W from [15] in, where neccessary, their corrected form. Here, equations (2.186) – (2.188) correspond to equations (55) – (57) in [15] and (2.189) – (2.191) similarly correspond to equations (68) – (70).

$$\omega_{,r} = \frac{W}{y\lambda} \tag{2.186}$$

$$\omega_{,rr} = -\frac{W_{,u}}{y\lambda} + \frac{MW}{\lambda} + \frac{1}{2}\frac{yW}{\lambda} + \frac{1}{2}\frac{y^2 W}{\lambda^2}(ym)_{,y} - \frac{1}{2}\frac{y^2 W_{,y}}{\lambda} \tag{2.187}$$

$$L_z^\phi = \frac{1}{2}\frac{\lambda W}{y} + \frac{1}{4}y(yw)_{,y} \tag{2.188}$$

$$w = \int r^{-1/2}e^{4\psi}\omega_{,r}\,dt + r^{1/2}\int r^{-1}e^{4\psi}\omega_{,t}\,dr \tag{2.189}$$

$$w_{,y} = 4rL_z^\phi - 2re^{4\psi}\omega_{,r} - \int e^{4\psi}\omega_{,r}\,dt + r\int r^{-1}e^{4\psi}\omega_{,t}\,dr \tag{2.190}$$

$$\begin{aligned}
w_{,yy} = {}& 2r^{5/2}e^{4\psi}\Big(8\psi_{,t}\omega_r + 8\psi_{,r}\omega_{,r} + 2\omega_{,rr} + 2\omega_{rt} + r^{-1}\omega_{,t} \\
& + 3r^{-1}\omega_{,r}\Big) - 8r^{5/2}\Big(L_{z,r}^\phi + L_{z,t}^\phi + r^{-1}L_z^\phi\Big) \\
& + 2r^{3/2}\Big[\int r^{-1}e^{4\psi}\omega_{,r}\,dt + \int r^{-1}e^{4\psi}\omega_{,t}\,dr\Big]
\end{aligned} \tag{2.191}$$

Now the revised versions of these become

$$\omega_{,r} = \frac{O}{y^2\lambda} \tag{2.192}$$

$$\begin{aligned}
\omega_{,rr} = {}& -\frac{O_{,u}}{y^2\lambda} + \frac{MO}{y\lambda} + \frac{1}{2}\frac{O}{\lambda} + \frac{1}{2}\frac{yO}{\lambda^2}(my)_{,y} \\
& - \frac{1}{2}\frac{y^2}{\lambda}\left(\frac{O}{y}\right)_{,y} \\
= {}& -\frac{O_{,u}}{y^2\lambda} + \frac{MO}{y\lambda} + \frac{1}{2}\frac{O}{\lambda} + \frac{1}{2}\frac{yO}{\lambda^2}(my)_{,y} - \frac{1}{2}\frac{y^2}{\lambda} \\
& \left(\frac{O_{,y}}{y} - \frac{O}{y^2}\right)
\end{aligned}$$

$$\omega_{,rr} = -\frac{O_{,u}}{y^2\lambda} + \frac{MO}{y\lambda} + \frac{O}{\lambda} + \frac{1}{2}\frac{yO}{\lambda^2}(my)_{,y} - \frac{1}{2}\frac{yO_{,y}}{\lambda} \tag{2.193}$$

$$L_z^\phi = \frac{1}{2}\frac{\lambda O}{y^2} + \frac{1}{4}yo_{,y} \tag{2.194}$$

$$o = y\left(\int r^{-1/2}e^{4\psi}\omega_{,r}\,dt + r^{1/2}\int r^{-1}e^{4\psi}\omega_{,t}\,dr\right) \qquad (2.195)$$

and then using equation (2.194)

$$o_{,y} = 4\frac{L_z^\phi}{y} - 2\frac{\lambda O}{y^3}$$

$$o_{,y} = 4r^{1/2}L_z^\phi - 2r^{1/2}e^{4\psi}\omega_r \qquad (2.196)$$

$$o_{,yy} = 2r^2e^{4\psi}\left(r^{-1}\omega_{,r} + 8\psi_{,r}\omega_{,r} + 8\psi_{,t}\omega_{,r} + 2\omega_{,rr} + 2\omega_{,rt}\right)$$

$$-2r^2\left(2r^{-1}L_z^\phi + 4L_{z,r}^\phi + 4L_{z,t}^\phi\right) \qquad (2.197)$$

2.4.2 Characteristic equations involving w and W

In our reformulation of the characteristic scheme from the variables m, w, M and W to the variables m, o, M and W we must isolate all equations involving w or W and amend them appropriately. Previously the w and W dependent equations in the characteristic region were given by the following, where (2.198) – (2.201) correspond to equations (39)–(42) in [15].

$$w_{,u} = \lambda W \qquad (2.198)$$

$$M_{,y} = \frac{1}{\lambda}(yw)_{,y}W + \frac{1}{4\lambda}\left(-y(m + y^2m_{,yy} + 3ym_{,y})\right.$$

$$\left. +\frac{1}{\lambda}y^2(m^2 + 2ymm_{,y} - w^2 - 2yww_{,y} + y^2m_{,y}^2 - y^2w_{,y}^2)\right) \qquad (2.199)$$

$$W_{,y} = \frac{1}{\lambda}(yw)_{,y}M + \frac{1}{4\lambda}\left(-y(w + y^2w_{,yy} + 3yw_{,y})\right.$$

$$\left. +\frac{1}{\lambda}2y^2(mw + ymw_{,y} + ywm_{,y} + y^2m_{,y}w_{,y})\right) \qquad (2.200)$$

$$\gamma_{,y} = -\frac{1}{8\lambda^2}y[m^2 + w^2 + 2y(mm_{,y} + ww_{,y}) + y^2(m_{,y}^2 + w_{,y}^2)] \qquad (2.201)$$

If we recall that

$$w = \frac{o}{y} \qquad (2.202)$$

$$w_{,y} = \frac{o_{,y}}{y} - \frac{o}{y^2} \qquad (2.203)$$

$$w_{,yy} = \frac{o_{,yy}}{y} - 2\frac{o_{,y}}{y^2} + 2\frac{o}{y^3} \qquad (2.204)$$

$$w_{,u} = \frac{o_{,u}}{y} \qquad (2.205)$$

$$W \;=\; \frac{O}{y} \tag{2.206}$$

$$W_{,y} \;=\; \frac{O_{,y}}{y} - \frac{O}{y^2} \tag{2.207}$$

then these transform to

$$o_{,u} \;=\; y\lambda W$$

$$o_{,u} \;=\; \lambda O \tag{2.208}$$

$$M_{,y} \;=\; -\frac{o_{,y}}{\lambda}\frac{O}{y} + \frac{1}{4\lambda}\Big[-y(m + y^2 m_{,yy} + 3y m_{,y})$$
$$+ \frac{1}{\lambda} y^2 \Big(m^2 + 2ym m_{,y} - \frac{o^2}{y^2} - 2o\Big(\frac{o_{,y}}{y} - \frac{o}{y^2}\Big)$$
$$+ y^2 m_{,y}^2 - y^2 \Big(\frac{o_{,y}}{y} - \frac{o}{y^2}\Big)^2 \Big) \Big] \tag{2.209}$$

i.e.
$$M_{,y} \;=\; -\frac{o_{,y}}{\lambda}\frac{O}{y} + \frac{1}{4\lambda}\Big[-y(m + y^2 m_{,yy} + 3y m_{,y})$$
$$+ \frac{1}{\lambda}\Big(y^2 m^2 + 2y^3 m m_{,y} - o^2 - 2oyo_{,y} + 2o^2$$
$$+ y^4 m_{,y}^2 - y^2 o_{,y}^2 - o^2 + 2oyo_{,y} \Big) \Big] \tag{2.210}$$

Therefore we have

$$M_{,y} \;=\; -\frac{o_{,y}}{\lambda}\frac{O}{y} + \frac{1}{4\lambda}\Big[-y(m + y^2 m_{,yy} + 3y m_{,y})$$
$$+ \frac{y^2}{\lambda}\Big(m^2 + 2ym m_{,y} + y^2 m_{,y}^2 - o_{,y}^2 \Big) \Big] \tag{2.211}$$

From equation (2.200) we obtain

$$\frac{O_{,y}}{y} - \frac{O}{y^2} \;=\; \frac{1}{\lambda} o_{,y} M + \frac{1}{4\lambda}\Big(-o - y^3\Big(\frac{o_{,yy}}{y} - 2\frac{o_{,y}}{y^2} + 2\frac{o}{y^3}\Big)$$
$$- 3y^2\Big(\frac{o_{,y}}{y} - \frac{o}{y^2}\Big) + \frac{2y^2}{\lambda}\Big(\frac{mo}{y} + ym\Big[\frac{o_{,y}}{y} - \frac{o}{y^2}\Big]$$
$$+ om_{,y} + y^2 m_{,y}\Big[\frac{o_{,y}}{y} - \frac{o}{y^2}\Big] \Big) \Big) \tag{2.212}$$

$$O_{,y} \;=\; \frac{O}{y} + \frac{yo_{,y}}{\lambda} M$$
$$+ \frac{1}{4\lambda}\Big(-y[o + y^2 o_{,yy} - 2yo_{,y} + 2o + 3yo_{,y} - 3o]$$
$$+ \frac{2y^2}{\lambda}\Big[mo + myo_{,y} - mo + oym_{,y} + oy^2 m_{,y} - oym_{,y}\Big]\Big) \tag{2.213}$$

$$O_{,y} \;=\; \frac{O}{y} + \frac{yo_{,y}}{\lambda} M - \frac{y^2}{4\lambda}(yo_{,yy} + o_{,y}) + \frac{y^3 o_{,y}}{2\lambda^2}(m + ym_{,y}) \tag{2.214}$$

Now, equation (2.201) can be rewritten as

$$\gamma_{,y} = -\frac{1}{8\lambda^2}y\Big((m + ym_{,y})^2 + (w + yw_{,y})^2\Big) \tag{2.215}$$

$$\text{or,} \qquad \gamma_{,y} = -\frac{1}{8\lambda^2}y\Big(m + ym_{,y})^2 + o_{,y}^2\Big) \tag{2.216}$$

The only other equation involving w and W is equation (43) in [15], which is not utilised in our evolution scheme, although it could be similarly altered to replace w and its derivatives with the appropriate o–equivalents, and similarly for W. We shall not, however, do this here.

Thus the complete set of regularised equations in the characteristic region are:

$$M = \frac{m_{,u}}{1 + my}, \tag{2.217}$$

$$O = \frac{o_{,u}}{1 + my}, \tag{2.218}$$

$$M_{,y} = -\frac{o_{,y}}{\lambda}\frac{O}{y} + \frac{1}{4\lambda}\Big[-y(m + y^2 m_{,yy} + 3ym_{,y})$$
$$+ \frac{y^2}{\lambda}\Big(m^2 + 2ymm_{,y} + y^2 m_{,y}^2 - o_{,y}^2\Big)\Big] \tag{2.219}$$

$$O_{,y} = \frac{O}{y} + \frac{yo_{,y}}{\lambda}M - \frac{y^2}{4\lambda}(yo_{,yy} + o_{,y}) + \frac{y^3 o_{,y}}{2\lambda^2}(m + ym_{,y}) \tag{2.220}$$

$$\gamma_{,y} = -\frac{1}{8\lambda^2}y\Big(m + ym_{,y})^2 + o_{,y}^2\Big) \tag{2.221}$$

2.4.3 Regular singular behaviour

The modified propagation equations (2.219 – 2.220) would appear to be singular for $y \to 0$, by virtue of the term in $\frac{1}{y}$. However, this pair of coupled singular equations are in fact regular singular equations, since their solutions remain regular for all values of y. The homogeneous parts of these are

$$M_{,y} + N\frac{O}{y} = 0 \tag{2.222}$$

$$O_{,y} - yNM - \frac{O}{y} = 0 \tag{2.223}$$

where for simplicity we set

$$N = \frac{o_{,y}}{1 + my}. \tag{2.224}$$

Now, $o_{,y}$ is given by

$$o_{,y} = y^2 e^{4\Psi}\Omega_{,y} \tag{2.225}$$

55

and so explicitly,

$$o_{,y} = y^2(1+my)^2\tilde{a}\sqrt{\alpha^2-1}\left(2(1+\sqrt{1-\alpha^{-2}}) - \frac{\bar{\bar{\Xi}}(y^2\lambda_u+\bar{\lambda}_v)^2}{y\sqrt{\lambda_u\bar{\lambda}_v}[\alpha^2(y^2-\lambda_u\bar{\lambda}_v)^2+(\bar{\lambda}_v+y^2\lambda_u)^2]}\right)_{,y}$$

$$o_{,y} = -y^2(1+my)^2\tilde{a}\sqrt{\alpha^2-1}\left(\frac{\bar{\bar{\Xi}}_{,y}(y^2\lambda_u+\bar{\lambda}_v)^2+2\bar{\bar{\Xi}}(y^2\lambda_u+\bar{\lambda}_v)(2y\lambda_u+\bar{\lambda}_{v,y})}{y\sqrt{\lambda_u\bar{\lambda}_v}[\alpha^2(y^2-\lambda_u\bar{\lambda}_v)^2+(\bar{\lambda}_v+y^2\lambda_u)^2]}\right.$$

$$-\frac{\bar{\bar{\Xi}}(y^2\lambda_u+\bar{\lambda}_v)^2}{y^2\lambda_u\bar{\lambda}_v[\alpha^2(y^2-\lambda_u\bar{\lambda}_v)^2+(\bar{\lambda}_v+y^2\lambda_u)^2]^2}\left[\sqrt{\lambda_u\bar{\lambda}_v}\left[\alpha^2(y^2-\lambda_u\bar{\lambda}_v)^2+(\bar{\lambda}_v+y^2\lambda_u)^2\right]\right.$$

$$+2y\sqrt{\lambda_u\bar{\lambda}_v}[\alpha^2(y^2-\lambda_u\bar{\lambda}_v)(2y-\lambda_u\bar{\lambda}_v)+(\bar{\lambda}_v+y^2\lambda_u)(\bar{\lambda}_{v,y}+2y\lambda_u)]$$

$$\left.\left.+\frac{1}{2}y\sqrt{\lambda_u/\bar{\lambda}_v}\bar{\lambda}_{v,y}[\alpha^2(y^2-\lambda_u\bar{\lambda}_v)^2+(\bar{\lambda}_v+y^2\lambda_u)^2]\right]\right) \tag{2.226}$$

In the limit as $y \to 0$, $\bar{\lambda}_v \to 4/a$, $\bar{\lambda}_{v,y} \to 0$, $\bar{\bar{\Xi}} \to 4\lambda_u/a$ and $\bar{\bar{\Xi}}_{,y} \to 0$. Thus ignoring terms of first or higher order, this reduces to

$$\lim_{y\to 0}(o_{,y}) = -\tilde{a}\sqrt{\alpha^2-1}\left(\frac{4\lambda_u/a(4/a)^2\sqrt{4\lambda_u/a}[16\alpha^2\lambda_u^2/a^2+16/a^2]}{4\lambda_u/a[16\alpha^2\lambda_u^2/a^2+16/a^2]^2}\right) \tag{2.227}$$

$$= -\tilde{a}\sqrt{\alpha^2-1}\frac{2\sqrt{\lambda_u/a}}{[\alpha^2\lambda_u^2+1]}$$

i.e. $$\lim_{y\to 0}(o_{,y}) = -\frac{2\sqrt{a\lambda_u(\alpha^2-1)}}{\alpha^2\lambda_u^2+1}+O(y) \tag{2.228}$$

so $o_{,y}$ is regular for $y \to 0$. Similarly we can obtain the asymptotic limit for m as $y \to 0$. We need to apply de l'Hôpital's rule in this case, since $m = (e^{2\phi} - 1)/y$ and the limit of $e^{2\phi}$ has already been found to be 1. We have

$$\lim_{y\to 0}(m) = \frac{1}{y}\left(\frac{\alpha^2(y^2-\lambda_u\bar{\lambda}_v)^2+(y^2\lambda_u+\bar{\lambda}_v)^2-\alpha^2\bar{\bar{\Xi}}^2-(\bar{\lambda}_v-y^2\lambda_u)^2}{\alpha^2\bar{\bar{\Xi}}^2+(\bar{\lambda}_v-y^2\lambda_u)^2}\right) \tag{2.229}$$

$$\lim_{y\to 0}(m) = \left(\frac{\alpha^2(y^2-\lambda_u\bar{\lambda}_v)^2+4y^2\lambda_u\bar{\lambda}_v-\alpha^2\bar{\bar{\Xi}}^2}{\alpha^2 y\bar{\bar{\Xi}}^2+y(\bar{\lambda}_v-y^2\lambda_u)^2}\right) \tag{2.230}$$

de l'Hôpital $\Rightarrow$

$$\lim_{y\to 0}(m) = \frac{2\alpha^2(y^2-\lambda_u\bar{\lambda}_v)(2y-\lambda_u\bar{\lambda}_{v,y})+8y\lambda_u\bar{\lambda}_v+4y^2\lambda_u\bar{\lambda}_{v,y}-2\alpha^2\bar{\bar{\Xi}}\bar{\bar{\Xi}}_{,y}}{\alpha^2\bar{\bar{\Xi}}^2+2\alpha^2 y\bar{\bar{\Xi}}\bar{\bar{\Xi}}_{,y}+(\bar{\lambda}_v-y^2\lambda_u)^2+2y(\bar{\lambda}_v-y^2\lambda_u)(\bar{\lambda}_{v,y}-2y\lambda_u)}$$

Ignoring terms of first or higher order, the only part of the numerator which survives

comes from the term $2\alpha^2 \bar{\Xi}\bar{\Xi}_{,y}$. We find that

$$\lim_{y \to 0}(m) = \frac{2\alpha^2 \lambda_u (4/a) 2\sqrt{(1 - \alpha^{-2}(4\lambda_u/a)}}{\alpha^2(4\lambda_u/a)^2 + (4/a)^2} = \frac{2\alpha\sqrt{a\lambda_u^3(\alpha^2 - 1)}}{\alpha^2\lambda_u^2 + 1} + O(y) \qquad (2.231)$$

Therefore, the function N as defined in equation(2.224) is regular as $y \to 0$. If we take the derivative of equation (2.220) with respect to y, we obtain

$$O_{,yy} - NM - yN_{,y}M - yNM_{,y} - \frac{O_{,y}}{y} + \frac{O}{y^2} = 0 \qquad (2.232)$$

By using equations (2.219 – 2.220) we can eliminate M and its derivative so that

$$O_{,yy} - \left(\frac{2}{y} + \frac{N_{,y}}{N}\right)O_{,y} + \left(\frac{2}{y^2} + \frac{N_{,y}}{yN} + N^2\right) = 0 \qquad (2.233)$$

where the dominant singular part is

$$O_{,yy} - \frac{2}{y}O_{,y} + \frac{2O}{y^2} = 0 \qquad (2.234)$$

The trial solution $O = y^x$ yields

$$x(x - 1)y^{x-2} - \frac{2}{y}xy^{x-1} + \frac{2}{y^2}y^x = 0 \qquad (2.235)$$

which simplifies to

$$x^2 - 3x + 2 = 0 \qquad (2.236)$$

with roots $x = 1$ and $x = 2$. Thus O has regular independent solutions y and y^2, and so exhibits regular singular behaviour as $y \to 0$.

2.4.4 Selection of the third comparison function

Having now converted the original scheme into an m, o, M and O scheme in the characteristic region and in the interface–matching area, we are in a position to proceed to run the program and to evaluate how well the evolving spacetime simulation matches the prescription given in [16]. All that remains is to decide what we are going to use to investigate how well the evolving system matches up with the expected analytic spacetime of Piran. It is obvious enough to take Ψ and Γ as two of the comparison functions, but what to use for the third is not so clear. As stated previously, Ω is unsuitable due to its behaviour as the radial distance increases to ∞. There is no evolution variable which exists in both Cauchy and characteristic region (with the possible exception of ψ,

which is closely related to m in the characteristic domain). We must therefore consider all remaining possibilities in turn, and shall choose for this purpose that which is most easily implemented, and which contains information about the rotational degree of freedom of the spacetime. The characteristic variable m is too closely related to Ψ for it to be used as an independent check, which leaves the best remaining alternative as o. The two further characteristic variables, M and O are calculated from m and o, and so are less attractive candidates as comparison functions. Using o as the third quantity for comparison also has the advantage that as an evolution variable itself, it is evolved through the code, and hence is readily exportable for graphics output and later when computing the absolute errors. However, it transpires that computing the corresponding values of o from the field equations of [15] and the metric expressions of Piran, in order to compare them with the evolved $o(i)$, is more difficult.

Recall that o is given by

$$o = -\int_F^P e^{4\psi(u,y)}(\frac{1}{2}y^5\omega(u,y)_{,y} + y^2\omega(u,y)_{,u})\,du \tag{2.237}$$

$$+ \int_F^P e^{4\psi(u,y)}y^2\omega(u,y)_{,y}\,dy \tag{2.238}$$

We shall obviously need to calculate $\dfrac{\partial\Omega}{\partial y}$ and $\dfrac{\partial\Omega}{\partial u}$ for Piran's metric function Ω in the characteristic region. We have

$$\Omega(u,y) = \tilde{a}\sqrt{\alpha^2 - 1}\left[2 + 2\sqrt{1 - \alpha^{-2}} \right.$$
$$\left. - \frac{\overline{\Xi}(y^2\lambda_{,u} + \overline{\lambda}_{,v})^2}{y\sqrt{\lambda_u\overline{\lambda}_v}[\alpha^2(y^2 - \lambda_u\overline{\lambda}_v)^2 + (\overline{\lambda}_v + y^2\lambda_u)^2]}\right] \tag{2.239}$$

$$\Omega_{,u} = -\tilde{a}\sqrt{\alpha^2 - 1}\left(\frac{\overline{\Xi}_{,u}(\overline{\lambda}_v + y^2\lambda_u)^2 + 2\overline{\Xi}(\overline{\lambda}_v + y_u^\lambda)(\overline{\lambda}_{v,u} + y^2\lambda_{u,u})}{y\sqrt{\lambda_u\overline{\lambda}_v}[\alpha^2(y^2 - \lambda_u\overline{\lambda}_v)^2 + (\overline{\lambda}_v + y^2\lambda_u)^2]}\right.$$
$$- \frac{\Xi(\overline{\lambda}_v + y^2\lambda_u)^2}{y\lambda_u\overline{\lambda}_v[\alpha^2(y^2 - \lambda_u\overline{\lambda}_v)^2 + (\overline{\lambda}_v + y^2\lambda_u)^2]^2} \times$$
$$\left(\frac{1}{2}\frac{\lambda_u\overline{\lambda}_{v,u} + \lambda_{u,u}\overline{\lambda}_v}{\sqrt{\lambda_u\overline{\lambda}_v}}\overline{\lambda}_{v,u}[\alpha^2(y^2 - \lambda_u\overline{\lambda}_v)^2 + (\overline{\lambda}_v + y^2\lambda_u)^2]\right.$$
$$+\sqrt{\lambda_u\overline{\lambda}_v}[2\alpha^2(y^2 - \lambda_u\overline{\lambda}_v)^2(-\lambda_u\overline{\lambda}_{v,u} - \lambda_{u,u}\overline{\lambda}_v)$$
$$\left.\left.+2(\overline{\lambda}_v + y^2\lambda_u)(\overline{\lambda}_{v,u} + y^2\lambda_{u,u})]\right)\right) \tag{2.240}$$

$$\Omega_{,y} = -\tilde{a}\sqrt{\alpha^2-1}\left(\frac{\overline{\Xi}_{,y}(\overline{\lambda}_v+y^2\lambda_u)^2+2\overline{\Xi}(\overline{\lambda}_v+y^2\lambda_u)(\overline{\lambda}_{v,y}+2y\lambda_u)}{y\sqrt{\lambda_u\overline{\lambda}_v}[\alpha^2(y^2-\lambda_u\overline{\lambda}_v)^2+(\overline{\lambda}_v+y^2\lambda_u)^2]}\right.$$
$$-\frac{\overline{\Xi}(\overline{\lambda}_v+y^2\lambda_u)^2}{y^2\lambda_u\overline{\lambda}_v[\alpha^2(y^2-\lambda_u\overline{\lambda}_v)^2+(\overline{\lambda}_v+y^2\lambda_u)^2]^2}\times$$
$$\left(\sqrt{\lambda_u\overline{\lambda}_v}[\alpha^2(y^2-\lambda_u\overline{\lambda}_v)^2+(\overline{\lambda}_v+y^2\lambda_u)^2]\right.$$
$$+\frac{1}{2}y\sqrt{\lambda_u/\overline{\lambda}_v}\,\overline{\lambda}_{v,y}[\alpha^2(y^2-\lambda_u\overline{\lambda}_v)^2+(\overline{\lambda}_v+y^2\lambda_u)^2]$$
$$+y\sqrt{\lambda_u\overline{\lambda}_v}[2\alpha^2(y^2-\lambda_u\overline{\lambda}_v)(2y-\lambda_u\overline{\lambda}_{v,y})$$
$$\left.\left.+2(\overline{\lambda}_v+y^2\lambda_u)(\overline{\lambda}_{v,y}+2y\lambda_u)]\right)\right) \tag{2.241}$$

where λ_u, $\overline{\lambda}_v$ and $\overline{\Xi}$ are as previously defined and

$$\lambda_{u,u} = \frac{1}{\tilde{a}}\left[\frac{u}{\sqrt{\tilde{a}^2+u^2}}-1\right] \tag{2.242}$$

$$\lambda_{u,y} = 0 \tag{2.243}$$

$$\overline{\lambda}_{v,u} = \frac{1}{\tilde{a}}\left[\frac{y^2(y^2u+2)}{\sqrt{y^4\tilde{a}^2+(y^2u+2)^2}}+y^2\right] \tag{2.244}$$

$$\overline{\lambda}_{v,y} = \frac{1}{\tilde{a}}\left[\frac{2y^3\tilde{a}^2+2yu(y^2u+2)}{\sqrt{y^4\tilde{a}^2+(y^2u+2)^2}}+2yu\right] \tag{2.245}$$

$$\overline{\Xi}_{,u} = \left(1+\frac{y\sqrt{1-\alpha^{-2}}}{\sqrt{\lambda_u\overline{\lambda}_v}}\right)\left(\lambda_{u,u}\overline{\lambda}_v+\lambda_u\overline{\lambda}_{v,u}\right) \tag{2.246}$$

$$\overline{\Xi}_{,y} = 2y+2\sqrt{1-\alpha^2}\sqrt{\lambda_u\overline{\lambda}_v}+\left(1+\frac{y\sqrt{1-\alpha^{-2}}}{\sqrt{\lambda_u\overline{\lambda}_v}}\right)\left(\lambda_{u,y}\overline{\lambda}_v+\lambda_u\overline{\lambda}_{v,y}\right) \tag{2.247}$$

In other words, we shall be evaluating at each point (u,y)

$$o = \int_F^P\left(\frac{\alpha^2(y^2-\lambda_u\overline{\lambda}_v)^2+(\overline{\lambda}_v+y^2\lambda_u)^2}{\alpha^2\overline{\Xi}^2+(\overline{\lambda}_v+y^2\lambda_u)^2}\right)^2 y^2\Omega(u,y)_{,y}\,dy$$
$$-\int_F^P\left(\frac{\alpha^2(y^2-\lambda_u\overline{\lambda}_v)^2+(\overline{\lambda}_v+y^2\lambda_u)^2}{\alpha^2\overline{\Xi}^2+(\overline{\lambda}_v+y^2\lambda_u)^2}\right)^2\left(\frac{y^5}{2}\Omega(u,y)_{,y}+y^2\Omega(u,y)_{,u}\right)du \tag{2.248}$$

with the derivatives of Ω as above. It transpired that o as given above could not be integrated directly, and therefore a numerical integration method must be implemented. The details of this procedure are dealt with in the next section.

Due to the slicing method implemented in the external characteristic region, i.e. the use of null $u = constant$ hypersurfaces, it is possible to perform the du and dy integrals

separately. In order to calculate the value of o at grid–point i on the jth u–surface, it will be neccessary to integrate with respect to u along the interface from the initial ($t = 0$) interface point (F, say) up to the interface point on level–j, and then with respect to y along that null slice out as far as point i (the final point, P say). This idea is illustrated in Figure 2.1.
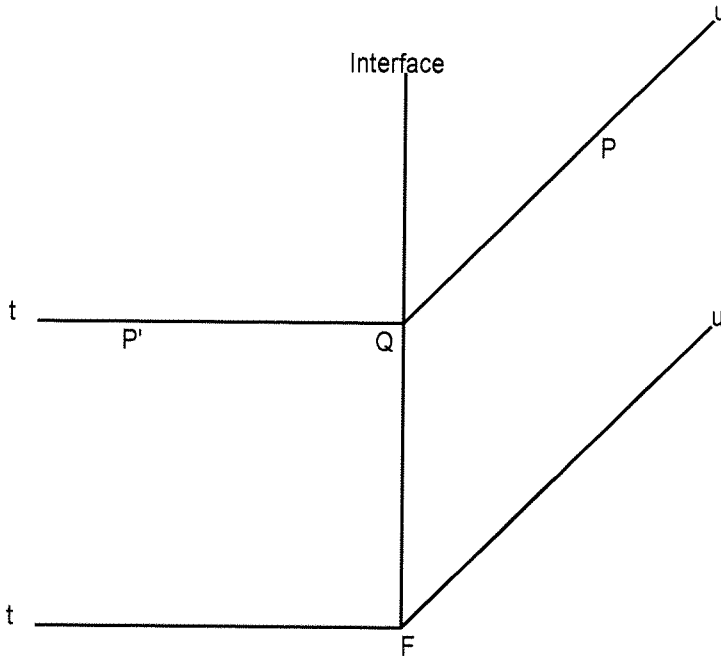
Figure 2.1: Paths of integration for o

It is to be noted that in this case, where the rotational degree of freedom is included, initial values shall need to be specified for both o on the characteristic slice, and for O on the interface. The initial value for $O(1)$ can be found from equation(2.192), while for the initial values for o on the characteristic slice we shall need to integrate equation(2.248) to obtain a value for o at each point. We then proceed as before.

Although o only exists as an evolution variable in the characteristic region, in the same way that we have constructed o in the characteristic region as a sum of integrals with respect to u and y, in the Cauchy region we can express o as a sum of integrals with respect to t and r. Thus we have

$$o_{P'} = \int_F^P \frac{1}{r} e^{4\psi} \omega_{,r} \; dt + \frac{1}{r} e^{4\psi} \omega_{,t} \; dr \tag{2.249}$$

where F is a fixed initial point, and P is the point at which o is being defined.

For the Piran interior o we use $\Psi(t,r)$, $\Omega(t,r)_{,t}$ and $\Omega(t,r)_{,r}$ as defined and calculated from the metric forms of [16]. Then

$$o = \int_F^P \frac{1}{r} e^{4\Psi} \Omega_{,r} \, dt + \int_F^P \frac{1}{r} e^{4\Psi} \Omega_{,t} \, dr \tag{2.250}$$

where Ψ is as given previously, and the derivatives of Ω are given by

$$
\begin{aligned}
\Omega_{,r} = -\tilde{a}\sqrt{\alpha^2 - 1} \Bigg(& \frac{\Xi_{,r}(\lambda_v + \lambda_u)^2 + 2\Xi(\lambda_v + \lambda_u)(\lambda_{v,r} + \lambda_{u,r})}{\sqrt{\lambda_u \lambda_v}[\alpha^2(1 - \lambda_u \lambda_v)^2 + (\lambda_v + \lambda_u)^2]} \\
& - \frac{\Xi(\lambda_v + \lambda_u)^2}{\lambda_u \lambda_v [\alpha^2(1 - \lambda_u \lambda_v)^2 + (\lambda_v + \lambda_u)^2]^2} \times \\
& \left(\frac{1}{2} \frac{\lambda_u \lambda_{v,r} + \lambda_{u,r} \lambda_v}{\sqrt{\lambda_u \lambda_v}} [\alpha^2(1 - \lambda_u \lambda_v)^2 + (\lambda_v + \lambda_u)^2] \right. \\
& + 2\sqrt{\lambda_u \lambda_v}[(\lambda_v + \lambda_u)(\lambda_{v,r} + \lambda_{u,r}) \\
& \left. \left. - \alpha^2(1 - \lambda_u \lambda_v)(\lambda_u \lambda_{v,r} + \lambda_{u,r} \lambda_v)] \right) \right)
\end{aligned} \tag{2.251}
$$

$$
\begin{aligned}
\Omega_{,t} = -\tilde{a}\sqrt{\alpha^2 - 1} \Bigg(& \frac{\Xi_{,t}(\lambda_v + \lambda_u)^2 + 2\Xi(\lambda_v + \lambda_u)(\lambda_{v,t} + \lambda_{u,t})}{\sqrt{\lambda_u \lambda_v}[\alpha^2(1 - \lambda_u \lambda_v)^2 + (\lambda_v + \lambda_u)^2]} \\
& - \frac{\Xi(\lambda_v + \lambda_u)^2}{\lambda_u \lambda_v [\alpha^2(1 - \lambda_u \lambda_v)^2 + (\lambda_v + \lambda_u)^2]^2} \times \\
& \left(\frac{1}{2} \frac{\lambda_u \lambda_{v,t} + \lambda_{u,t} \lambda_v}{\sqrt{\lambda_u \lambda_v}} [\alpha^2(1 - \lambda_u \lambda_v)^2 + (\lambda_v + \lambda_u)^2] \right. \\
& + 2\sqrt{\lambda_u \lambda_v}[(\lambda_v + \lambda_u)(\lambda_{v,t} + \lambda_{u,t}) \\
& \left. \left. - \alpha^2(1 - \lambda_u \lambda_v)(\lambda_u \lambda_{v,t} + \lambda_{u,t} \lambda_v)] \right) \right)
\end{aligned} \tag{2.252}
$$

with

$$\lambda_u = \frac{1}{\tilde{a}}\left[(\tilde{a}^2 + (t - r)^2)^{1/2} - (t - r)\right] \tag{2.253}$$

$$\lambda_v = \frac{1}{\tilde{a}}\left[(\tilde{a}^2 + (t + r)^2)^{1/2} + t + r\right] \tag{2.254}$$

$$\Xi = 1 + \lambda + u\lambda_v + 2\sqrt{1 - \alpha^{-2}}\sqrt{\lambda_u \lambda_v} \tag{2.255}$$

$$\lambda_{u,r} = \frac{1}{\tilde{a}}\left[\frac{r - t}{\tilde{a}^2 + (t - r)^2} + 1\right] \tag{2.256}$$

$$\lambda_{v,r} = \frac{1}{\tilde{a}}\left[\frac{t + r}{\tilde{a}^2 + (t + r)^2} + 1\right] \tag{2.257}$$

$$\Xi_{,r} = (\lambda_u \lambda_{v,r} + \lambda_{u,r} \lambda_v)\left(1 + \sqrt{\frac{1 - \alpha^{-2}}{\lambda_u \lambda_v}}\right) \tag{2.258}$$

$$\lambda_{u,t} = \frac{1}{\tilde{a}}\left[\frac{t - r}{\tilde{a}^2 + (t - r)^2} - 1\right] \tag{2.259}$$

$$\lambda_{v,t} = \frac{1}{\tilde{a}}\left[\frac{t + r}{\tilde{a}^2 + (t + r)^2} + 1\right] \tag{2.260}$$

$$\Xi_{,t} = (\lambda_u \lambda_{v,t} + \lambda_{u,t} \lambda_v)\left(1 + \sqrt{\frac{1 - \alpha^{-2}}{\lambda_u \lambda_v}}\right) \tag{2.261}$$

For the interior part of the evolving o we shall express the integrands in terms of the Cauchy evolution variables, namely ψ, ω, L_z^ϕ and $\tilde{L}$. We can write, from equation (15) of [15]

$$\omega_{,t} = -2e^{-4\psi}L_z^\phi \tag{2.262}$$

so that o can be expressed in terms of the Cauchy evolution variables thus:

$$o = \int_F^P \frac{1}{r}e^{4\psi}\omega_{,r}\,dt + \int_F^P \frac{1}{r}(-2L_z^\phi)\,dr \tag{2.263}$$

i.e.

$$o = \frac{1}{r}\int_F^P e^{4\psi}\omega_{,r}\,dt - 2\int_F^P \frac{1}{r}L_z^\phi\,dr \tag{2.264}$$

Thus we now possess explicit expressions for o both in terms of the evolving variables and the analytic forms of Piran. The first case, which we shall refer to as the evolving o, is given by equation(2.264) in the Cauchy region and simply by the evolution variable o in the characteristic region. The second case taken from [16] is given by equation(2.250) in the Cauchy region and equation(2.248) in the characteristic region, and shall be referred to as Piran's o.

2.5 Numerical Integration

2.5.1 Procedure for computing the integrals

The expressions for o which have been obtained involve a sum of two integrals. In the Cauchy region these are with respect to t and r, while in the exterior characteristic region the integrals are with respect to u and y. In the case where there is no rotational degree of freedom present, $\omega = 0$ throughout. Since the Geroch potential o is defined in terms of derivatives of ω, clearly $o = 0$ also, or equivalently $w = 0$. This also fixes O and W

as zero. This significantly simplifies the initialisation of these variables. Unfortunately when ω is non–zero, o and O are also non–zero, and cannot be expressed in terms of the other variables except in terms of an integral. Thus in order to establish values for the evolving o on the initial characteristic slice at each grid–point $y(i)$ there is no suitable alternative method than to numerically integrate

$$
\begin{aligned}
o = & -\int_F^Q e^{4\Psi(u,y)}(\frac{1}{2}y^5\Omega(u,y),_y + y^2\Omega(u,y),_u)\, du \\
& + \int_Q^P e^{4\Psi(u,y)}y^2\Omega(u,y),_y\, dy
\end{aligned} \tag{2.265}
$$

We have set the fixed point F as the interface point on the initial slice. Thus the du integral above has limits F and Q, which in this case are the same point. Recall that Q is defined as the interface point on the slice in question. Hence the expression for o which is to be integrated via a numerical method reduces to

$$
o(i) = \int_{y(1)}^{y(i)} e^{4\Psi(i)}[y(i)]^2\Omega,_y(i)\, dy \tag{2.266}
$$

Once these values have been calculated, they can then be evolved in conjunction with the other variables to form the basis of the numerical scheme. All other evolution variables are initialised via their derivations from the formulae of Piran et al. [16] and no further integration is required throughout the evolution proper. However, as noted previously o can only be explicitly expressed in terms of integrals. Thus when calculating the values of Piran's o–function for the purpose of computing the errors involved in the evolution, numerical integration is again the only means by which these values may be obtained. The same is true for the Cauchy part of the evolving o–function. It is important to remember that these numerical integrations are not a part of the evolution process, merely a means by which the accuracy of the code can be determined.

In each case, the expressions obtained for o (with the exception of the evolving o in the code itself) involve one integral along the Cauchy–characteristic slice (t =constant in the Cauchy region, and $u = constant$ in the characteristic region), and one other in a direction parallel to the direction of propagation of the slices. That is, in the interior region, there is an integral with respect to time, and in the characteristic regime the second integral is with respect to the null variable u, although for purposes within the code we have $u = t - r_{interface}$, or rather $u = t - 1$. Since the code employs a second–order

accurate differencing scheme, with information stored on three successive time–levels, it is clear that in order to calculate the integrals in directions orthogonal to the slices, it will be neccessary to calculate a piece at each time–step, and then take a cumulative total from the initial slice to the current level.

The method employed in order to calculate the time integral up the interface was to evaluate the integrand at the mid–point between r_n^j and r_n^{j+1}, the time slice at that moment in the evolution being number $j + 1$, and then multiply the result by the spacing between time levels, i.e. Δt. Equivalently in the characteristic portion we do the analagous thing to calculate the u integral, taking the value of the relevant integrand at the mid–point between y_1^j and y_1^{j+1} and multiplying this by the spacing between null hypersurfaces, Δu.

Here the fixed initial point F which appears as the lower limit on the integrals which make up the o function is taken to be the interface point on the initial slice. This makes it simple to construct the o–function. The first integral with respect to t or u is cumulatively calculated up the interface as far as point Q, then the second integral with respect to the radial variable r or y is numerically calculated along the relevant slice as far as the point in question, P.

We then apply a numerical integration routine, which combines a trapezoidal integration method with a polynomial interpolation routine, to calculate o along the slices. This produces a value for each grid point in the Piran–o scheme, and for Cauchy points with the evolving–o scheme. We can then perform a comparison between the evolving–o and Piran's–o.

Thus this modified version of the original code has three comparison functions, ψ and γ as before, and the Geroch potential function o. These were then used to establish the accuracy of the code in the case of Piran's family of exact solutions [16].

2.6 Convergence results

The code when compared with the Weber–Wheeler wave [22] had showed robust second–order convergence [15]. The modified code, produced in order to examine its performance when evolving with solutions containing two degrees of freedom [16] had also been programmed to second–order accuracy. However, the neccessary change of variable
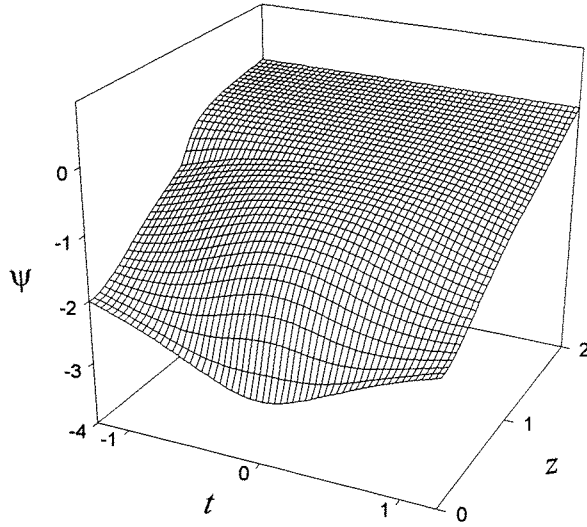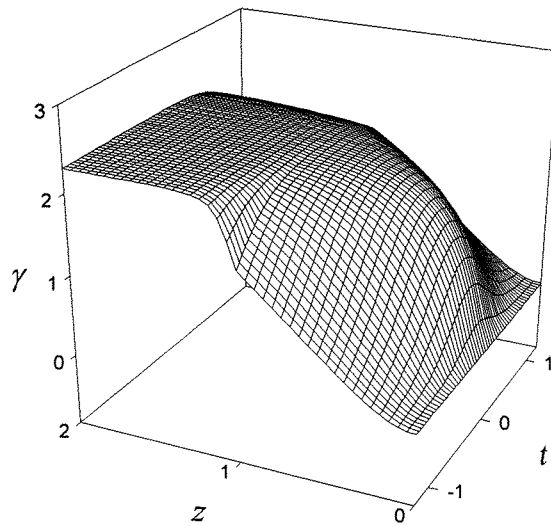
Figure 2.2: Function plot for ψ.

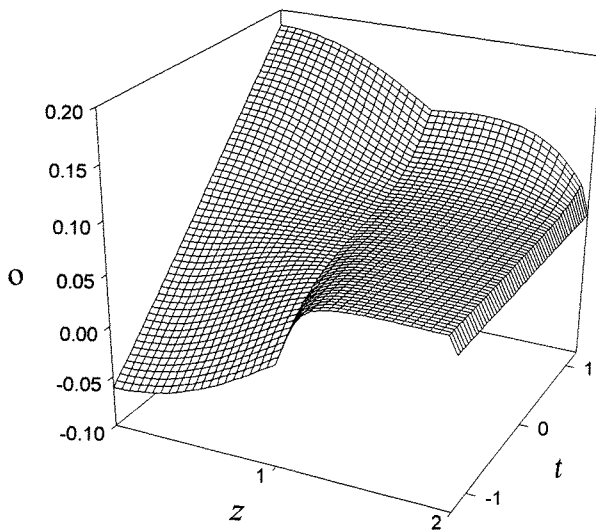Figure 2.3: Function plot for γ.

65

Figure 2.4: Function plot for o.

in the characteristic region from w to o, and especially the initialisation of this variable by means of a numerical integration method, was expected to reduce the accuracy of the evolution. The degree of this reduction in accuracy was something we wished to determine.

Figures 2.2 – 2.4 show plots of the three comparison functions Ψ, Γ and o, from the analytic prescription of [17]. Ψ and Γ are both symmetric in time. Ψ corresponds to the translational mode, and the main activity is in the Cauchy region, near the centre of the system. A pulse comes in from infinity, the centre coincides with the $r = 0$ axis when $t = 0$, and then the pulse rebounds. Γ corresponds to the energy of the system, and again we see more activity in the Cauchy region than the characteristic. As might be expected, there is a build up of energy around the $r = 0$ axis for $t \sim 0$, when the pulse has come in and is about to rebound. The graph of o, the Geroch potential is more difficult to interpret, since unlike Ψ and Γ it has less of a clear physical meaning.

The evolving variables ψ and γ were compared with the corresponding Piran functions as follows. A value was chosen for the parameter which determines how often output is drawn from the evolving data. This value is typically in the region of 20. Then in that case, after the original slice data is taken from the 20th, 40th, 60th slices, and so on. On each of these designated slices the pointwise error for ψ and γ is calculated

at each point using a formula of the following form:

$$\xi(\psi)_i = \psi(z_i)_{exact} - \psi(z_i)_{evolved} \qquad (2.267)$$

and similarly for $\xi(\gamma)$. The functions ψ and γ labelled as '*exact*' are those taken from the formulae of [16], in standard form in the Cauchy region and in their regularised (barred) forms in the characteristic region. z_i is the value at the ith point of the grid of the spatial coordinate which combines the r and y coordinates into one coordinate as follows.

$$z = \begin{cases} r & \text{for } 0 \leq z \leq 1 \\ 2 - y & \text{for } 1 \leq z \leq 2 \end{cases} \qquad (2.268)$$

The use of this unifying coordinate enables plots across the whole radial range to be produced. In interpreting these, however, it is important to appreciate that when $z > 1$, the physical spacing between adjacent z points is not uniform, since $y = r^{-1/2}$. Hence as z increases beyond the interface point, situated at $z = 1$, the distance between adjacent points increases, even though on the grid itself Δz is constant. This means that on the plots with z as the spatial coordinate the graph is distorted once $z \geq 1$. However, the general trends in behaviour can be clearly seen. To define the pointwise error for our o function we state the following.

$$\xi(o)_i = o(z_i)_{exact} - o(z_i)_{evolved} \qquad (2.269)$$

where o_{exact} is the function previously defined as Piran's o, and $o_{evolved}$ is that previously defined as the evolving o. These pointwise errors are plotted here, (figures 2.5 - 2.7), with the appropriate functions above, in surface plots for times ranging from -1.25 to 1.25. Here the curvature parameter α was taken as 2. The length scale $\tilde{a}$ was equal to 0.5, thus the quantity $t/\tilde{a}$ satisfies

$$\left| \frac{t}{\tilde{a}} \right| \leq 2.5 \qquad (2.270)$$

Since the real time has no physical meaning without reference to the length scale, this gives a more realistic indication of the period of evolution. For example, if a very large value of $\tilde{a}$ were chosen, say $\tilde{a} = 10$, the scheme would run for about 25 time units, but this would give no additional information.

Different values of $\tilde{a}$ gave similar plots to those shown but on different scales. When α was set equal to 1, Minkowski spacetime was recovered. For values of α greater than

about 10 singular behaviour was observed. For ease of viewing the parameters were assigned the values $\alpha = 2$, $\tilde{a} = 0.5$ for all plots shown here.
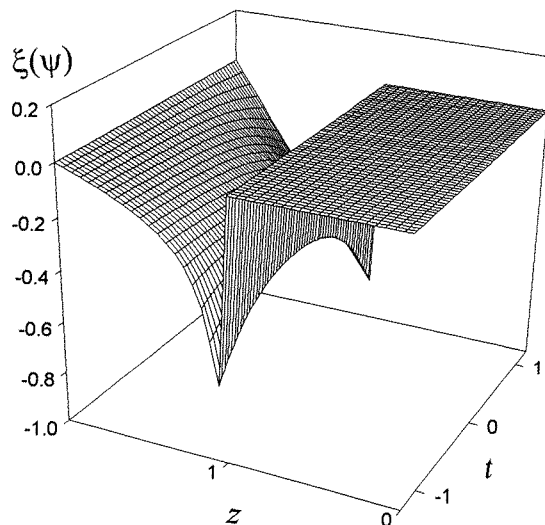

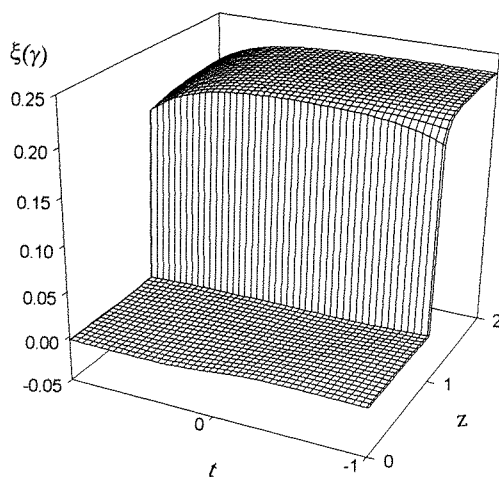Figure 2.5: Pointwise errors for ψ, multiplied by 10^4.

Figure 2.6: Pointwise errors for γ, multiplied by 10^4.

The errors as shown in figures (2.4) to (2.6) were obtained with $\alpha = 2$ and $\tilde{a} = 0.5$. It is here that the effect of numerically initialising the evolution variable o in the
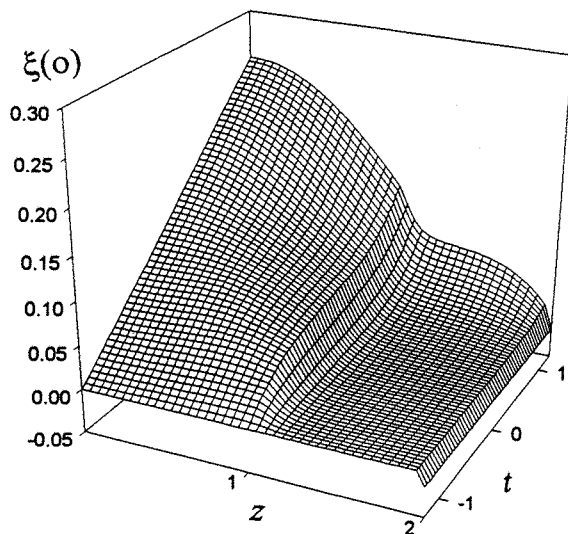
Figure 2.7: Pointwise errors for o, multiplied by 10^4.

characteristic region can be seen. In the Cauchy region, $0 \leq z \leq 1$, the errors for ψ and γ are small. The errors shown for o in the Cauchy region have little significance since they only give the differences between two numerically calculated integrals. Recall that o only evolves in the characteristic region. However in the characteristic region, $1 \leq z \leq 2$, the errors for o are significantly smaller. Notice however the shearing effect at the interface as t increases from its starting value -1. This indicates a loss of accuracy in the non–evolving o as it was calculated along the interface. This was not unexpected, since the only way of calculating the du portion of the integral, up the interface, was to evaluate the integral for each section between successive slices and sum from the first slice to the current one. The graph suggests that errors in the calculation of the dy integral were less significant. A similar jump in error at the interface was observed for ψ and γ, and the strong interrelations between evolution variables meant that the error in numerically initializing o contaminated these variables as well.

Thus the need to set initial values for the evolution variable o via a numerical integration method greatly affected the errors of the scheme. Were it not for the singular behaviour of Ω, this function could have been used instead. It could have been initialised without the use of numerical integration, and would almost certainly have given much

smaller errors. However in the case of the exact solution being used this was not possible, and so we were constrained to the use of numerics in spite of the loss of accuracy incurred.

In order to determine the rate of convergence the norms would need to be calculated for each of these functions. Previously when the rotational degree of freedom was absent, the code displayed second order convergence, and the l_2 norm was required to show this. However, on this occasion second order convergence was not observed. We therefore need to consider instead the l_1 norm. This is defined as

$$l_1 = \frac{1}{N} \sum |f(z_i)_{exact} - f(z_i)_{evolved}| \tag{2.271}$$

The values of this function were computed at each time slice for each of the three comparison functions, ψ, γ and o. These values are plotted in figures 2.8—2.10. Note that in each case the y–axis shows the norm multiplied by 10^4 for convenience. As would be expected the norm for o was the largest of the three. All three graphs show an increasing trend as the evolution progressed as one would predict. The reason for the fluctuations in the norm for Γ is unclear, however the graphics show l_1 norms of reasonable order.
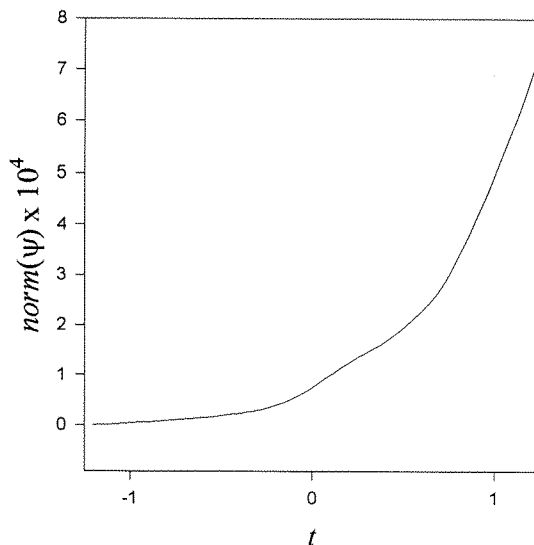
Figure 2.8: Plot of the l1 norm for ψ.

Table 2.1 shows the values of the $l1$ norm of the three functions, ψ, γ and o at $t = 0$, for a range of grid resolutions. Each time the number of grid points is doubled,
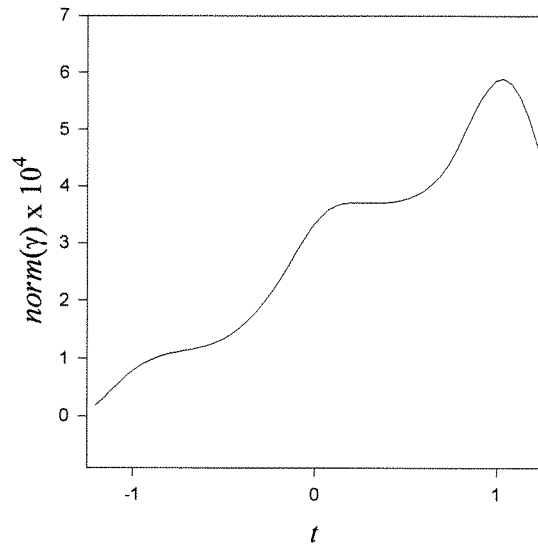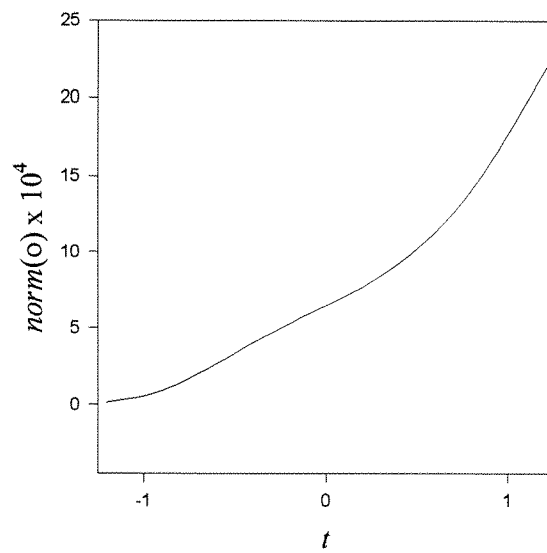
Figure 2.9: Plot of the l1 norm for γ.

Figure 2.10: Plot of the l1 norm for o.

71

Grid Points	Norm l_1 for ψ	Factor	Norm l_1 for γ	Factor	Norm l_1 for o	Factor
75	$1.036\mathrm{x}10^{-3}$	-	$4.709\mathrm{x}10^{-3}$	-	$8.741\mathrm{x}10^{-3}$	-
150	$2.877\mathrm{x}10^{-4}$	3.6	$1.308\mathrm{x}10^{-3}$	3.6	$2.498\mathrm{x}10^{-3}$	3.5
300	$7.378\mathrm{x}10^{-5}$	3.9	$3.352\mathrm{x}10^{-4}$	3.9	$6.574\mathrm{x}10^{-4}$	3.7
600	$1.845\mathrm{x}10^{-5}$	4.0	$8.382\mathrm{x}10^{-5}$	4.0	$1.685\mathrm{x}10^{-4}$	3.9

Table 2.1: Convergence results for Piran's solution at time $t = 0$

for first order convergence the norm should decrease by a factor of 2 and then by a further factor of 2 since the time–step is also automatically halved. Thus overall the norm would be expected to show a decrease by a factor of 4 each time the resolution is doubled. In Table 2.1 the resolution refers to the number of grid points in both the Cauchy and characteristic regions, thus the total number of grid points is twice the resolution. The columns labelled 'factor' show the factor by which the l_1 norm for each of the three functions has decreased from the previous resolution. This shows that the function o displays only first order convergence. This was predicted due to the neccessary construction of this function through numerical integration methods. This meant that even if the evolving o was accurate to second order, the function constructed from Piran's solution which was used to test the convergence would show only first order convergence. The fact that the other two functions, ψ and γ, also showed first–order rather than second–order convergence was more surprising. It had been hoped that the use of the integration routine to set initial values for o would have only a minimal effect on the accuracy of the evolution. Indeed it is not obvious as to why this initial procedure should cause the accuracy to be reduced to this extent. The variables are all closely interrelated, and this would explain some of this reduction in the order of convergence of the variables ψ and γ. Thus the revised code displays first–order convergence in all three comparison functions, ψ, γ and o. The adjustments neccessary to cope with Piran's solution had been more involved than expected, but the problems that were generated were overcome. Therefore the code had been tested in a case where both degrees of freedom were involved. Furthermore, the exact solution of Piran is not asymptotically flat. Despite the fact that the convergence is less rapid than for the case where there

was no rotational degree of freedom present, this still shows that the amended code was able to successfully reproduce the functions as prescribed from the solution of Piran.

Chapter 3

Principal Null Directions

3.1 Motivation

The methods described previously have been able to show the accuracy of the code, but involve computing metric functions which are coordinate dependent. The idea has been suggested of employing instead principal null directions (PNDs), which provide gauge–invariant information about solutions of Einstein's equations. Principal null direction calculations are generally approached through the use of spinors and null tetrads, while numerical relativity traditionally utilises ADM '3 + 1' slicing to produce a series of 3–dimensional spacelike slices. At first sight these two approaches seem irreconcilable. However, a method for computing PNDs from a '3 + 1' scenario, assuming as an input the intrinsic metric and extrinsic curvature on a spacelike slice, has recently been proposed by Gunnarsen et al. [17]. This method makes PNDs more accessible to numerical relativistic schemes, and could provide a suitable bridge between the two previously separate approaches. The advantages of this would be appreciable. For example, the orientation of the PNDs relative to each other can determine the Petrov type of the system. Hence if the four PNDs could be calculated at various points on each evolution slice, then a spacetime 'map' of the PNDs could be produced. This would then clearly demonstrate the generic behaviour at each designated point, from the relationship between PND directions and Petrov type as shown overleaf. In Table 3.1 it is assumed that further to the conditions stated, the remaining PND directions are all distinct and in a different direction to those already considered. In this context, however, a direction is considered

Relative directions of PNDs	Petrov type
Four distinct directions	Type I
One identical pair	Type II
Three identical directions	Type III
Two distinct pairs of directions	Type D
All in same direction	Type N
$\Psi = 0$	Type O

Table 3.1: Petrov types

as a vector direction, that is $\mathbf{v}$ and $-\mathbf{v}$ have the same direction. An introduction to the Petrov classification can be found in, e.g. [23].

In [17] the '3+1' method is applied to Kastor–Traschen solutions to obtain various 'snapshot' PND pictures with various configurations of black holes. Our aim is to produce similar pictures of our vacuum cylindrically symmetric solutions at various time intervals.

3.2 The '3+1' method for computing PNDs

We outline the method for calculating the PNDs as proposed in [17]. The input required is the induced 3–dimensional metric h_{ab}, and extrinsic curvature p_{ab}, of the spacelike hypersurface Σ, and the method finally outputs the projections of the PNDs in that hypersurface. The constraint equations are

$$R - p_{ab}p^{ab} + p^2 = 2\Lambda \tag{3.1}$$

$$D_a(p^{ab} - ph^{ab}) = 0 \tag{3.2}$$

Here p and R are the fully contracted forms of p_{ab} and R_{ab}. Note that it is the 3–metric that is used to raise and lower indices. Thus $p = p_{ab}h^{ab}$ and $R = R_{ab}h^{ab}$. D_a is the unique torsion free derivative operator compatible with the 3–metric. The electric and magnetic field tensors are defined by:

$$E_{ab} = R_{ab} - p_a^m p_{bm} + p p_{ab} - \frac{2}{3}\Lambda h_{ab} \tag{3.3}$$

$$B_{ab} = \varepsilon_{a|}^{\ mn} D_m p_{n|p} \tag{3.4}$$

75

respectively, where ε_{abc} is the Levi–Civita alternating tensor, with $\varepsilon_{abc}\varepsilon^{abc} = 3!$. Both tensors are symmetric and trace–free by virtue of the constraint equations (3.1) and (3.2). A unit vector field $\hat{z}^a$ in the slice Σ is selected, and the tensor fields E_{ab} and B_{ab} are then decomposed into components along and perpendicular to $\hat{z}^a$. The following quantities are then defined

$$s_{ab} = h_{ab} - \hat{z}_a \hat{z}_b \tag{3.5}$$

$$e = E_{ab}\hat{z}^a \hat{z}^b \tag{3.6}$$

$$e_a = E_{bc}\hat{z}^b \left(\delta_a^c - \hat{z}_a \hat{z}^c\right) \tag{3.7}$$

$$e_{ab} = E_{cd}\left(\delta_a^c - \hat{z}_a \hat{z}^c\right)\left(\delta_b^d - \hat{z}_b \hat{z}^d\right) + \frac{1}{2}e s_{ab} \tag{3.8}$$

$$b = B_{ab}\hat{z}^a \hat{z}^b \tag{3.9}$$

$$b_a = B_{bc}\hat{z}^b \left(\delta_a^c - \hat{z}_a \hat{z}^c\right) \tag{3.10}$$

$$b_{ab} = B_{cd}\left(\delta_a^c - \hat{z}_a \hat{z}^c\right)\left(\delta_b^d - \hat{z}_b \hat{z}^d\right) + \frac{1}{2}b s_{ab} \tag{3.11}$$

Note that in equation (10) of [17] the last term is erroneously given as $\frac{1}{2}e s_{ab}$ rather than $\frac{1}{2}b s_{ab}$. If a rotation by $\frac{\Pi}{2}$ in the plane orthogonal to the field $\hat{z}^a$ is denoted by

$$J_a{}^b \equiv \varepsilon_a{}^{bc}\hat{z}^c \tag{3.12}$$

and two orthogonal unit vector fields in the plane orthogonal to $\hat{z}^a$ are chosen and written $\hat{x}^a$ and $\hat{y}^a$, then we can define the complex null vector $\hat{m}^a$ by

$$\hat{m}^a = \frac{1}{\sqrt{2}}(\hat{x}^a - i\hat{y}^a) \tag{3.13}$$

Finally the Weyl scalars can be expressed in terms of these quantities as follows:

$$\Psi_0 = \left(-e_{ab} + J_a{}^c b_{bc}\right)m^a m^b \tag{3.14}$$

$$\Psi_1 = \frac{1}{\sqrt{2}}\left(e_a - J_a{}^c b_c\right)m^a \tag{3.15}$$

$$\Psi_2 = \frac{1}{2}\left(-e + ib\right) \tag{3.16}$$

$$\Psi_3 = \frac{1}{\sqrt{2}}\left(e_a + J_a{}^c b_c\right)\bar{m}^a \tag{3.17}$$

$$\Psi_4 = \left(-e_{ab} - J_a{}^c b_{bc}\right)\bar{m}^a \bar{m}^b \tag{3.18}$$

Once these Weyl scalars have been calculated, then the PNDs can be obtained by finding the roots of the quartic

$$\Psi_4 z^4 + 4\Psi_3 z^3 + 6\Psi_2 z^2 + 4\Psi_1 z + \Psi_0 = 0 \tag{3.19}$$

For each root, z_i say, (i=1,...,4), writing

$$z_i = \tan(\theta_i/2)e^{-i\phi_i} \qquad (3.20)$$

then the unit vectors, $P_{(i)}{}^a$ describe the principal null direction, where

$$P_{(i)}{}^a = \cos\theta_i \hat{z}^a + \sin\theta_i \cos\phi_i \hat{x}^a + \sin\theta_i \sin\phi_i \hat{y}^a \qquad (3.21)$$

Thus in the four-dimensional scheme, $t^a + P_{(i)}{}^a$ is a principal null direction for each i ($i \in \{1, 2, 3, 4\}$) where t^a is the unit normal to the slice Σ in the original four–manifold.

3.2.1 Solving the Weyl quartic

It is clear from the previous section that in order to calculate the PNDs it is neccessary to solve equation (3.19). The d'Inverno–Russell–Clark method is used for this purpose [24]. First, substituting $y = \Psi_4 z + \Psi_3$ into (3.19), the equation becomes

$$y^4 + 6Hy^2 + 4Gy + K = 0 \qquad (3.22)$$

where

$$I = \Psi_4\Psi_0 - 4\Psi_1\Psi_3 + 3\Psi_2^2 \qquad (3.23)$$

$$J = \begin{vmatrix} \Psi_4 & \Psi_3 & \Psi_2 \\ \Psi_3 & \Psi_2 & \Psi_1 \\ \Psi_2 & \Psi_1 & \Psi_0 \end{vmatrix} \qquad (3.24)$$

$$K = \Psi_4^2 I - 3H^2 \qquad (3.25)$$

$$H = \Psi_4\Psi_2 - \Psi_3^2 \qquad (3.26)$$

$$G = \Psi_4^2\Psi_1 - 3\Psi_4\Psi_3\Psi_2 + 2\Psi_3^3 \qquad (3.27)$$

The solutions to (3.22) are more easily expressed in terms of the solutions to the reducing cubic,

$$\lambda^3 - I\lambda + 2J = 0 \qquad (3.28)$$

These solutions are misquoted in [17] and should be stated as

$$\lambda_1 = \left(P + \frac{I}{3P}\right) \qquad (3.29)$$

$$\lambda_2 = \left(e^{2\Pi i/3}P + e^{4\Pi i/3}\frac{I}{3P}\right) \qquad (3.30)$$

$$\lambda_3 = \left(e^{4\Pi i/3}P + e^{2\Pi i/3}\frac{I}{3P}\right) \qquad (3.31)$$

77

where

$$P = \left[-J + \sqrt{J^2 - (I/3)^3} \right]^{1/3} \tag{3.32}$$

Although the expressions for P and the roots λ_i in [17] satisfy the reducing cubic (3.22), they finally produce roots for the quartic equation which are inconsistent with those obtained from [25] and with the formulation of [24], from which they were taken. The next step is to define three complex numbers α, β, γ, by

$$\alpha^2 = 2\Psi_4\lambda_1 - 4H \tag{3.33}$$

$$\beta^2 = 2\Psi_4\lambda_2 - 4H \tag{3.34}$$

$$\gamma^2 = 2\Psi_4\lambda_3 - 4H \tag{3.35}$$

where the signs are determined by the constraint

$$\alpha\beta\gamma = 4G \tag{3.36}$$

Now, [17] gives

$$\gamma^2 = \alpha^2 + \beta^2 + 4H \tag{3.37}$$

However, this in conjunction with (3.35) yields

$$
\begin{aligned}
2\Psi_4\lambda_3 - 4H &= \alpha^2 + \beta^2 + 4H \\
&= 2\Psi_4\lambda_1 - 4H + 2\Psi_4\lambda_2 - 4H + 4H \\
\Rightarrow \lambda_3 &= \lambda_1 + \lambda_2
\end{aligned} \tag{3.38}
$$

From (3.29) – (3.31) this would require that

$$\left(P + \frac{I}{3P} \right) + \left(e^{2\Pi i/3} P + e^{4\Pi i/3} \frac{I}{3P} \right) - \left(e^{4\Pi i/3} P + e^{2\Pi i/3} \frac{I}{3P} \right) = 0 \tag{3.39}$$

Thus taking real parts of (3.39) we obtain

$$P + \frac{I}{3P} - \frac{1}{2}P - \frac{1}{2}\frac{I}{3P} + \frac{1}{2}P + \frac{1}{2}\frac{I}{3P} \neq 0 \tag{3.40}$$

and taking the imaginary parts,

$$\frac{\sqrt{3}}{2}P - \frac{\sqrt{3}}{2}\frac{I}{3P} + \frac{\sqrt{3}}{2}P - \frac{\sqrt{3}}{2}\frac{I}{3P} \neq 0 \tag{3.41}$$

So clearly the expression given for γ^2 (3.37) is incorrect. Following the method of [25] we have

$$\begin{aligned}
\lambda_3 &= (\gamma^2 + 4H)/2\Psi_4 \\
&= -(8H + \alpha^2 + \beta^2)/2\Psi_4 \\
\Rightarrow \gamma^2 &= -\left(\alpha^2 + \beta^2 + 12H\right)
\end{aligned} \tag{3.42}$$

Thus the expression for γ^2 in terms of α^2, β^2 and H should read

$$\gamma^2 = -\left(\alpha^2 + \beta^2 + 12H\right) \tag{3.43}$$

Finally we obtain four complex numbers which are the solutions of (3.19). They are given by

$$z_1 = -\left[\Psi_3 + \frac{1}{2}(\alpha + \beta + \gamma)\right]/\Psi_4 \tag{3.44}$$

$$z_2 = -\left[\Psi_3 + \frac{1}{2}(\alpha - \beta - \gamma)\right]/\Psi_4 \tag{3.45}$$

$$z_3 = -\left[\Psi_3 + \frac{1}{2}(-\alpha + \beta - \gamma)\right]/\Psi_4 \tag{3.46}$$

$$z_4 = -\left[\Psi_3 + \frac{1}{2}(-\alpha - \beta + \gamma)\right]/\Psi_4 \tag{3.47}$$

If each of the z_i is then written $z_i = |z_i|e^{i\arg(z_i)} = \tan(\theta_i/2)e^{-i\phi_i}$ then the projections of the four PNDs in the spacelike slice Σ are given by the unit vectors

$$P^a_{(i)} = \cos\theta_i \hat{z}^a + \sin\theta_i \cos\phi_i \hat{x}^a + \sin\theta_i \sin\phi_i \hat{y}^a \tag{3.48}$$

3.3   Calculation of the Weyl scalars

To remain consistent with the notation of [17] we shall let h_{ab} be the 3–metric on the spacelike slice Σ, and p_{ab} be the extrinsic curvature of Σ. Here the indices a and b can each take three values. We shall consider here the method of [17] as applied to the general vacuum cylindrical case. In our (t, r, ϕ, z) coordinates the full metric is

$$g_{ij} = \begin{pmatrix} -e^{2(\psi - \gamma)} & 0 & 0 & 0 \\ 0 & e^{2(\psi - \gamma)} & 0 & 0 \\ 0 & 0 & r^2 e^{-2\psi} + \omega^2 e^{2\psi} & \omega e^{2\psi} \\ 0 & 0 & \omega e^{2\psi} & e^{2\psi} \end{pmatrix} \tag{3.49}$$

Thus the induced 3–metric on a constant time slice in (r, ϕ, z) coordinates is

$$
h_{ab} = \begin{pmatrix} e^{2(\psi-\gamma)} & 0 & 0 \\ 0 & r^2 e^{-2\psi} + \omega^2 e^{2\psi} & \omega e^{2\psi} \\ 0 & \omega e^{2\psi} & e^{2\psi} \end{pmatrix} \tag{3.50}
$$

with contravariant components

$$
h^{ab} = \begin{pmatrix} e^{2(\gamma-\psi)} & 0 & 0 \\ 0 & r^{-2} e^{2\psi} & -\omega r^{-2} e^{2\psi} \\ 0 & -\omega r^{-2} e^{2\psi} & e^{-2\psi} + \omega^2 r^{-2} e^{2\psi} \end{pmatrix} \tag{3.51}
$$

The extrinsic curvature components have previously been calculated to be

$$
p_{rr} = -\chi_{,t} e^{\chi} \tag{3.52}
$$

$$
p_{\phi\phi} = r^2 \psi_{,t} e^{-\psi-\gamma} - \omega\omega_{,t} e^{3\psi-\gamma} - \omega^2 \psi_{,t} e^{3\psi-\gamma} \tag{3.53}
$$

$$
p_{\phi z} = -e^{3\psi-\gamma}\left(\frac{1}{2}\omega_{,t} + \omega\psi_{,t}\right) \tag{3.54}
$$

$$
p_{zz} = -\psi_{,t} e^{3\psi-\gamma} \tag{3.55}
$$

where since p_{ab} is symmetric, $p_{z\phi} = p_{\phi z}$ and the other components are zero. The non–zero contravariant components of the extrinsic curvature in (r, ϕ, z) coordinates are given by

$$
p^{rr} = -e^{-3\chi}\chi_{,t} \tag{3.56}
$$

$$
p^{\phi\phi} = r^{-2} e^{2\psi-\chi}\psi_{,t} \tag{3.57}
$$

$$
p^{\phi z} = -\frac{1}{2r^2} e^{2\psi-\chi}(\omega_{,t} + 2\omega\psi_{,t}) = p^{z\phi} \tag{3.58}
$$

$$
p^{zz} = e^{-\chi}\left(r^{-2} e^{2\psi}(\omega^2 \psi_{,t} + \omega\omega_{,t}) - e^{-2\psi}\psi_{,t}\right) \tag{3.59}
$$

The tensors E_{ab} and B_{ab} were calculated using the expressions found for the components of the 3–metric and extrinsic curvature in the formulae of equations(3.3) and (3.4). The next step was to choose the three unit vector fields $\hat{x}^a$, $\hat{y}^a$, $\hat{z}^a$. For ease of plotting and interpretation, we chose a Cartesian frame XYZ, rather than a frame with the vectors pointing in the directions of $R\Phi Z$. In (t, r, ϕ, z) coordinates a standard cylindrically symmetric orthonormal frame is

$$
\hat{t}^a = \left(-e^{\psi-\gamma}, 0, 0, 0\right) \tag{3.60}
$$

80

$$\hat{r}^a = \left(0, e^{\psi-\gamma}, 0, 0\right) \tag{3.61}$$

$$\hat{\phi}^a = \left(0, 0, e^{\psi}/r, -\omega e^{\psi}/r\right) \tag{3.62}$$

$$\hat{z}^a = \left(0, 0, 0, e^{-\psi}\right) \tag{3.63}$$

with

$$\hat{t}^a \hat{t}_a = -\hat{r}^a \hat{r}_a = -\hat{\phi}^a \hat{\phi}_a = -\hat{z}^a \hat{z}_a = 1 \tag{3.64}$$

and all other combinations zero. The cylindrical polar basis $(\hat{r}, \hat{\phi}, \hat{z})$ and the Cartesian basis $(\hat{x}, \hat{y}, \hat{z})$ are connected by

$$\hat{\mathbf{r}} = \cos\phi\mathbf{i} + \sin\phi\mathbf{j} \tag{3.65}$$

$$\hat{\mathbf{\Phi}} = -\sin\phi\mathbf{i} + \cos\phi\mathbf{j} \tag{3.66}$$

$$\hat{\mathbf{z}} = \mathbf{k} \tag{3.67}$$

with reciprocal relations

$$\hat{\mathbf{x}} = \mathbf{i} = \cos\phi\hat{\mathbf{r}} - \sin\phi\hat{\mathbf{\Phi}} \tag{3.68}$$

$$\hat{\mathbf{y}} = \mathbf{j} = \sin\phi\hat{\mathbf{r}} + \cos\phi\hat{\mathbf{\Phi}} \tag{3.69}$$

$$\hat{\mathbf{z}} = \mathbf{k} = \hat{\mathbf{z}} \tag{3.70}$$

Hence, using equations (3.61) and (3.62) we get

$$\hat{x}^a = \cos\phi \begin{pmatrix} e^{\psi-\gamma} \\ 0 \\ 0 \end{pmatrix} - \sin\phi \begin{pmatrix} 0 \\ e^{\psi}/r \\ -\omega e^{\psi}/r \end{pmatrix} \tag{3.71}$$

$$\hat{y}^a = \sin\phi \begin{pmatrix} e^{\psi-\gamma} \\ 0 \\ 0 \end{pmatrix} + \cos\phi \begin{pmatrix} 0 \\ e^{\psi}/r \\ -\omega e^{\psi}/r \end{pmatrix} \tag{3.72}$$

The components of $\hat{x}^a, \hat{y}^a$ and $\hat{z}^a$ are then

$$\hat{x}^a = \begin{pmatrix} e^{\psi-\gamma}\cos\phi \\ -r^{-1}e^{\psi}\sin\phi \\ \omega r^{-1}e^{\psi}\sin\phi \end{pmatrix} \tag{3.73}$$

$$\hat{y}^a = \begin{pmatrix} e^{\psi-\gamma}\sin\phi \\ r^{-1}e^{\psi}\cos\phi \\ -\omega r^{-1}e^{\psi}\cos\phi \end{pmatrix} \tag{3.74}$$

$$\hat{z}^a = \begin{pmatrix} 0 \\ 0 \\ e^{-\psi} \end{pmatrix} \qquad (3.75)$$

The components e, e_a, e_{ab}, b, b_a and b_{ab} were calculated from the expressions in [17] and given previously here as (3.6)–(3.11). The specialist GR computer algebra system STENSOR was used to calculate these components, and this system was also used to obtain explicit expressions for the Weyl scalars, Ψ_0, Ψ_1, ..., Ψ_4 for our chosen unit vector fields $\hat{x}^a$, $\hat{y}^a$, $\hat{z}^a$. An outline of the capabilities and procedures of STENSOR and SHEEP can be found in [26].

The expressions obtained for the '3+1' Weyl scalars were as follows:

$$
\begin{aligned}
\Psi_0 &= \frac{1}{2}e^{2\psi-2\gamma}\Bigg[\left(2\cos^2\phi-1\right)\left(\gamma_{,t}\psi_{,t}-\gamma_{,r}\psi_{,r}+3\psi_{,r}^2+\psi_{,rr}-r^{-1}\psi_{,r}+\frac{1}{4}r^{-2}e^{4\psi}\omega_{,t}^2\right) \\
&\quad +e^{4\psi-2\gamma}r^{-3}\cos\phi\sin\phi\left(6\psi_{,r}\omega_{,t}-\gamma_{,r}\omega_{,t}-\gamma_{,t}\omega_{,r}+\omega_{,rt}-2r^{-1}\omega_{,t}\right)\Bigg] \\
&\quad + ie^{2\psi-2\gamma}\Bigg[\frac{1}{4}e^{4\psi-2\gamma}r^{-3}\left(2\cos^2\phi-1\right)\left(6\psi_{,r}\omega_{,t}-\gamma_{,r}\omega_{,t}-\gamma_{,t}\omega_{,r}+\omega_{,rt}-2r^{-1}\omega_{,t}\right) \\
&\quad +\cos\phi\sin\phi\left(\gamma_{,r}\psi_{,r}-\gamma_{,t}\psi_{,t}-3\psi_{,r}^2-\psi_{,rr}+r^{-1}\psi_{,r}-\frac{1}{4}e^{4\psi}r^{-2}\omega_{,t}^2\right)\Bigg] \qquad (3.76)
\end{aligned}
$$

$$
\begin{aligned}
\Psi_1 &= \frac{1}{4}r^{-1}e^{4\psi-2\gamma}\Bigg[\sin\phi\left(\gamma_{,t}\omega_{,t}-\gamma_{,r}\omega_{,r}+5\psi_{,r}\omega_{,r}-\psi_{,t}\omega_{,t}+\omega_{,rr}-r^{-1}\omega_{,r}\right) \\
&\quad +r^{-1}e^{-2\gamma}\cos\phi\left(4\psi_{,r}\psi_{,t}-2\gamma_{,r}\psi_{,t}-2\gamma_{,t}\psi_{,r}+2\psi_{,rt}+r^{-1}\gamma_{,t}-r^{-2}e^{4\psi}\omega_{,r}\omega_{,t}\right)\Bigg] \\
&\quad + \frac{1}{4}ir^{-1}e^{4\psi-2\gamma}\Bigg[\cos\phi\left(\gamma_{,t}\omega_{,t}-\gamma_{,r}\omega_{,r}+5\psi_{,r}\omega_{,r}-\psi_{,t}\omega_{,t}+\omega_{,rr}-r^{-1}\omega_{,r}\right) \\
&\quad +r^{-1}e^{-2\gamma}\sin\phi\left(2\gamma_{,r}\psi_{,t}+2\gamma_{,t}\psi_{,r}-4\psi_{,r}\psi_{,t}-2\psi_{,rt}-r^{-1}\gamma_{,t}+r^{-2}e^{4\psi}\omega_{,r}\omega_{,t}\right)\Bigg] (3.77)
\end{aligned}
$$

$$
\begin{aligned}
\Psi_2 &= \frac{1}{2}e^{2\psi-2\gamma}\Bigg[\gamma_{,t}\psi_{,t}-\gamma_{,r}\psi_{,r}+\psi_{,r}^2-2\psi_{,t}^2+\psi_{,rr}+r^{-1}\psi_{,r}-\frac{1}{4}r^{-2}e^{4\psi}\left(2\omega_{,r}^2+\omega_{,t}^2\right)\Bigg] \\
&\quad + \frac{1}{4}ir^{-2}e^{5\psi-3\gamma}\Bigg[2\psi_{,r}\omega_{,t}-\gamma_{,r}\omega_{,t}-\gamma_{,t}\omega_{,r}+4\psi_{,t}\omega_{,r}+\omega_{,rt}\Bigg] \qquad (3.78)
\end{aligned}
$$

$$
\begin{aligned}
\Psi_3 \;=\; & \frac{1}{4}r^{-1}e^{4\psi-2\gamma}\left[\sin\phi\left(\gamma_{,t}\omega_{,t}-\gamma_{,r}\omega_{,r}+5\psi_{,r}\omega_{,r}-\psi_{,t}\omega_{,t}+\omega_{,rr}-r^{-1}\omega_{,r}\right)\right. \\
& \left.+r^{-1}e^{-2\gamma}\cos\phi\left(2\gamma_{,r}\psi_{,t}+2\gamma_{,t}\psi_{,r}-4\psi_{,t}\psi_{,r}-2\psi_{,rt}-r^{-1}\gamma_{,t}+r^{-2}e^{4\psi}\omega_{,r}\omega_{,t}\right)\right] \\[2mm]
& +\;\frac{1}{4}ir^{-1}e^{4\psi-2\gamma}\left[\cos\phi\left(\gamma_{,r}\omega_{,r}-\gamma_{,t}\omega_{,t}-5\psi_{,r}\omega_{,r}+\psi_{,t}\omega_{,t}-\omega_{,rr}+r^{-1}\omega_{,r}\right)\right. \\
& \left.+r^{-1}e^{-2\gamma}\sin\phi\left(2\gamma_{,r}\psi_{,t}+2\gamma_{,t}\psi_{,r}-4\psi_{,r}\psi_{,t}-2\psi_{,rt}-r^{-1}\gamma_{,t}+r^{-2}e^{4\psi}\omega_{,r}\omega_{,t}\right)\right]
\end{aligned}
$$

$$
\begin{aligned}
\Psi_4 \;=\; & \frac{1}{2}e^{2\psi-2\gamma}\left[\left(2\cos^2\phi-1\right)\left(\gamma_{,t}\psi_{,t}-\gamma_{,r}\psi_{,r}+3\psi_{,r}^2+\psi_{,rr}-r^{-1}\psi_{,r}+\frac{1}{4}r^{-2}e^{4\psi}\omega_{,t}^2\right)\right. \\
& \left.+r^{-3}e^{4\psi-2\gamma}\cos\phi\sin\phi\left(\gamma_{,r}\omega_{,t}+\gamma_{,t}\omega_{,r}-6\psi_{,r}\omega_{,t}-\omega_{,rt}+r^{-1}\omega_{,t}\right)\right] \\[2mm]
& +\;ie^{2\psi-2\gamma}\left[\cos\phi\sin\phi\left(\gamma_{,t}\psi_{,t}-\gamma_{,r}\psi_{,r}+3\psi_{,r}^2+\psi_{,rr}-r^{-1}\psi_{,r}+\frac{1}{4}r^{-2}e^{4\psi}\omega_{,t}^2\right)\right. \\
& \left.+\frac{1}{4}r^{-3}e^{4\psi-2\gamma}\left(2\cos^2\phi-1\right)\left(6\psi_{,r}\omega_{,t}-\gamma_{,r}\omega_{,t}-\gamma_{,t}\omega_{,r}+\omega_{,rt}-2r^{-1}\omega_{,t}\right)\right] \quad (3.79)
\end{aligned}
$$

Identical expressions for these Weyl scalars were obtained when they were calculated in SHEEP directly from the frame and the four–dimensional metric. This means that the decomposition given in Gunnarsen's method is consistent with classical '3+1' decomposition techniques, since both give the same result. Thus having specified the frame, it makes no difference by which of these methods the Weyl scalars are calculated.

3.4 Adaptation of the computer code

The evolution routines in the simulation were left as before, but in addition routines for computing the values of the Weyl scalars, Ψ_0–Ψ_4 were written. Thus from the evolving values of the metric functions Ψ, Γ, Ω we derived a value for each of these scalars at every grid point on the current evolution level. Once these were known, the method of Gunnarsen et al. was applied to obtain the PNDs for the grid point in question. So, we needed to solve the Weyl polynomial, (3.19), where the coefficients of z and its powers were functions of Ψ, Γ, Ω and their derivatives. The standard leapfrog scheme was used to express these functions and their derivatives in suitable form. Once the five Weyl scalars had been calculated at any one grid point the d'Inverno–Russell–Clark method

was applied as described in section 3.2.1 to obtain the complex numbers z at that point. Finally standard routines split the complex numbers into their modulus and argument forms where

$$z_i = \tan\left(\theta_i/2\right) e^{-i\phi_i} \qquad (i = 1...4) \qquad (3.80)$$

Thus θ_i and ϕ_i are defined as

$$\theta_i = 2\arctan|z| \qquad (3.81)$$

$$\phi_i = -arg(z) \qquad (3.82)$$

and then these inserted into equation (3.48) to finally obtain the principal null directions at that point (as projected into the spacelike hypersurface $t = constant$).

3.5   Problems with identification of roots

The first observation to make about this method as applied to a numerical approach is the ambiguity involved in proceeding from the Weyl scalars, $\Psi_0, ..., \Psi_4$ to the four complex numbers $z_1, ..., z_4$. The z_i are expressed in terms of three complex numbers, α, β and γ, which are themselves only defined as α^2 etc. Indeed, from equations (3.14)–(3.18) we see that in calculating the z_i from the Ψ_i no fewer than 3 roots are taken, two being square roots and the other a cube root. Since all the quantities involved are complex, this leads to a significant problem in isolating one unique solution throughout the evolution process. The choice of solution obtained from the first slice is to a large extent immaterial, but what is very important is that it is the same solution that is obtained on each future slice. If one unique root is not isolated and the program jumps from root to root, then the PND pattern becomes meaningless. Recall that to calculate values for $\lambda_1, ..., \lambda_3$ we require a value for P which is given as $P = \{-J + \sqrt{J^2 - (I/3)^3}\}^{1/3}$. Let us define

$$\Lambda = J^2 - (I/3)^3 \qquad (3.83)$$

Then obtaining a value for P involves firstly taking the square root of Λ, and then the cube root of the complex number $-J + \sqrt{\Lambda}$. However, the fact that all these quantities are complex numbers means that each time a root must be taken there is choice as to which of the roots is the 'right' one. The first occasion when this problem arises is in calculating the square root that occurs in the definition of P. However, in the case of

applying the PND approach of Gunnarsen et al. to the Weber Wheeler wave, we can utilise the fact that this solution has no rotational element, and thus $\omega = 0$. If this constraint is applied to the definitions of the Weyl scalars, (3.76)–(3.79), the imaginary components are all found to vanish. Thus in the case of non–rotating systems, the Weyl scalars are necessarily real. This means that unlike the general case where Λ is fully complex and thus has no preferred square root, we can choose to always take either the positive or the negative square root when computing $\sqrt{\Lambda}$. Hence without loss of generality, in this case one can always take the positive square root of Λ, so that

$$\sqrt{\Lambda} = \begin{cases} A & or \\ Bi \end{cases} \tag{3.84}$$

where $A, B \in \Re$ and $A, B > 0$. In the general case where a rotational element is present, this simplification is not easily applied. Although when taking a square root, the first quadrant root would always be preferred over the third quadrant root, it is difficult to choose between the second and fourth quadrants as to which is the preferred one. Having applied this constraint there still remained the significant numerical problem of isolating one solution through the remaining cube root and final square rooting processes. In order to obtain any meaningful information from the PND evolution it was essential that the choosing of roots was consistent. This problem was particularly important when calculating P. For as previously noted, the first square root can be confined to the upper half plane but the choice of the cube root P cannot be restricted in the same way. Since it is the argument of the complex number that distinguishes between the three roots, it was this that was used to select the preferred root. Various methods of tracking the position on the Argand diagram of the previous root were attempted, in each of the stages from Ψ_i to z_i. A simple procedure which recorded the argument of the complex number on the previous slice was successful, where we defined (using the case of $P^{1/3}$ for illustration)

$$\begin{aligned} arg_1^P &= \left| \arg(P_i^n) - \arg(P_i^{n-1}) \right| \\ arg_2^P &= \left| \arg(P_i^n) - \left(\arg(Pn-1_i) + \frac{2}{3}\Pi \right) \right| \\ arg_3^P &= \left| \arg(P_i^n) - \left(\arg(Pn-1_i) + \frac{4}{3}\Pi \right) \right| \end{aligned} \tag{3.85}$$

We then simply select the argument of our function P at point i of the slice by finding the minimum of these, that is $min\left(arg_1^P, arg_2^P, arg_3^P\right)$. Then if arg_1^P is the minimum, the argument of P_i^n is taken to lie in the region $0 \leq arg(P_i^n) < \frac{2}{3}\Pi$, if arg_2^P is the minimum it is taken in the region $\frac{2}{3}\Pi \leq arg(P_i^n) < \frac{4}{3}\Pi$ and if the minimum is found to be arg_3^P the region is $\frac{4}{3}\Pi \leq arg(P_i^n) < 2\Pi$. This approach was wholly successful except in the cases when the solution crossed the axes. On these occasions significant problems were encountered in that the root was forced to be that nearest the previous root, and hence would not go through the axis but instead was reflected in it. Thus despite extensive work it was not possible to successfully isolate one root through the entire evolution process, and the simulation sporadically jumped from one root to another. The PNDs obtained were erratic and therefore we could draw no conclusions from them through this method.

If, instead, we work with a standard cylindrical frame

$$\hat{t}^a = \left(-e^{\psi-\gamma}, 0, 0, 0\right) \tag{3.86}$$

$$\hat{r}^a = \left(0, e^{\psi-\gamma}, 0, 0\right) \tag{3.87}$$

$$\hat{\phi}^a = \left(0, 0, e^{\psi}/r, -\omega e^{\psi}/r\right) \tag{3.88}$$

$$\hat{z}^a = \left(0, 0, 0, e^{-\psi}\right) \tag{3.89}$$

then the '3+1' Weyl scalars are given by

$$
\begin{aligned}
\Psi_0 = {} & e^{2\psi-2\gamma}\left[\gamma_{,t}\psi_{,t} - \gamma_{,r}\psi_{,r} + \psi_{,r}^2 - \psi_{,t}^2 + \psi_{,rr} + \frac{1}{2}r^{-1}\left(\gamma_{,r} + \psi_{,r} - r^{-1}e^{4\psi}\omega_{,r}^2\right)\right.\\
& \left.+ r^{-2}e^{2\psi-2\gamma}\left(\gamma_{,r}\psi_{,t} + \gamma_{,t}\psi_{,r} - 2\psi_{,r}\psi_{,t} - \psi_{,rt} - \frac{1}{2}r^{-1}\gamma_{,t} + \frac{1}{2}r^{-2}e^{4\psi}\omega_{,r}\omega_{,t}\right)\right]\\
& + \frac{1}{2}ir^{-1}e^{4\psi-2\gamma}\left[\gamma_{,r}\omega_{,r} - \gamma_{,t}\omega_{,t} - 5\psi_{,r}\omega_{,r} + \psi_{,t}\omega_{,t} - \omega_{,rr} + r^{-1}\omega_{,r}\right.\\
& \left.+ r^{-2}e^{2\psi-2\gamma}\left(3\psi_{,r}\omega_{,t} + 3\psi_{,t}\omega_{,r} - \gamma_{,r}\omega_{,t} - \gamma_{,t}\omega_{,r} + \omega_{,rt} - \frac{1}{2}r^{-1}\omega_{,t}\right)\right] \tag{3.90}
\end{aligned}
$$

$$\Psi_1 = 0 \tag{3.91}$$

$$\Psi_2 = \frac{1}{4}r^{-1}e^{2\psi-2\gamma}\left[4r\psi_{,r}^2 - 2\gamma_{,r} - 2\psi_{,r} + r^{-1}e^{4\psi}\omega_{,r}^2\right]$$
$$+ \frac{1}{4}ir^{-2}e^{5\psi-3\gamma}\left[2\psi_{,r}\omega_{,t} - 2\psi_{,t}\omega_{,r} - r^{-1}\omega_{,t}\right] \tag{3.92}$$

$$\Psi_3 = 0 \tag{3.93}$$

$$\Psi_4 = e^{2\psi-2\gamma}\left[\gamma_{,t}\psi_{,t} - \gamma_{,r}\psi_{,r} + \psi_{,r}^2 - \psi_{,t}^2 + \psi_{,rr} + \frac{1}{2}r^{-1}\left(\psi_{,r} + \gamma_{,r} - r^{-1}e^{4\psi}\omega_{,r}^2\right)\right.$$
$$\left. + \frac{1}{2}r^{-2}e^{2\psi-2\gamma}\left(4\psi_{,r}\psi_{,t} - 2\gamma_{,r}\psi_{,t} - 2\gamma_{,t}\psi_{,r} + 2\psi_{,rt} + r^{-1}\gamma_{,t} - r^{-2}e^{4\psi}\omega_{,r}\omega_{,t}\right)\right]$$
$$+ \frac{1}{2}ir^{-1}e^{4\psi-2\gamma}\left[\gamma_{,t}\omega_{,t} - \gamma_{,r}\omega_{,r} + 5\psi_{,r}\omega_{,r} - \psi_{,t}\omega_{,t} + \omega_{,rr} - r^{-1}\omega_{,r}\right.$$
$$\left. + r^{-2}e^{2\psi-2\gamma}\left(3\psi_{,r}\omega_{,t} + 3\psi_{,t}\omega_{,r} - \gamma_{,r}\omega_{,t} - \gamma_{,t}\omega_{,r} + \omega_{,rt} - \frac{1}{2}r^{-1}\omega_{,t}\right)\right] \tag{3.94}$$

Notice that in this case, two of the Weyl scalars vanish, namely Ψ_1 and Ψ_3. This means that in the analysis, a simplification arises. For, recall that the equation we need to solve in order to calculate our complex numbers $z_1...z_4$ is

$$\Psi_4 z^4 + 4\Psi_3 z^3 + 6\Psi_2 z^2 + 4\Psi_1 z + \Psi_0 = 0 \tag{3.95}$$

Thus in this case, for this chosen tetrad our quartic equation in z reduces to a quadratic in z^2:

$$\Psi_4(z^2)^2 + 6\Psi_2 z^2 + \Psi_0 = 0 \tag{3.96}$$

with solution

$$z^2 = -\frac{3\Psi_2}{\Psi_4} \pm \frac{\sqrt{9\left(\Psi_2\right)^2 - \Psi_0\Psi_4}}{\Psi_4} \tag{3.97}$$

Hence we can extract unambiguous solutions for z, our complex number (up to sign), and thus this tetrad enables us to calculate the associated PNDs in this frame. Interpretation of these vectors is much more difficult, however, since the PNDs were found to be of the form

$$\alpha d\phi + \beta dz \tag{3.98}$$

and in a cylindrically symmetric model where we have effectively factored out ϕ, $d\phi$ is rather difficult to interpret.

So to sum up the PND work, implementing the method of Gunnarsen et al. in the program was not too difficult, but there was difficulty in achieving meaningful results. Two different choices of tetrad were tried, but each had serious drawbacks: one gave unambiguous solutions with little physical meaning, while the solutions of the other would have been easy to understand but could not be satisfactorily obtained. However, there is scope for using a similar method in numerical relativistic work, and with the right tetrad this may prove to provide useful information. Unfortunately we were unable to do this for the exact solutions [22] [16] under consideration.

Chapter 4

Conclusions

We have studied the numerical model of vacuum cylindrical symmetry developed by the Southampton Group, which combines an inner Cauchy region with an outer characteristic region via an interface. Its validity was proven by rigourously checking all analytic calculations and their implementation in the code. The exact solution of Piran et al. was used as a further test of the code, involving all three degrees of freedom. This solution is not asymptotically flat, and the rotational element Ω for the solution is not bounded at future null infinity. This meant that care had to be taken in the discretisation of the functions to ensure that all computed quantities were bounded. Due to the unbounded nature of the metric function Ω it was decided to use the Geroch potential function o as the third comparison function along with the other two metric functions, Ψ and Γ, which were well–behaved for all radial values. The evolution produced by the code followed the analytic prediction well, but the convergence was only first order despite the fact that the differencing methods employed were second order. This was as a result of the need to evolve the Geroch potential o rather than Ω, for o is defined in terms of the derivative of Ω. Thus numerical integration was needed to obtain values for o on the initial slice, and also on every iteration to calculate the values for comparison with the evolving function. Although the integration routine was second order, the overall accuracy of the evolution was reduced to first order in this case. However, the errors were still of acceptable size.

The code was also investigated in terms of the feasibility of producing principal null directions numerically, as suggested by Gunnarsen et al. [17]. In this work, an

89

algorithm is given for calculating the principal null directions when the induced 3-metric and extrinsic curvature of a spacelike hypersurface are known. This computation of the PNDs clearly suited '3+1' codes. However, the steps required to translate the induced 3-metric and extrinsic curvature into solutions for the PNDs are of tensorial form. This means that without a programming language which can perform tensor manipulations (eg. products, contractions, implied summation etc.) this method is not as immediately applicable as is suggested. Also generally it is the metric functions, in our case Ψ, Γ and Ω which are evolved, and not the nine components of the 3-metric h_{ab}. It was neccessary therefore to calculate analytic forms for the final stage of the tensor calculation, namely the Weyl scalars $\Psi_0 - \Psi_4$ and to proceed numerically from that point. Another major problem with this approach is the ambiguity involved in taking roots of complex numbers, which led to significant difficulties in obtaining meaningful values for the principal null directions by this method. However it is possible that in a suitable frame where some of the Weyl scalars vanish more success might be possible. It is unlikely however that this would be the case for a general spacetime with no symmetries.

Where now for Numerical Relativity?

The future for numerical relativistic work looks bright. Certainly there still remains some distrust of work in numerical relativity compared with wholly analytical approaches. The fact that much of classical research is not applicable to situations of astrophysical interest has meant that numerical studies are becoming more attractive. As detectors become more sensitive and astrophysical measurements more accurate, new observations will require explanations. It is likely that numerical, rather than analytical work will be able to provide these explanations. Yet numerical work in this area must be supported by analytical work, for without calculating the governing equations in as simple and appropriate a form as possible, progress is highly unlikely. Thus numerical relativists must continue to develop techniques and methods which can be applied to more and more general situations.

Numerical relativity may still be a young field of research, but much progress has already been made. The key to making real progress in relativistic understanding is to obtain a better grasp of the physical processes involved. While many numerical

codes in this area of research may have limited applicability, any insight gained into physically relevant problems is invaluable. Indeed every successful program adds another piece to the puzzle. A method successfully applied in one case may lead another group to overcome a similar obstacle in their work. Similarly an approach found to have significant problems involved may save another group from proceeding down a dead end. By combining the advances made through various programs which focus on one specific area, there exists a real possibility of successfully tackling much more complicated problems.

Bibliography

[1] E. Poisson. Measuring black–hole parameters and testing General Relativity using gravitational wave data from space–based interferomters. *Phys. Rev. D*, 54:5939, 1996.

[2] M.M May, R.H White. Hydrodynamic calculations of general-relativistic collapse. *Phys. Rev*, 141:1232–1241, 1964.

[3] S.G. Hahn, R.W. Lindquist. The two body problem in geometrodynamics. *Ann. Phys.*, 29:304–331, 1964.

[4] R. Arnowitt, S. Deser, C.W. Misner. *Gravitation: An Introduction to Current Research (ed. L. Witten)*.

[5] J.W.York. *Sources of Gravitational Radiation, (ed. L. Smarr)*, pages 83–126. Cambridge University Press, 1979.

[6] C.W. Misner, K.S. Thorne, J.A. Wheeler. *Gravitation*. W.H. Freeman and Company, 1970.

[7] T. Piran. *Gravitational Radiation, (ed. N Deruelle and T. Piran)*, pages 203–256. 1982.

[8] L.Smarr. *Sources of Gravitational Radiation (ed. L. Smarr)*, pages 139–160. Cambridge University Press, 1979.

[9] X. Zhuge, J.M. Centrella, and S.L.W. McMillan. Gravitational radiation from the coalescence of binary neutron stars: Effects due to the equation of state, spin, and mass ratio. *Phys. Rev. D*, 54:7261, 1996.

[10] R. Gomez, L Lehner, R.L. Marsa, and J.. Winicour. Moving black holes in 3D. *Phys. Rev. D*, 57(8):4778, 1998.

[11] L. Rezzolla, A.B. Abrahams, T.W. Baumgarte, G.B. Cook, M.A. Scheel, S.L. Shapiro, and S.A. Teukolsky. Waveform propagation in black hole spacetimes: Evaluating the quality of numerical solutions. *Phys. Rev. D*, 57(4):1084, 1997.

[12] T.W. Baumgarte, G.B. Cook, M.A. Scheel, S.L. Shapiro, and S.A. Teukolsky. General Relativistic models of binary neutron stars in quasiequilibrium. *Phys. Rev. D*, 57(12):7299, 1998.

[13] R. A. d'Inverno. *Approaches to Numerical Relativity.* Cambridge University Press, 1992.

[14] Chris J.S. Clarke, Ray A. d'Inverno, James A. Vickers. Combining Cauchy and characteristic codes I. The vacuum cylindrically symmetric problem. *Physical Review D*, 52(12), December 1995.

[15] Mark R. Dubal, Ray A. d'Inverno, Chris J.S.Clarke. Combining Cauchy and characteristic codes II. The interface problem for vacuum cylindrical symmetry. *Physical Review D*, 52(12), December 1995.

[16] T. Piran, P.N. Safier, J.Katz. Cylindrical gravitational waves with two degrees of freedom: An exact solution. *Physical Review D*, 34(2), July 1986.

[17] L. Gunnarsen, H. Shinkai, K. Maeda. A '3 + 1' method for finding principal null directions. *Class. Quantum Grav.*, 12, 1995.

[18] P. Jordan, J. Ehlers, W. Kundt. *Abh. Wiss. Mainz. Math. Naturwiss*, Kl. 2, 1960.

[19] A. S. Kompaneets. *Sov. Phys. JETP 7*, 1958.

[20] R. Geroch. A method for generating solutions of Einstein's equations. *Journal of Mathematical Physics*, 12, 1971.

[21] R.M. Wald. *General Relativity.* University of Chicago Press, 1984.

[22] J.Weber, J.A.Wheeler. Reality of the cylindrical gravitational waves of Einstein and Rosen. *Reviews of Modern Physics*, 29, 1957.

[23] F. De Felice, C.J.S. Clarke. *Relativity on curved manifolds.* Cambridge University Press, 1990.

[24] R.A. d'Inverno, R.A. Russell-Clark. Classification of the Harrison Metrics. *Journal of Mathematical Physics*, 12, 1971.

[25] J. Åman, R. d'Inverno, G. Joly, M. MacCallum. Quartic equations and classification of Riemann tensors in general relativity. *General Relativity and Gravitation*, 23, 1991.

[26] M.A.H. MacCallum, J.E.F. Skea, R.G. McLenaghan, J.D. Mcrea. *Algebraic Computing in General Relativity.* Clarendon Press, 1994.